TU Delft
Delft
University of
Technology

Design of the Jumbo City Flyer

Group D06

FINAL REPORT
version 2.0   29/01/2013

Team 06 - Group members

Name	Initials	Student number	Email address
Alfons van der Beek	A.G.J.A.	4022432	
Dries Decloedt Ivan	D.	4048571	
Eng'alut	D.O.I.	1338455	
Patrick van Ginneken	P.	1507044	
Yannick Janssen	Y.S.	1356747	
Hamza Mehmood	M.H.	4051998	
Eelco Naarding	E.W.	1356925	
Roel Nous	R.J.M.	4030745	
Jasper Tiemstra	J.C.	4012569	
Stefan Verkaik	S.	4024591	

Change record

Version	Date	Pages affected	Brief description of change
1.0	21/01/2013	all	first draft version
2.0	29/01/2013	all	final version

Deadline: 25/01/2013

Principal tutor: Dr. A.G. Rao

Coach: Ir. V.P. Brugemann

Coach: P. Lv, MSc.

Advisor: Prof. dr. Ir. G. Eitelberg

Preface

This report is the fourth and final installment in a series of reports for the design synthesis exercise. The challenge of this exercise was to design a high capacity aircraft optimised for short range missions.

This report was written in a period of 3 weeks by 10 students. It intends to give a complete overview of the preliminary design process of the Jumbo City Flyer, the design which was chosen from the 3 concepts analysed in the midterm report.

It is recommended that the readers of this report have some fundamental knowledge in the field of aeronautics in order to obtain a thorough understanding of the process.

A word of thanks goes to our tutor and coaches Dr. A.G. Rao, Ir. V.P. Brugemann and L.V. Peijian, MSc. for their support and advice in the project. We would also like to thank Prof. Dr. Ing. G. Eitelberg for initiating the project and for his advice.

DSE group 06

Summary

A market analysis of the 50 busiest aerial routes indicated that 47 of these routes are shorter than 2500 km. Additionally it was observed that these routes have a high potential for future growth, which is driven by the mega cities of Asia and BRIC countries. Currently, long range high capacity aircraft, e.g., the Boeing 747 and A330, are used on these routes, resulting in a high fuel consumption per passenger km. Furthermore, increasing pressure to lower emissions and rising fuel costs create business opportunities for those able to overcome these challenges.

This report details the preliminary design of the Jumbo City Flyer, an aircraft specifically tailored to the unique market described above. To gain an early advantage in this highly competitive market, this aircraft needs to have its maiden flight by 2025. Also, it was estimated that by 2025 there is a total market for 1200 aircraft such as the Jumbo City Flyer, and this number is expected to have increased to 5500 by 2050. This assumes that the Jumbo City Flyer completely saturates the market. The preliminary design of the Jumbo City Flyer has been performed by 10 students from the Faculty of Aerospace Engineering at the Delft University of Technology as part of their bachelor thesis.

Roskam's airplane design series, consisting of 8 books, has been used as main guideline for the Jumbo City Flyer's preliminary design. The results presented in this report have been obtained by running through design sequence I and II in the Roskam books. Additional literature was used for topics not fully considered in Roskam, e.g., composite structures.

The result is an aircraft capable of transporting 514 passengers in a 2 class configuration together with a cargo load of 20 tonnes over a maximum distance of 2500 kilometres. This aircraft will cruise at Mach 0.62 at an altitude of 8.5 kilometres and will be powered by 4 turboprop engines, each capable of providing almost 13,300 kW. The structure of the Jumbo City Flyer will primarily consist of an epoxy/HS carbon fibre composite. Also, as the Jumbo City Flyer can take off within 2400 metres, land using 2200 metres, and fits in the 80-80-25 box, it is able to operate from the airports investigated in the market analysis.

To overcome the challenge of reducing CO_2-emissions, the Jumbo City Flyer will be using LNG instead of Jet A-1. Secondly, drag is reduced by flying slower, as the cruise speed of the Jumbo City Flyer is Mach 0.62 compared to Mach 0.85 for the 747-400, thus lowering fuel consumption and emissions. On the altitude and cruise speed the Jumbo City Flyer operates at, turboprops are more efficient than turbofans, hence these are chosen to power the Jumbo City Flyer. Furthermore, as the maximum take-off weight of 239 tonnes is half that of the 747-400, emissions are lowered even further. Finally, the Jumbo City Flyer will make use of an electrical taxiing system, it is thus capable of taxiing without using its engines. These features combined result in an average reduction of 47 percent in CO_2 emission per passenger per kilometre compared to the Boeing 747-400.

The Jumbo City Flyer not only outperforms the Boeing 747-400 with respect to

the emissions, but also considering operating costs. Crew costs increase because of the lower cruising speed, however, compared to the gain obtained in the fuel costs, this increase is negligible. Because the Jumbo City Flyer requires less fuel than the Boeing 747-400 and because liquefied natural gas is cheaper than Jet A-1, the total operating cost of the Jumbo City Flyer is 16 percent lower compared to the Boeing 747-400. Additionally, the purchase price of the Jumbo City Flyer is estimated to be around $170 million compared to $350 million for the 747-8.

Concluding, it is shown the Jumbo City Flyer is an economically viable concept and it is proven that the promised performance of the Jumbo City Flyer is technologically feasible by 2025. The team thus concluded that a continuation of this preliminary design is worthwhile, keeping in mind that more iterations in the preliminary design can improve the Jumbo City Flyer further.

Table of contents

List of Figures

List of Tables

List of symbols

Symbol	Unit	Description
α	rad	Angle of attack
$\alpha_{0,L}$	rad	Zero lift angle of attack
α_s	rad	Stall angle
$\Gamma_{hinge-line}$	rad	Angle between fuselage and the extension line of the flap
σ_{yield}	MPa	Yield strength
σ_x, σ_y	MPa	Tensile strength
A	-	Aspect ratio
A_i	m^2	Section area
A	m	Rim width
A_h	-	Aspect ratio of the horizontal tailplane
A_v	-	Aspect ratio of the vertical tailplane
$\bar{c}$	m	Chord length of the MAC
b	m	Wing span
b_h	m	Span of the horizontal tailplane
b_v	m	Span of the vertical tailplane
c	m	Chord length
C_l	-	Lift coefficient of the airfoil
C_L	-	Lift coefficient of the aircraft
$C_{L,max}$	-	Maximum lift coefficient of the aircraft
C_m	-	Pitching moment coefficient
$C_{m,\alpha}$	1/rad	Pitching moment coefficient rate
$C_{m,ac}$	-	Pitching moment coefficient in the a.c.
$C_{root,h}$	m	Root chord of the horizontal tailplane
$C_{root,v}$	m	Root chord of the vertical tailplane
$C_{tip,h}$	m	Tip chord of the horizontal tailplane
$C_{tip,v}$	m	Tip chord of the vertical tailplane
D	m	Bead seat diametre
D_0	m	Outside diametre
$D_{s,max}$	m	Maximum shoulder diametre
ϵ	rad	Downwash angle at the horizontal tailplane
e	-	Oswald efficiency factor
E_x, E_y	GPa	Young's modulus
G_{xy}	GPa	Shear modulus
H	m	Section height
h_v	m	Height of the vertical tailplane
k	W/mK	Thermal conductivity
$\Lambda_{LE,h}$	rad	Leading edge sweep angle of the horizontal tailplane
$\Lambda_{LE,v}$	rad	Leading edge sweep angle of the vertical tailplane
λ_h	-	Taper ratio of the horizontal tailplane
λ_v	-	Taper ratio of the vertical tailplane
l_h	m	Horizontal length between the wing a.c. and the horizontal tailplane a.c.
m	kg	Mass

n		Load factor
P	W	Power
q	N/m	Shear flow
$\frac{\delta Q}{\delta t}$	W	Heat transfer
ρ	kg/m^3	Density
Re	-	Reynolds number
S	m^2	Area of the wing planform
S$_{flapped}$	m^2	Wing area affected by the flap devices
S$_e$	m^2	Area of the elevator
S$_h$	m^2	Area of the horizontal tailplane
S$_r$	m^2	Area of the rudder
S$_{ref}$	m^2	Area of the wing planform
S$_v$	m^2	Area of the vertical tailplane
t	m	Skin and section thickness
τ_{23}	Pa	Shear stress
T	Nm	Torque
T	°C	Temperature
θ	rad	Twist
$\frac{\delta\theta}{\delta z}$	rad/m	Rate of twist
V	m/s	Undisturbed airflow speed
V	l	Volume
VA	VA	Voltampere or power
V$_h$	m/s	Airflow speed at the horizontal tailplane location
ν_{xy}, ν_{yx}		Poisson's ratio
W	m	Section width
W$_i$	kg	Aircraft component weight
W$_s, max$	m	Maximum shoulder width
x$_{ac}$	m	Distance from reference frame to the aircraft a.c.
x$_{cg}$	m	Distance from reference frame to the c.g in X-direction
x$_i$	m	Distance from reference frame to the c.g of the aircraft component in X-direction
x$_{np}$	m	Distance from reference frame to the n.p.
z$_i$	m	Distance from reference frame to the c.g of the aircraft component in Z-direction

Abbreviations

Abbreviation	Description
AC	Alternating current
a.c.	Aerodynamic center
APU	Auxiliary power unit
BOG	Boil-off gas
c.g.	Centre of gravity
CS	Certification Specifications
DC	Direct current
DOC+1	Direct operating cost plus interest
DSE	Design synthesis exercise
ESWL	Equivalent single wheel load
EW	Empty weight
FADEC	Full authority digital engine control
FAR	Federal aviation regulations
FW	Fuel weight
GD	General Dynamics
HS	High strength
ICAO	International Civil Aviation Organisation
ISA	International standard atmosphere
L/D	Lift over drag ratio
LNG	Liquefied natural gas
LPG	Liquefied petroleum gas
MAC	Mean aerodynamic chord
MTOW	Maximum take-off weight
n.p.	Neutral point
OEW	Operative empty weight
RAMS	Reliability, availability, maintainability, and safety
SF	Safety factor
W/P	Power loading
W/S	Wing loading ratio

1 Introduction

The aviation market is expected to grow with 5 percent per year in the coming decades. An increase of up to 7 percent in air traffic is expected on flights shorter than 2500 km [2]. Today no high capacity, short range aircraft to serve this growing market.

This report describes the preliminary design of the Jumbo City Flyer. A short range, high capacity aircraft that will be ready for its first test flight in 2025. The Jumbo City Flyer will be able to carry around 500 passenger over a range of maximum 2500 km. It should reduce the CO_2-emissions by 50 percent compared to a Boeing 747-400 on the same mission. The Jumbo City Flyer also strives to reduce operational cost for the airliners.

The Jumbo City Flyer is designed by 10 students of the faculty of Aerospace Engineering at the Delft University of Technology as part of their design synthesis exercise (DSE), see appendix D for the group structure. The aim of this report is to detail the preliminary design of the Jumbo City Flyer, and to investigate if the Jumbo City Flyer is the right aircraft for the market.
The outline of this report is based on the separate aircraft parts:

- Chapter 2 describes the different specifications that must be taken into account for the Jumbo City Flyer.
- Chapter 3 explains the process and results from this process up to the start of this report.
- Chapter 4 shows a study of the performance of the Jumbo City Flyer.
- Chapter 5 gives a detailed study of the different wing characteristics.
- Chapter 6 gives an overview of the aerodynamic capabilities of the Jumbo City Flyer.
- Chapter 7 explains the type of propulsion the Jumbo City Flyer uses and shows the performance of the aircraft with respect to emissions.
- Chapter 8 gives an overview of the selection and types of material used.
- Chapter 9 details the design of the empennage to achieve the desired stability of the aircraft.
- Chapter 10 shows the method for and results from determining the weight and centre of gravity position of the aircraft.
- Chapter 11 describes the different characteristics of the fuselage.
- Chapter 12 explains the characteristics of the landing gear.
- Chapter 13 discusses the reliability, availability, maintainability, and safety analysis, the operability characteristics, and shows the risk analysis.
- Chapter 14 details the market fit, the overall geometry, the family options on the Jumbo City Flyer, the operational aspects of the aircraft, the compliance matrix and the development timeline.
- Chapter 15 gives the conclusion of the design process.
- Chapter 16 presents an overview of the different recommendations for the continuation of the design per topic.

2 General requirements

The general requirements, which followed from market research, were stated in the midterm report [3]. For coherence of this report, an overview of these are given in this chapter. The final design is named the Jumbo City Flyer. The need of such a design and the accompanying market research are discussed in this chapter.

From the market research it followed that a range of 2500 km is required. The capacity of the Jumbo City Flyer was determined to be around 500 passengers, while the optimum cruise Mach number for the Jumbo City Flyer was found to be Mach 0.62. Finally the cruise height of the Jumbo City Flyer was determined to be 8.5 km. These requirements are derived in sections 2.1-2.5. Finally, sections 2.6 and 2.7 state the considerations with respect to sustainability and the requirements originating from other sources.

2.1 The global market

The aviation industry is expected to grow on average by 5 percent annually for the next decades. Figure 1 shows the growth realised in 2011 compared to 2010. As can be seen, air traffic is increasing on a global level. Furthermore, studies show that the air traffic between megacities in a short range is expected to increase substantially over the next few decades [2]. Currently aircraft like the Boeing 747-400 are being used for this mission. However, these aircraft are optimized for high range missions and are thus inefficient. Due to this, a potentially large market for short range high capacity is available. Keeping the stringent future requirements regarding environmental impact in mind, a new, innovative type of aircraft will be needed which is efficient for this mission.

Furthermore, Boeing estimates that 34,000 aircraft need to be build before 2031 to accomodate growth [4], whereas Airbus expects 27,347 aircraft [5] for the same. These numbers do not include the older aircraft that need to be replaced. With currently around 15,000 aircraft available, the market offers a big opportunity for a new type of aircraft to enter the market. Due to this, there is a large viable market for an innovative aircraft like the Jumbo City Flyer.
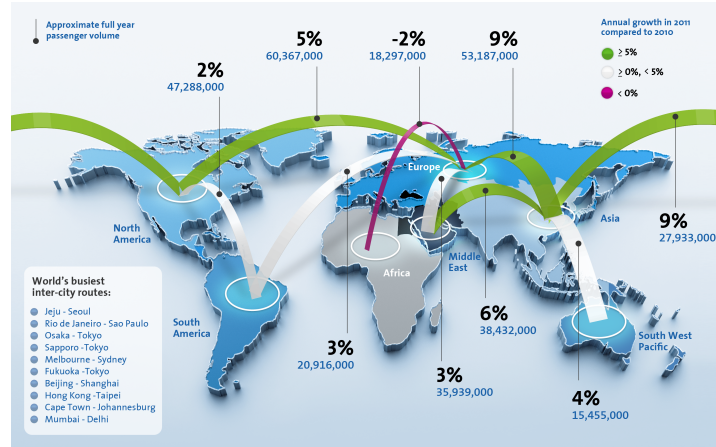
Figure 1: Expected growth of global air traffic.

2.2 Range

As the need for the Jumbo City Flyer has been explained, it would be appropriate to specify its characteristics. For the range, current flight distances and predictions were analysed. It is expected that 25 percent of all flights are under 3000 km in 2031 [5]. Furthermore, from the 50 busiest flight routes, 47 are below 2500 km [6], see A. These flights transport 4.7 percent of all passengers worldwide [7].

Combining the aforementioned, it can be concluded that the majority of the busiest flight routes are in a short range below 2500 km. Furthermore, it is expected that in the future a significant percentage of flights will be in this range. Therefore it was decided that the Jumbo City Flyer will have a range of 2500 km.

2.3 Transport capacity

In this section the passanger capacity and the cruise Mach number shall be discussed

2.3.1 Passenger capacity

As a passenger capacity of 500 was given as an costumer requirement, this value was used as an initial value. To check whether this is a good value to use, a market analysis was done, researching the economic, population and urbanisation growth of the Asia-Pacific region, as the air traffic in this region is expected to grow most.

Due to expected growth in economy [8], population and urbanisation of the Asia-Pacific region, the air traffic within the region is expected to grow. A need of approximately 31,000 medium capacity aircraft, carrying 100-250 passengers, and 600 high capacity aircraft, carrying 400-800 passengers, is expected by Boeing [4] and Airbus [5] by the year 2031.

The city population densities of the mature markets of North America and Europe mean that cities 2500 km apart can be comfortably served by the medium sized aircraft. These aircraft are designed specifically for this range. However, given the growth of GDP per capita in the Asia-Pacific region, air travel between the very

high densely populated cities of the Asian-Pacific region will need aircraft with higher capacity.

Due to the high demand for medium sized aircraft, it is anticipated that constraints in the capacity of the megacity airports in the Asia-Pacific region will occur between 2025-2050 [5]. This will mean that airliners will need large capacity aircraft to replace the role covered by the medium sized aircraft. This to increase the carrying capacity of the aircraft. As mentioned earlier, more high capacity aircraft will be needed, which carry 400-800 passengers. Taking a higher value in this range would mean that the passenger flexibility would have to be compromised on, while a low value would reduce the essence of producing a family of such aircraft. Due to this, it was found that the initial value of 500 passengers was a likeable value and therefore the Jumbo City Flyer was set to carry around 500 passengers.

2.3.2 Cruise Mach number

Now the number of passengers is determined, the cruise Mach number is to be investigated. The cruise Mach number is influenced mostly by crew costs and fuel costs. When flying slower, fuel costs go down but crew costs go up. To analyse the optimum cruise speed, an imaginary airliner is considered that has a market share of 100 percent on the 47 flights of interest from the busiest routes in appendix A. To set a benchmark, it was assumed that the entire fleet of this airliner flies at Mach 0.8. The flight speed was then varied for the whole fleet, while everything else was kept the same. The following assumptions were made during this analysis.

- Fuel costs vary linearly with the drag force.
- Flying slower results in more aircraft required to transport everyone, increasing rental cost and depreciation cost. This relation is assumed to be linear with the number of aircraft needed.
- Flying slower means more flight hours in total and thus more crew. This relation is assumed to be linear with the total flight time, including turnaround time.
- Engine run time for the entire fleet increases when flying slower, increasing the maintenance cost. It has a linear relation with the flight hours.
- The number of passengers transported and the total number of flights stay the same. Assuming a fixed ticket price, total income is the same in this analysis. Therefore, when cost are optimised, profit is optimised.
- Transport costs, landing fees, passenger service, airframe maintenance costs, and other flying operations costs are considered fixed costs.

The annual reports of Japan Airlines of 2009 [9], American Airlines of 2011 [10] and All Nippon Airlines of 2012 [11], are studied to find out how much of their operating expenses consist of the costs listed above. From this information, an estimation was made on how much the imaginary airliner of this section would spend on these costs, as percentage of its total operating expenses.

To calculate the fuel cost, the drag during cruise is calculated using equation 1. With equation 1 the fuel cost for each cruise Mach number can be calculated. The fuel cost is estimated to make up 33 percent of all operating costs.

$$D = C_{D_0} \cdot \frac{1}{2} \cdot \rho \cdot V^2 \cdot S + \frac{2 \cdot W^2}{\rho \cdot V^2 \cdot S \cdot \pi \cdot A \cdot e} \qquad (1)$$

The flight time is calculated over the average distance, weighted by passengers [6], of 1250 km. To account for the taxiing and climbing phases of the mission 30 minutes are added to the flight time. This is the total run time of the engine. For the crew time, the turnaround time of 70 minutes is added. Engine maintenance is estimated to be 2.5 percent of all operating costs and personnel cost is estimated to be 17 percent of all operating costs.

The total mass flux for the Jumbo City Flyer is 2800 passengers over a 16 hour operation time per day, [3]. This results in 600 airplanes to serve the total market in 2025, when flying at Mach 0.8. The rental cost and depreciation are considered 8.5 percent of the total cost of an airliner by 2025.

All the costs are calculated for cruise speeds varying between Mach 0.5 and Mach 0.9. A percentage of cost relative to the cost at Mach 0.8 is obtained, where the cost at Mach 0.8 is always 100 percent. These percentages are multiplied by the total number of aircraft needed and the relative cost of the subject considered. Finally, the fixed cost are added. The resulting cost-cruise Mach number diagram can be seen in figure 2. In the figure the cost with a cruise Mach number of 0.8 is 100 percent, as baseline value.
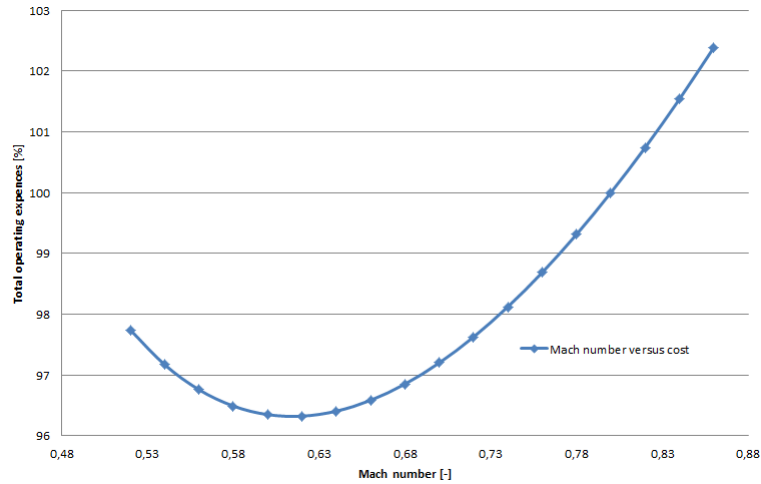
Figure 2: Cruise Mach number versus cost.

The figure shows an optimal cruise Mach number of Mach 0.62. This result is verified with the direct operating cost plus interest (DOC+1) method of NASA [12]. From the DOC+I method a cruise Mach number of Mach 0.63 is found. For the DOC+I method the following assumptions were made:

- The addition to the total flight time of 1 hour to obtain the block hours of the crew.
- The calculations corresponding to international flights for crew-, landing- and navigation fees are used.

- The airframe weight is equal to the empty weight (EW).
- The following values were used to determine the depreciation costs: period = 15 years, residual = 0.1, airframe spares = 0.06, engine spares = 0.23.
- As it is impossible to predict the future value of the aircraft in the conceptual phase, this value was set to 0 for the interest calculations.

The 2 approaches above have a result very close to each other. A cruise speed of Mach 0.62 is selected for the Jumbo City Flyer. It is important to note that economic predictions are prone to errors. Assumptions can be wrong and that will influence the results significantly. It does not say which cruise Mach number is the best cruise Mach number, the analysis merely shows that the Mach number chosen is reasonable.

2.4   Cruise altitude

After the cruise Mach number is determined, the cruise altitude is investigated. A first step is to determine the minimal altitude. For flight routes in Asia, mountains need to be considered. This resulted in a minimum cruise altitude of 6.5 km for the Jumbo City Flyer. The regulations state no minimum cruise height.

The second step is to look at the air routes used by other aircraft. Using the list of the 50 busiest air routes, it turns out that for flights between Tokyo - Sapporo a cruise altitude of 11 km is used. For Tokyo - Asaka a cruise altitude of 10 km and Beijing and Shanghai at a cruise altitude of 9 km. All flights are below a distance of 1000 km. These aircraft operate on turbofans and have a cruise Mach number of 0.8. Taking into considerations the busy air routes, an aircraft flying on the same altitude would cause a traffic jam.

The cruise altitudes are checked with reference aircraft flying with the same type of engines as the Jumbo City Flyer, see table 3. Looking at their cruise heights a cruise height of 8.5 km is chosen for the Jumbo City Flyer.

Table 3: Cruise altitudes of different kinds of aircraft.

Aircraft type	Aircraft name	Cruise altitude [km]
Military aircraft	A400M	9
	An-70	12
	Lockheed Martin C130-J	8.5
Short-range low capacity civil aircraft	An-140	7.3
	ATR-42	5.2
	ATR-72	6.1
	EMB-120	9

2.5   Field performance

The runway lengths were investigated for the 50 busiest air routes, see appendix A. From these 50 busiest routs, all airports but 3 have at least 1 runway that is 2800 metres or longer. The 3 that do not, have such an airport in close approximity as alternate destination.

Another topic of interest when investigating the runway length, is the case described in the baseline report, where China Southern Airlines' A380's made a loss when operated on domestic flights [13]. This was partly because an A380 can not land on every destination this airliner offers. To make a profit, the Jumbo City Flyer should be able to land on all these airports. So, these destinations [14] are added to this analysis and can be found in appendix B. The shortest runway length found is 2490 m.

Concluding, every airport investigated has at least 1 runway that is 2490 m or longer. To add a safety margin, a take-off and landing distance of 2200 m is selected as starting point.

2.6 Sustainable development strategy

Since "sustainable development, although a widely used phrase and idea, has many different meanings and therefore provokes many different responses" [15] the following sustainability approach has been developed to avoid ambiguity and confusion.

The Jumbo City Flyer is to fit in a growing aircraft industry with a minimal environmental impact. This means for the Jumbo City Flyer it was aimed at reducing the CO_2-emissions per passenger with 50 percent with respect to the Boeing 747-400 on the same mission and also decrease the noise levels. Another aspect of the life cycle of the Jumbo City Flyer is the construction and end-of-life. How the impact on the environment can be reduced in those phases is part of the research in the detailed design and operations planning phase.

2.7 Impact of civil airworthiness requirements and aviation regulations

Now the first 4 main requirements set by the market are known, other requirements can be discussed. These requirements originate from the customer, the team, and regulations, such as from the Federal Aviation Regulation (FAR) parts 25 and 36 [16, 17], Certification Specifications (CS) part 25 [18], and the International Civil Aviation Organisation (ICAO) [19].

The leading requirements for the design of the aircraft are listed in this section. More detailed requirements can be found in the midterm report [3]. The requirements are divided into their relevant categories:

Aerodynamics and structures

- Noise levels should at least conform to national regulations and standards.
- Limit loads have a safety factor of at least 1.5. The structure should be able to withstand these limit loads for at least 3 seconds while also satisfying:
  o The effects of deformation are not significant.
  o The deformations involved are fully accounted for in the analysis.
  o The methods and assumptions used are sufficient to cover the effects of these deformations.

Control and stability

- Locations of centre of gravity, centre of moments and aerodynamic centre should be designed such that stable manoeuvres are possible. The controllability, stability, trim, and stall characteristics of the aircraft must be demonstrated to work for each altitude expected during service.

Performance

- Emissions and fuel consumption cut by at least 50 percent as compared to a Boeing 747-400 on the same mission.

Design integration and safety

- The first test flight shall be conducted no later than 2025.
- Safe operation shall not be jeopardised in order to meet any other requirement.

Now that the requirements are set, the next step in the design process can be made.
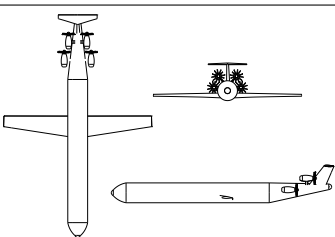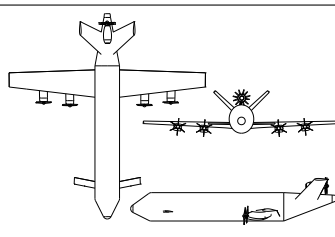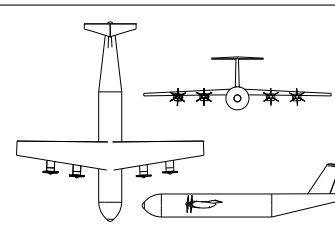
3 Aircraft configuration

The requirements for the Jumbo City Flyer have been specified in chapter 2 and in this chapter the general characteristics of the aircraft are detailed. The methodology behind the development of the Jumbo City Flyer's configuration is briefly explained in section 3.1. Furthermore in section 3.2, the general arrangement of the aircraft is explained, discussing the fuselage, wing arrangement, engines, type of fuel, empennage and the undercarriage. In section 3.3, the most important configuration parameters are summarised. Concluding, the usage of Roskam's books as main guideline during the project is validated in section 3.4.

3.1 Configuration development

In the first stage of the project different ideas were generated, as stated in the baseline report [20]. From those ideas, 3 concepts were generated of which the general lay-out can be found in table 34. The dimensions are shown in appendix C. These 3 concepts were elaborated upon in Class I-level, using Roskam [21, 22]. Next, a trade-off had to determine the best concept to be further developed into the Jumbo City Flyer. Because of inaccuracies in Class I methods, it was decided that a difference of at least 10 percent in score was necessary to indicate a clear winner. This was not the case, thus it was decided to make a new concept combining the best elements from the 3 concepts. A detailed explanation of the above procedure can be found in the midterm report [3], while the explanation of combining the 3 concepts can be found in section 3.2.

Table 4: Planform of the 3 concepts.

| JCF500-1 | JCF500-2 | JCF500-3 |

3.2 General arrangement

This section discusses the general characteristics of the Jumbo City Flyer, which combined form the baseline for the class II design. The following sections deal with the fuselage, wing, engines, fuel, empennage, and undercarriage arrangement, respectively.

3.2.1 Fuselage type

The midterm report describes the study of 3 concepts, the JCF500-1, -2 and -3. Each of which has different fuselage characteristics, which are summarised in this section. An overview of the fuselage parameters of each concept can be found in

table 5.

Since the JCF500-1 has just 1 deck to fit 508 passengers,it is a long and slender aircraft. Having a circular fuselage with 1 passenger deck, there is sufficient room in the belly to accommodate cargo and check-in luggage. With its length of 77 metres, it does not exceed the maximum of 80 metres, and according to the regulations [18] this fuselage is thus acceptable. However, a fuselage this long and slender has a suboptimal pressure-drag-over-skin-friction-drag ratio, ruining aerodynamic performance[23]. This was found sufficient to discard the JCF500-1's fuselage.

Because the JCF500-2 has 2 passenger decks it is shorter compared to the JCF500-1. Also, as the fuselage is elliptical, cargo and check-in luggage can be accommodated below the passenger decks. It was recommended to continue working with this type of fuselage since it has sufficient room for payload and reasonable aerodynamic performance[3]. Also, this fuselage provides potential to develop a family of aircraft. This fuselage will be further elaborated upon in chapter 11.

The JCF500-3 has a circular fuselage with 2 decks, resulting in little to no room for any type of cargo. This was created on purpose as passengers bringing only cabin luggage, which saves weight and decreases door to door times. However as it was found that from a commercial perspective it is generally more attractive to have space for cargo and check-in luggage, this fuselage is thus not further developed.

Table 5: Fuselage characteristics of the 3 concepts.

	JCF500-1	**JCF500-2**	**JCF500-3**
Shape	Circular	Elliptical	Circular
Diameter [m]	7	h: 7.5 w: 6.5	6.1
Length [m]	77	55	57
Decks	single	double	double
Passengers [-]	508	504	504
Cargo	available	available	unavailable
Luggage	allowed	allowed	not allowed

3.2.2 Wing arrangement

The basic consideration that needs to be made about the wing arrangement is whether a high or a low mounted wing should be used.

Compared to a low mounted wing, a high mounted wing requires additional reinforcement at its connection with the fuselage [21]. In addition, if connected to the wing, the landing gear needs to be longer for a high mounted wing. This makes the landing gear heavier and requires additional space inside the wing for the retraction system. It was found that these effects can lead to a 20 percent heavier wing structure [24].

Regarding the tail, the horizontal tail area of an aircraft with a high wing is about 20 percent larger than the horizontal tail area of an aircraft with a low wing. This is because the effect of the downwash on the tail is larger for a high mounted wing.

The result is a heavier aircraft, having adverse effects on performance.

Structural advantages of a low wing are that the landing gear retraction mechanism can be fitted inside the wing while the gear can be retracted in the fuselage. Also, if connected to the wing the landing gear is shorter, making the landing gear lighter and requiring less space inside the wing for the retraction system. This will result in a lighter structure and is the reason why it was decided to continue with a low wing configuration.

3.2.3   Location and type of engines

The Jumbo City Flyer will use turboprops, as these have the lowest fuel consumption at the cruise speed and altitude of the Jumbo City Flyer when compared to other types of engines, as found in the midterm report [3]. This is supported by figure 3 [2], showing the propulsive efficiencies of different engine types as function of the airspeed. The 4 engines still need to be developed. Each will provide at least 13,300 kW of power and 2 will be placed on each side of the aircraft, at 6.77 and 13.08 m from the fuselage centre.
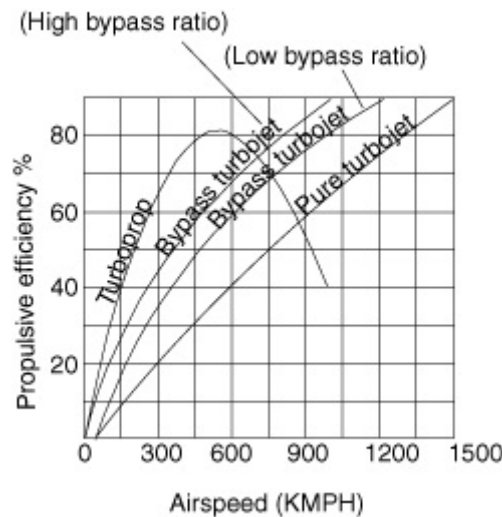
Figure 3: Thermal efficiency of engines.

3.2.4   Fuel type selection

It was found that liquefied natural gas (LNG) is the best option to fuel the Jumbo City Flyer. The advantages over previously considered fuels like the normally used Jet A-1 Kerosene, but also liquid hydrogen, liquefied petroleum gas (LPG) and compressed natural gas (CNG) are decisive, and will be summarised below after a short introduction on LNG.

LNG is natural gas, mostly consisting of methane, converted into liquid by cooling it to -162° Celsius, which allows for easier storage. LNG has 610 times the energy density compared to non liquefied natural gas and 2/3 of the energy density of Jet A-1 kerosene. Since the Jumbo City Flyer has significantly lower maximum design range than most commercial aircraft, the added 50 percent required volume to use

LNG instead of Jet A-1 is not an issue.

To keep the LNG cooled at -162° Celsius, a method called auto-refrigeration is used. This works as follows: the LNG is stored very close to its boil temperature. Some of the liquid fuel would boil off, which absorbs energy as latent heat in the boiling process. The boil-off gas (BOG) is vented which keeps the pressure constant, which in turn keeps the temperature in the gas tank constant [25].

The LNG tanks would need insulation for which 2 materials are considered, silica aerogel and phenolic foam. Thin layers of a combination of these insulators can limit the temperature rise from taxi to landing to within 5 degrees without considering boil off. If the LNG is stored slightly below its boiling temperature, this would mean that around 1 percent of the total fuel would boil off as described in section 7.6.1, around 500 kg [26]. This amount is deemed acceptable. The most important advantages of LNG as a fuel are listed below as compared to using Jet A-1 kerosene.

Advantages of LNG over Jet A-1 kerosene

- 25 percent less CO_2 than Jet A-1 per Joule generated [27].
- Less CO, NO_x and reactive hydrocarbons by around 80 percent [28, 29].
- Reduction of fuel costs [29].
- Reduction of engine noise due to high octane number [29].
- Reduction of fuel weight (FW) by 25 percent because of the increased specific energy of LNG over Jet A-1 [27].
- Possibility of increased engine efficiency as the cryogenic fuel can be used to cool the incoming air in a heat exchanger. The lower temperature allows lighter materials to be used, a higher mass-flow through the engines, and permits combustors to inject more fuel without overheating the engine [30].

3.2.5   Empennage arrangement

In the midterm report it was recommended to further investigate the considered options for the empennage. The best solution was found to be to use a conventional tail. This followed from a more detailed analysis that was performed on the empennage. The options considered were a conventional tail, a canard configuration, a V-tail, a twin tail and a T-tail. An overview of the main advantages and disadvantages of the remaining options is shown in table 6.

Table 6: Empennage characteristics concepts.

	V-tail	Canard	Conventional tail
Advantages	Noise shielding	Additional lifting surfaces	Large c.g. range
	Lighter structue	Increased cabin comfort	Undisturbed airflow on main wing
	Reduced aerodynamic drag	Reduced induced drag	More efficient use of fuselage
	Less interference	Improved manoeuvrability	
Disadvantage s	More difficult control	Difficult sizing	A rolling moment is generated
	Requires complex system	Limited c.g. range	Tail creates negative lift
	Higher torsion loads on fuselage	Difficult use of HLD's	Tail in the wake of the wing

It was found that using a V-tail would not be the most efficient option. From the trade-off conducted in the midterm report [3], it was decided that using an engine

in between the tail surfaces would not be advantageous. Hence the noise shielding advantage as stated in table 6 become irrelevant. Also, the impact of the other advantages in table 6 do not outweigh the disadvantages. It was thus decided that the option to use a V-tail is discarded.

Considering the remaining 2 options, the decisive factor is the range in which the c.g. may vary during flight. For a canard configuration this c.g. range is greatly restricted in order to remain stable. This could lead to great difficulty during the design process, since the c.g. for the design is expected to fluctuate significantly in a canard configuration. If a canard configuration is used, the wing and thus the fuel system will have to be placed further to the aft of the fuselage, in order to ensure stability. Due to this the distance between the c.g. of the fuselage and the c.g. of the wing and fuel system increases and thereby increases the c.g. range. Furthermore, as the design aims to carry a large number of passengers, the fluctuation of the c.g. will be even stronger as the fuel will decrease. As this is in contrast with the restricted c.g. range required for a canard configuration, this option is not suitable.

Summarising, it was found that a conventional tail has the potential to meet all requirements regarding stability and control [20]. In addition, a larger c.g. range is allowed in the design. Therefore, it was decided that the best solution is to use a conventional tail.

3.2.6 Undercarriage arrangement

Considering the initial configuration, there are 2 major decisions that need to be noted before going further with the preliminary design.

First, it was decided that the Jumbo City Flyer will use a retractable landing gear. A retractable gear is heavier than a non-retractable gear, however the additional drag of a non-retractable gear becomes too large at cruise speeds above 80 m/s [22].

The second decision taken is that a tricycle configuration will be used. The reason for this choice is that this configuration offers a wide range of advantages. The most important characteristics are a stable ground loop behavior, good visibility over the nose, a level floor, good steering characteristics after touch down and during taxiing, easy rotation at take-off and an easy take-off procedure [31].

3.3 Final design

After reconsidering all main characteristics, the final configuration was determined. A detailed analysis was performed with the final concept. An elliptical 2 deck fuselage with cargo hole was chosen. It was also decided to use a low wing, mounted with 4 turboprops. A conventional tail was chosen for stability and control. The fuel used is LNG. The fundamental parameters can be found in table 7. The planform of the final concept can be found in figure 4. Further elaboration of the parameters and values will be given in this report. In figure 5 the top view of the

747-400 overlayed with the top view of the Jumbo City Flyer can be seen. For rendered images of the Jumbo City Flyer, see Appendix G.

Table 7: Overview of the Jumbo City Flyer's main features.

Feature	Jumbo City Flyer
General	
Fuselage height [m]	7.2
Fuselage width [m]	6.2
Total length [m]	58.3
Total height [m]	21.9
Passengers [ec/bu]	418/96
Cargo	32 LD1 containers
Performance	
Design range [km]	2500
Stall speed [m/s]	76.6
Cruise speed [m/s]	190
Cruise altitude [m]	8500
Minimum take-off length [m]	2300
Minimum landing length [m]	2200
Propulsion	
Fuel	LNG
Reference engine type	Europrop TP400
Thrust per engine [kW]	13,300
Number of engines	4
CO_2-emissions [kg/MJ]	0.05
Wing	
Span [m]	62.5
Area [m^2]	391
Aspect ratio [-]	10
Airfoil type	Updated version of NACA 63A-613
Incidence angle [deg]	3
Dihedral [deg]	6
Weight	
MTOW [tonne]	239
EOW [tonne]	114
FW [tonne]	56.7
Payload weight [tonne]	68.7
Aerodynamics	
$C_{l,max,clean}$ [-]	1.7
$C_{l,max,land}$ [-]	2.3
$C_{l,max,take-off}$ [-]	2.1
$C_{d,0}$ [-]	0.0165

63.5

Side view

54.6

Front view

17.2
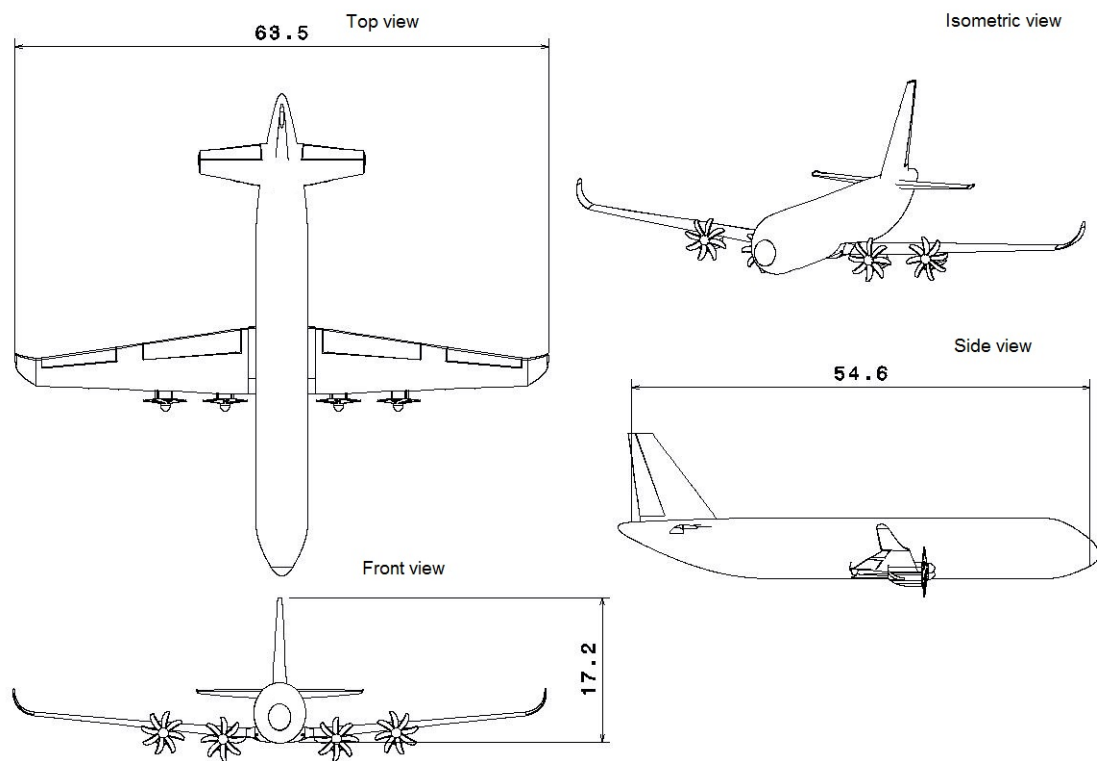
Figure 4: Planform of the Jumbo City Flyer.
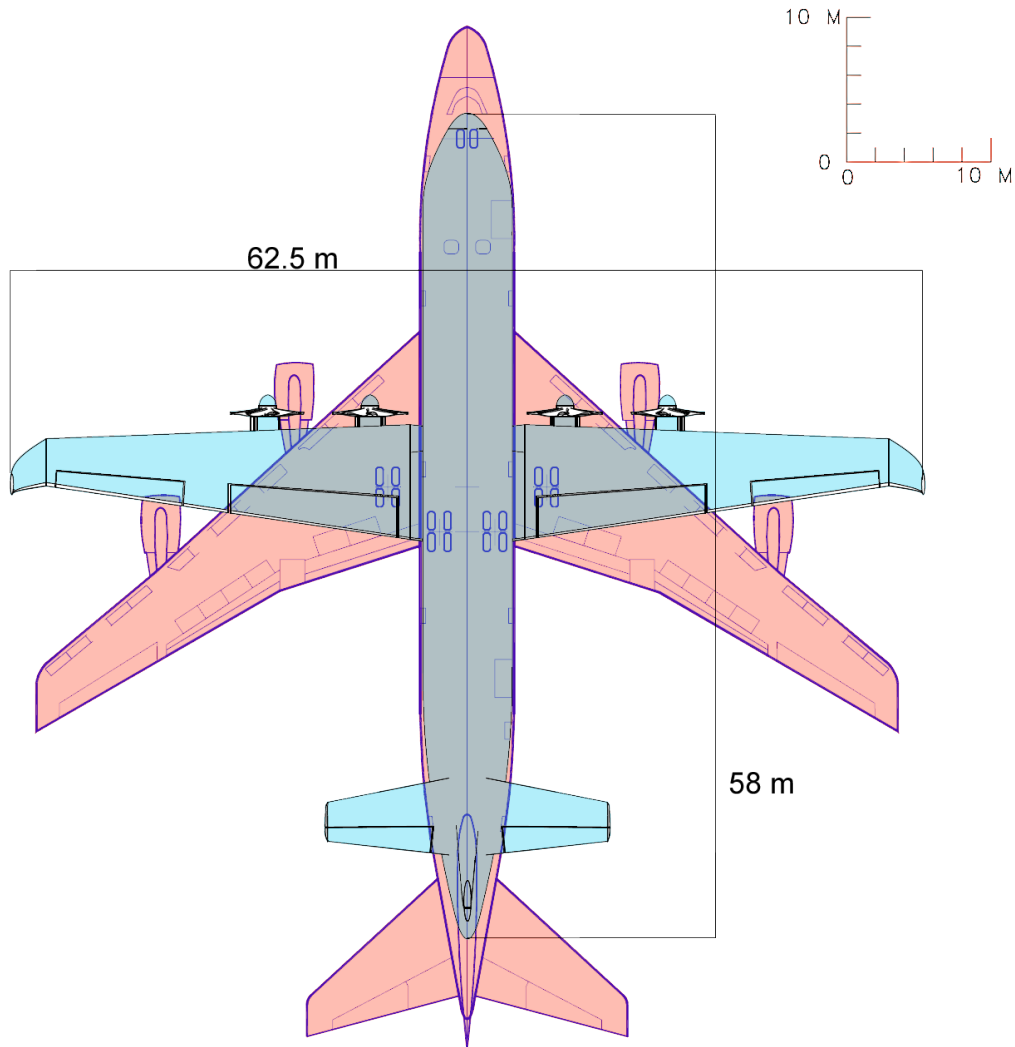
Figure 5: Top views of the Jumbo City Flyer and the 747-400 overlayed.

3.4   Validation of methodology

During the development of the configuration, but also throughout the preliminary design, Roskam's books on airplane design [21, 22, 23, 31, 32, 33, 34, 35] have been used as the main guideline. In this section, Roskam's methodology will be validated for the design of the Jumbo City Flyer.

A first aspect of validation is that the method used should be suitable for the product to be designed. Roskam provides a set of 282 reference aircraft divided into 12 categories, of which 2 categories are comparable to the Jumbo City Flyer. This was found to be sufficient reference to consider the method to be applicable for design of the Jumbo City Flyer. It needs to be noted that the reference aircraft are relatively old, only including aircraft designed before 1997. This means that the results are conservative, not including developments of for instance materials, and less accurate for innovative aircraft like the Jumbo City Flyer.

Secondly to validate the method, the results should be reproducible using other methods. Conveniently Roskam refers to other methodologies for several aspects of the design, such as for instance Torenbeek [36]. In chapter 10 it will be explained that 2 methods were used for the Class II weight estimation. This was done to check that the results in Roskam are reproducible. Toorenbeek's method resulted in a maximum take-off weight (MTOW) of 229 tonnes, while the GD-method [32] predicted a MTOW of 245 tonnes. This is reasonably accurate as in general for Class II methods accuracies up to 5 percent can be expected [22].

4 Performance analysis

In this chapter the different performance characteristics of the Jumbo City Flyer are discussed. In section 4.1 the aircraft's mission and the corresponding flight envelope are given. The Class I weight estimation is discussed in section 4.2, while in section 4.3 the initial approximations for the aircraft's performance are discussed. Finally, in section 4.4 the Class II performance analysis is elaborated upon, presenting the Jumbo City Flyer's most up-to-date performance characteristics.

The most important aspects of the performance of the Jumbo City Flyer are found in table 9, and the maximum range and the ferry range are around 4500 km and 5600 km, respectively. The runway lenght required for take-off is 2250 metre.

4.1 Mission analysis

The Jumbo City Flyer has to be designed such that it is capable of withstanding a specified range of loads without failure. The fact that wind gusts create extra loads on the aircraft must be taken into account. The maximum load factors can be found in the V-n diagram, which is elaborated upon in section 4.1.1. In section 4.1.2 the mission profile, illustrating the different phases of flight, is discussed.

4.1.1 Flight envelope

CS-25 identifies 2 types of V-n diagrams for certified aircraft [18]. The first is the V-n manoeuvre diagram and the other is the V-n gust diagram. These diagrams are used to determine the combinations of flight conditions and load factors for which the aircraft structure must be designed. Also, it is a useful tool in determining the manoeuvring capability of the aircraft. Both diagrams are illustrated in figure 6.
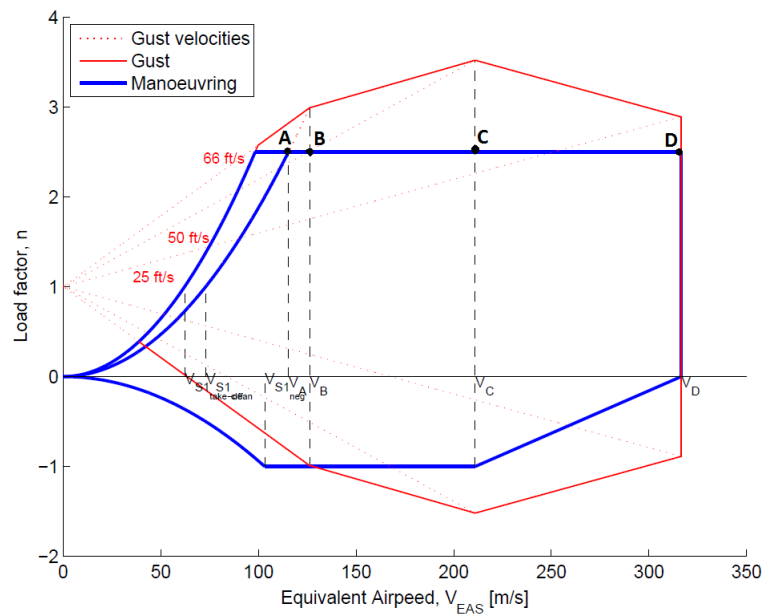
Figure 6: V-n manoeuvre and gust diagram.

Designing the V-n diagram in accordance with CS-25 regulations brings certain

restrictions to the process. As can be seen on the top of figure 6, the positive design limit load factor, $n_{lim,pos}$, is equal to 2.5. Since the Jumbo City Flyer has a MTOW of more than 170 tonne, $n_{lim,pos}$ may not be less than 2.5 and need not to be greater than 3.8. This is why a limit load factor of 2.5 is selected. Also, a lower limit load factor is provided by CS-25, the negative design limit load factor, $n_{lim,neg}$. This may not be less than -1.0 for speeds smaller or equal to V_C, and varies linearly between V_C and V_D. The manoeuvring diagram is further restricted by a curve from point 0 to A, which represents the maximum normal force coefficient, $C_{N,max}$. For preliminary analysis purposes it is acceptable to use equation 2 to calculate $C_{N,max}$:

$$C_{N,max} = 1.1 \cdot C_{L,max} \tag{2}$$

The same relation holds for $C_{L,max,neg}$. The design manoeuvring speed, V_A, the cruise speed, V_C, and the design diving speed, V_D, are also indicated in the diagram. The design manoeuvring speed is the intersection between the $C_{N,max}$-curve and limit load factor. At speeds close to this, full deflection of any of the flight control surfaces should not be attempted because of the risk of damaging the aircraft. The cruise speed is determined using the Mach number and cruise altitude assuming the International Standard Atmosphere (ISA). The design diving speed is then computed by multiplying the cruise speed with a factor of 1.25, which forms the right border of the diagram. When flying at speeds higher than the design diving speed, there is a risk of damaging the aircraft's structure when manoeuvring.

To account for gusts that may occur during flight, a load associated with vertical gust must also be evaluated over the range of speeds. CS-25 describes the calculations in some detail for different altitudes. However, since this diagram shows the flight envelope at sea level, the gust velocities are fixed at 20.12 m/s for V_B, 15.24 m/s for V_C and 7.62 m/s for V_D. These gust velocities provide additional lift, which means that the load factor increases. The structure of the aircraft should be designed to cope with the gust load factor if it is higher than the limit load factor. Therefore the maximum gust load is the decisive load factor that the structure should be designed for.

4.1.2 Flight profile analysis

Based on requirements set by the customer and the earlier performed market analysis, a typical mission profile for the Jumbo City Flyer can be constructed, which is illustrated in figure 7.
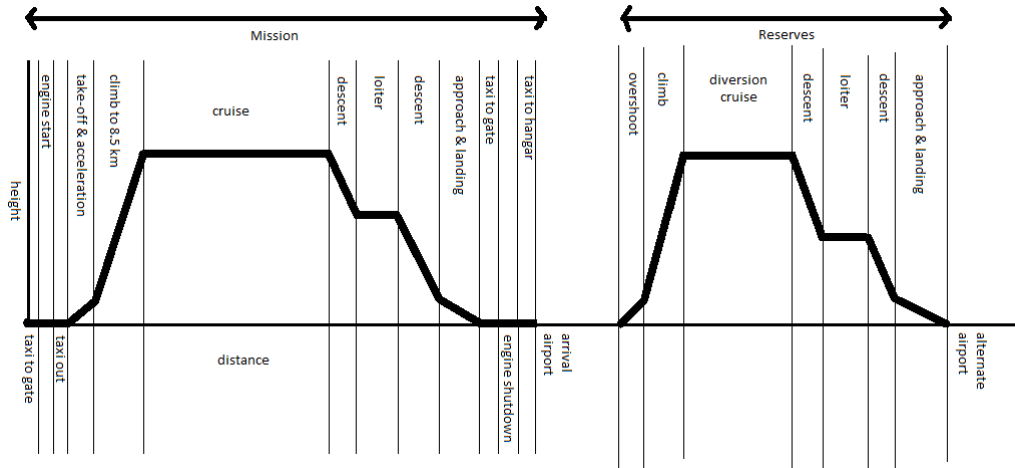
Figure 7: Mission profile for the Jumbo City Flyer.

The distance is plotted on the x-axis and the height on the y-axis, neither of them are to scale. An overview of a conventional mission, from rolling out of the hangar to storage back into the hangar, can be seen in the left part of the figure. The right part of the mission profile indicates the reserves. When landing has to be cancelled, the Jumbo City Flyer has to be capable of performing this part of the mission. A diversion cruise of 45 minutes is accounted for and fuel for diversion should always be included.

4.2 Class I weight estimation

A Class I weight estimation for the Jumbo City Flyer was made using Roskam I [21]. The results of this calculation are summarized in table 8.

Table 8: Class I weight estimation of the Jumbo City Flyer.

Parameter	Weight [tonne]
MTOW	197
EOW	80.4
EW	79.4
FW	46.7
PW	68.7

To make the Class I weight estimation, the following assumptions were made:

- The weight of 1 passenger or crew member including luggage is assumed to be 97.4 kg.
- The Jumbo City Flyer is assumed to fly 500 passengers over 2500 kilometres.
- The Jumbo City Flyer requires 12 crew members for operation.
- The usage of composites will decrease the empty weight of the Jumbo City Flyer with 20 percent compared to using aluminium for the structure [37].
- The Jumbo City Flyer will be able to carry 20 tonnes of cargo.
- The specific fuel consumption for LNG is determined, using equation 3:

$$c_{p,a} = \frac{H_{s,b}}{H_{s,a}} c_{p,b} \tag{3}$$

where H is the calorific value, c is the specific fuel consumption and the subscripts a and b refer to the respective fuel types considered.

4.3   Evaluation of performance requirements

In the previous section, the Class I weight estimation for the Jumbo City Flyer was performed. In this section, the sizing of the aircraft to meet the requirements as defined in chapter 2 is explained.

The power loading (W/P) and the wing loading (W/S) have been determined with an aircraft performance diagram. The next step was to pick an optimal design point in the performance diagram. Figure 8 shows the the Jumbo City Flyer's performance diagram in which the chosen design point is indicated with a red dot. Once the design point was determined, the maximum lift coefficient for take-off, landing, and clean configuration, as well as other design aspects like wing area and aspect ratio, were obtained. The results are summarised in table 9.
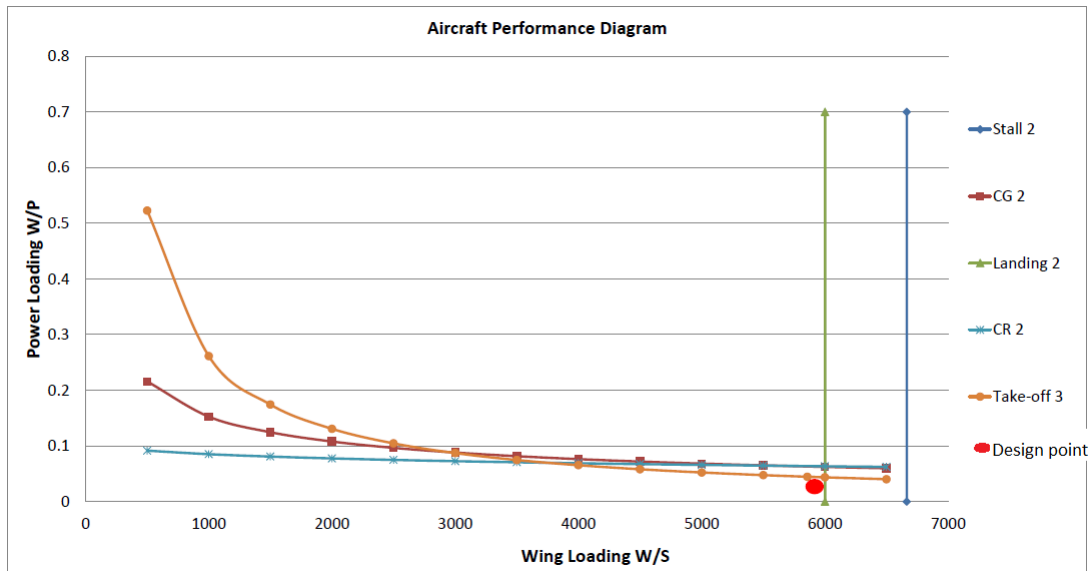
Figure 8: Power and wing loading of the Jumbo City Flyer.

Table 9: Performance results of the Jumbo City Flyer.

Parameter	Value	Parameter	Value
W/S [N/m^2]	6001	Root chord [m]	8.87
W/P [N/W]	0.044	Tip chord [m]	3.64
Power required [MW]	53	Taper Ratio [-]	0.3
Wingspan [m]	62.51	Wing area [m^2]	391
Aspect ratio [-]	10	Quarter chord sweep angle [degree]	0
$C_{L,max,clean}$ [-]	1.67	Stall speed clean [m/s]	80
$C_{L,max,take-off}$ [-]	2.10	Stall speed take-off [m/s]	68
$C_{L,max,landing}$ [-]	2.30	Stall speed landing [m/s]	65

The procedure used to create the power loading diagram is described in chapter 3 of Roskam I [21]. To obtain the results in table 9 the following assumptions were

made:

- Oswald efficiency factor: 0.85
- Design climb rate: 7 m/s
- Design climb gradient: 5.5 percent
- Equivalent skin-friction drag coefficient: 0.003
- Wetted area ratio: 5.5
- Take-off parameter: 193
- Cruise altitude: 8500 m
- Take-off distance: 2200 m
- Density ratio: 0.78

4.4   Class II performance analysis

In section 4.3 the Jumbo City Flyer was sized according to the Class I performance analysis. It has to be verified whether the performance requirements are still met in the Class II performance analysis. The method used as well as the results from the Class II performance analysis are explained in this section. In general, the procedure used is described in chapter 5 of Roskam VII [34]. The results from the Class II weight estimation can be found in table 10.

Table 10: Class II weight estimation of the Jumbo City Flyer.

Parameter	Weight [tonne]
MTOW	239
EOW	114
EW	113
FW	56.3
PW	68.7

4.4.1   Stall

The stall speed is the first characteristic for which the Class II performance analysis has been conducted. The results of the calculations are summarised in table 11. Similar to the Class I performance analysis 3 stall speeds were calculated. These are the stall speed in clean, take-off and landing configuration. As stated in CS-25 [18] and FAR 25 [16], these stall speeds need to determined at most forward c.g., while assuming MTOW. Note that the stall characteristics given in table 11 were determined at sea level in ISA.

Table 11: Class II stall speeds for the Jumbo City Flyer.

Parameter	Speed [m/s]
$V_{stall,clean}$	77
$V_{stall,take-off}$	68
$V_{stall,landing}$	65

4.4.2   Take-off performance

The take-off distance is the second parameter for which the Class II performance has been investigated. The runway lengths for airports on the 50 busiest routes

were determined, resulting in the conservative requirement that the total take-off length should be below 2200 m [3]. In the Class II performance analysis the length of the ground run for the Jumbo City Flyer was calculated to be 2180 m. Keep in mind that the aircraft still needs approximately 200 m to climb to the screening height of 15 m. As most airports have a clearway and since the requirement was taken to be conservative, it is assumed that this will not be a problem.

Several assumptions have been made for determining the ground run length and they are listed below:

- FAR 25 is used and verified to be coherent with CS-25.
- Only concrete and asphalt runways are considered.
- Take-off power is assumed to be the maximum available power.
- Density ratio (σ) is 0.78, corresponding to an airfield elevation of 2300 metres.

4.4.3 Climb performance

The Class II maximum rate of climb at sea level for the Jumbo City Flyer was determined to be 19.32 m/s, corresponding to 3800 fpm. This climb rate was determined for sea level in ISA. Additionally, the aircraft was assumed to fly in clean configuration at the cruising lift over drag ratio. Concluding, it should be checked whether the regulations' requirements are met in exceptional cases, for instance in landing configuration with 1 engine inoperative.

4.4.4 Payload-range diagram

The requirement for the Jumbo City Flyer's range when fully loaded was set at 2500 km [20]. However, when the payload is decreased and the amount of fuel aboard remains the same, this range will increase. Hence, a payload-range diagram can be constructed. The payload-range diagram for the Jumbo City Flyer can be found in figure 9.

On the y-axis the operative empty weight (OEW) plus the payload is indicated while the x-axis indicates the corresponding range. Point A indicates the maximum range for the aircraft loaded with 514 passengers and 20 tonnes of cargo. From point A the range increases as the payload is reduced until it reaches point B. This point indicates the maximum range of 4459 km for the aircraft transporting 100 passengers and 20 tonnes of payload. Finally, at point C the aircraft has a range of 5567 km, which corresponds to the aircraft flying at its OEW. This range is the so-called ferry range and is not that interesting from a commercial perspective. It is mainly important for when the aircraft has to be relocated for delivery or maintenance.
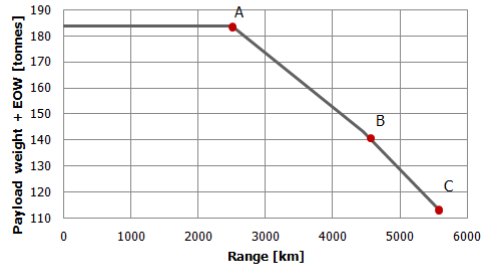
Figure 9: Payload-range diagram of the Jumbo City Flyer.

4.4.5 Landing performance

The final performance parameter for which a Class II performance analysis was done is the landing distance. It was calculated that the Jumbo City Flyer requires a maximum landing field length of 2241m. This value slightly exceeds the 2200m requirement set in chapter 2 but since the requirement was set at a conservative value, no changes to the design have to be considered for landing.

To determine the landing distance, the following assumptions were made:

- The average flight path angle is assumed to be 0.1 radians, an average value for commercial aircraft.
- The average deceleration in the ground run is assumed to be 0.4, an average value for turboprops.
- It is assumed that no reverse thrust is available.

5 Wing design

In this chapter, the wing will be discussed in more detail. Sections 5.1 to 5.3 describe wing characteristics such as wing area, aspect ratio, type of airfoil, type and size of control surfaces. Section 5.4 describes the preliminary design of the wing structure of the Jumbo City Flyer.

5.1 Wing characteristics

This section summarizes the main characteristics of the wing, including the wing area, the layout of the planform and the type of airfoil used.

5.1.1 Wing area

From the design point, a wing loading of 6000 N/m^2 was selected, and the weight was estimated With the weight estimated to be 239 tonne, a wing area of 391 m^2 will be needed.

5.1.2 Planform

An aspect ratio of 10 was selected for the Jumbo City Flyer, resulting in a span of 62.5 metres. There is no need for sweep when flying at a Mach number of 0.62. At this speed the critical Mach number is not reached. To account for the critical Mach number sweep is used, in this case this is not necessary. The taper ratio was set to 0.41 in the midterm report [3] remains the same in the final design. The chord length at the root is 8.87 metre and the chord length at the tip of the wing is 3.64 metre. An overview of the wing planform is given in figure 10. The dimensions are given in meters. The positioning and sizing of both the high-lift devices and the ailerons is done in sections 6.2 and 5.3 respectively.
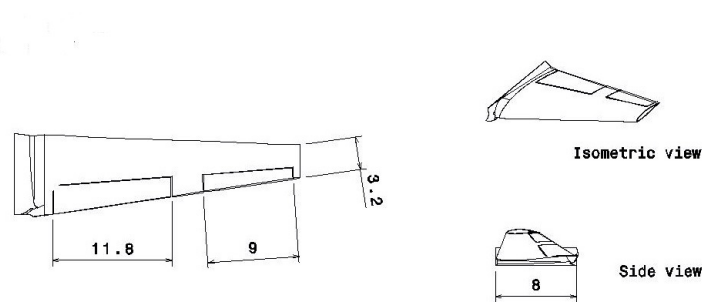
Figure 10: Overview of the wing planform of the Jumbo City Flyer

5.1.3 Airfoil selection

In the midterm report [3], an airfoil for the wing was selected: the NACA 64A-719 profile. It provides a maximum lift coefficient of 1.5 in clean configuration, whereas it should provide a $C_{L,max}$ of 1.79. Note that the $C_{L,max}$ requirement in clean configuration is 1.7 for the Jumbo City Flyer, but the wing should provide 1.05 times that value [33]. Additionally the airfoil has a thickness of 19 percent while a

thickness of 13 percent is sufficient to store the LNG in the wing.

More airfoils were investigated in JavaFoil [38] and the best standard airfoil found is the NACA 63A-613 airfoil. It generates more lift than the NACA 64A-719 profile, $C_L, max = 1.75$, and the 2D drag is 35 percent lower. However, this airfoil still does not fulfill the C_L, max requirement and improvements are thus necessary.

For this purpose, XFLR5 [39] is used, this program allows for modification of standard airfoils to meet specified requirements. Several iteration steps were performed in which the location of the thickness, the camber and the location of maximum camber were varied. Combinations of these options were also considered. The NACA 63A-613 airfoil served as basis for the modifications.

It was found that increasing the $C_{l,max}$ is possible, but then the moment increases as well. This means that a bigger tail and thus an even higher $C_{L,max}$ are required. Therefore this option is discarded, hence only minor improvements remain possible. This resulted in an airfoil providing $C_{L,max}$ of 1.76, with a moment during cruise and climb lower than the moment of the NACA 63A-613 profile. The decreased moment results in less trim drag and thus a better value for the lift over drag ratio (L/D). Due to time limitations this is not the optimum value. Using more iteration will result in an improved $C_{L,max}$ and will meet the requirements set as explained in chapter 6.
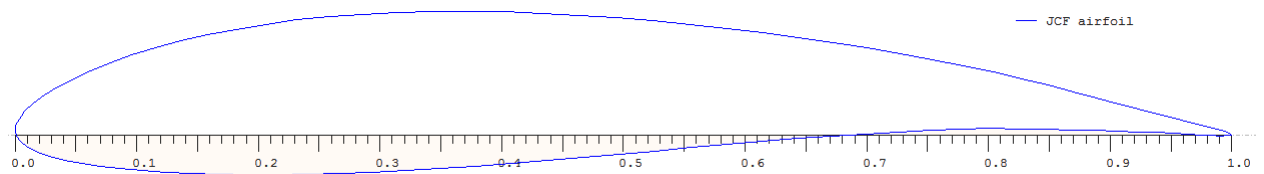
Figure 11: Profile of the airfoil selected for the Jumbo City Flyer

In figures 12 through 13, the Jumbo City Flyer's airfoil is compared to the NACA 63A-613 profile, for 2D analysis only. A Reynolds number (Re) of 35 million is used for these graphs. Table 12 gives the changes with respect to the NACA 63A-613 profile as obtained. The 3D characteristics will be discussed in chapter 6.
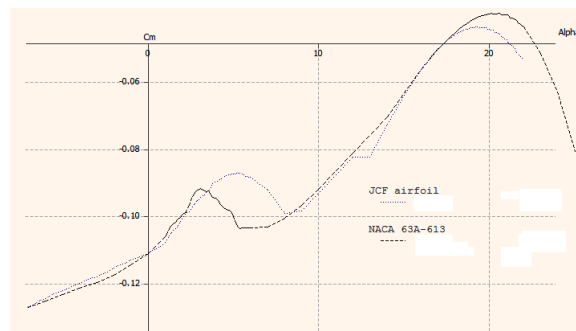
Figure 12: C_m versus α curve for the Jumbo City Flyer airfoil. Re = 35 million.

Table 12: Input parameters in XFLR5 of Jumbo City Flyer airfoil compared with NACA 63A-613 airfoil.

Name	Thickness (% c)	at (% c)	camber (% c)	at (% c)
NACA 63A-613	13.00	34.95	3.99	52.36
Jumbo City Flyer Airfoil	12.99	29.40	3.99	52.40
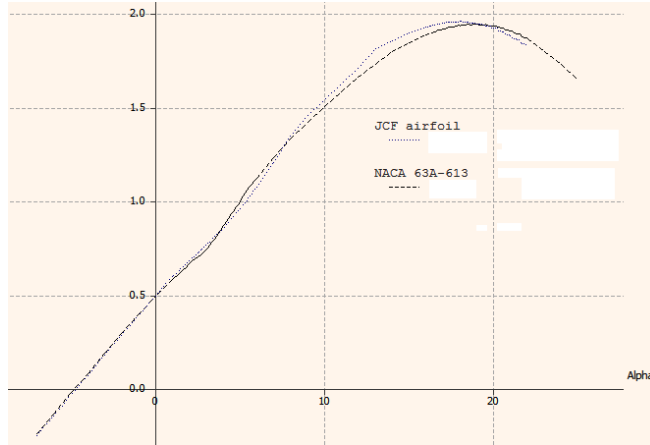
Figure 13: C_l versus α curve for the Jumbo City Flyer airfoil. Re = 35 million.
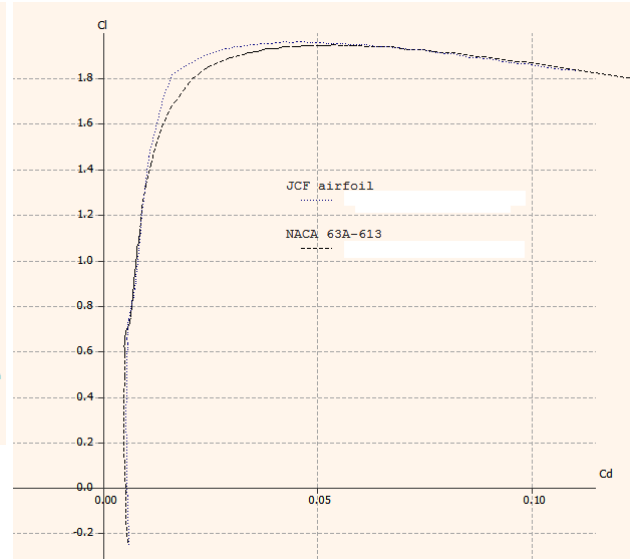
Figure 14: C_l versus C_d curve for the Jumbo City Flyer airfoil. Re = 35 million.

With the airfoil selected in this section and a cruise Mach number of 0.62, there is no need for a sweep angle in the wing. An important point for sweep is the critical Mach number. The critical Mach number is the Mach number when turbulent flow occurs due to flying close to the speed of sound. At a speed of mach 0.62 the critical Mach number is not reached so it is not necessary to use sweep.

5.2 Verification of method

Both XFLR and Javafoil are programs recommended by staff at the faculty of Aerospace Engineering of TU Delft for doing initial research on airfoils. However, there are limitations on JavaFoil. First of all, JavaFoil does not model laminar separation bubbles and flow separation, which may lead to incorrect results. Furthermore an airfoil analysed beyond stall will give inaccurate results [38]. Therefore, this program is used to evaluate at low Mach numbers: Mach 0.2. The maximum lift coefficient is important for this analysis, however what happens beyond stall is not of importance in this chapter. Only conventional airfoils are considered with this program.

Similar limitations are found for XFLR5. Furthermore the warning is given that XFLR5 is designed for low Reynolds numbers applications. The same airfoils are

investigated in both XFLR5 and JavaFoil to check the performance of XFLR5 at high Reynolds numbers. It was found that XFLR5 indeed tends to overestimate the maximum lift coefficient at high Reynolds numbers. To account for this problem, Reynolds numbers found for the wing are divided by 2 when analysed with XFLR5. Concretely, to do the analysis in XFLR5 at a Reynolds number of 35 million, the value of 18 million is given as input. For standard NACA values, this is found to give results more comparable with JavaFoil then using 35 million as Reynolds number.

To further validate the results of this chapter, a model of the wing will have to be tested in a wind tunnel.

5.3 Control surfaces

The ailerons have to be sized such that they provide sufficient control, as defined by equation 4, during all phases of the aircraft's mission. The sizing of Jumbo City Flyer' ailerons is based on the procedures as described in Aircraft Preliminary Design Handbook by professor Gudmundsson [40] and data from the Flight Dynamics Lecture Notes [41].

$$\frac{pb}{2V} \geq 0.07 \tag{4}$$

It was assumed that the Jumbo City Flyer uses plain flap ailerons. This type of aileron is commonly used in a wide range of aircraft. Additionally, while this aileron type is very effective, it is also relatively simple to design and produce. It is recommended to further investigate other aileron types, such as Frise ailerons, during future development of the Jumbo City Flyer.

As such, the ailerons can be sized using equations 6 and 7 and inserting the obtained values in equation 5. Using these equations, it was determined that an aileron span of 9 metres is sufficient to meet the requirement set in equation 4.

$$\frac{pb}{2V} = -\frac{C_{l_{d\alpha}}}{C_{lp}} d\alpha \tag{5}$$

$$C_{l_{d\alpha}} = \frac{c_{l_{d\alpha}} c_r}{Sb} \left[\left(b_2^2 - b_1^2 \right) + \frac{4 \left(\lambda - 1 \right)}{3b} (b_2 - b_1)^3 \right] \tag{6}$$

$$C_{lp} = \frac{- \left(C_{l_\alpha} + C_{d\_0} \right) C_r b}{24S} \left[1 + 3\lambda \right] \tag{7}$$

5.4 Wing structure

The wing structure will be made of epoxy/high strength (HS) carbon fibre, the decision for this material is explained in chapter 8. Carbon fibre presents a few challenges that require special attention, these are:

- More challenging to use and less predictable because experience in the aircraft industry is lacking.
- Complex damage, e.g., fibre cracks, matrix cracks, interface debonding, delamination, and microbuckling.
- Brittle, no ductile failure.
- Flammability, lightning strikes.
- Structural health monitoring and non destructive inspection of composites is much more difficult than for metals.

Because of these challenges the safety factor (SF) for the wing box of epoxy/HS carbon fibre is doubled as compared to the aluminium wing box calculations. A SF of 3 instead of a SF of 1.5 is used. The wing structure can be seen in figure 15.
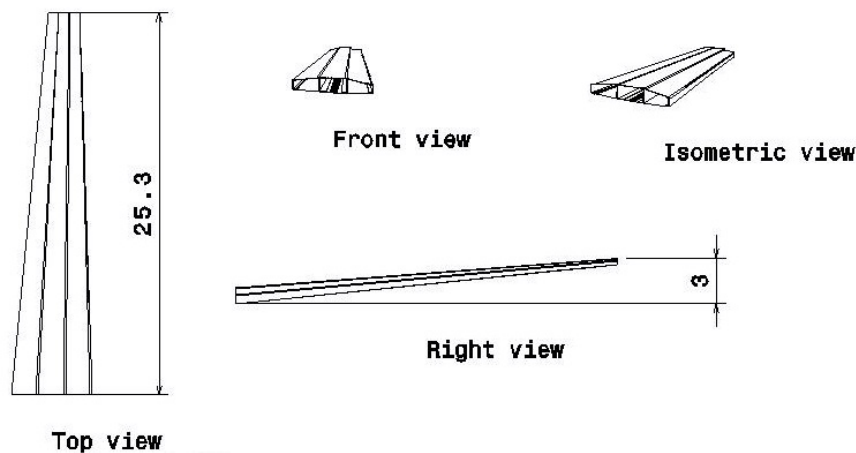
Figure 15: The wing structure including the wingbox.

5.4.1 Preliminary wing box design

The lift, drag, thrust and moments are calculated using the MTOW. For all corners of the flight envelope the corresponding aerodynamic maximum load factors were calculated, and then multiplied with the SF. The maximum load factor is 3.5. Multiplied wit the safety factor resulting in a maximum load of 10.5 times the MTOW. The resulting aerodynamic lift is used to calculate the internal moment, shear force, and torque [42]. A simplified drawing is given in figure 16. The drag force is considered negligible and is left out of this calculation.

For the internal load calculation each half wing is divided into 100 beam elements for which the lift force is assumed to act at the quarter-chord in the middle of the element. Also, it is assumed that the lift portion the wing section carries is linearly dependent on the surface it has.
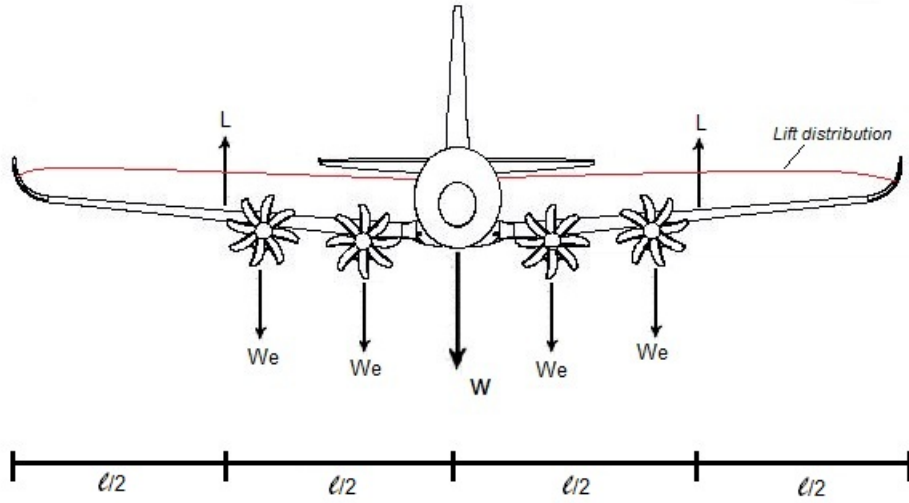
Figure 16: Forces on the Jumbo City Flyer during symmetric flight.

Constraints are defined for the wing tip displacement and rotation. Wingtip displacement should not exceed ±15 percent of the total span of the wing, and wingtip twist should not exceed ± 10°. These maxima were used to obtain the required bending and torsional stiffness of each beam element. The bending moments and torsion include the moments caused by the lift forces, thrust from the engines, weight of the engines, weight of the fuel and weight of the wing [43]. For the wing weight an initial value was estimated and later updated with the calculated value.

The stiffness distributions of the the wing box needs to be determined. These are assumed to be constant throughout a beam element and is constrained by the shape of the airfoil. For the calculations thin wall assumptions are used. In thin-walled beams the wall thickness is much smaller than a representative dimension of the cross-section allowing higher powers of it to be left out of the calculation. Where possible however all thicknesses were taken into account to avoid over designing as much as possible.

Lift is assumed to act at the quarter chord, where the front spar will be positioned. It followed from the high lift device calculation that the second spar could be positioned at 0.75c. However, to account for the structural control mechanism and some room for the aileron fly-by-optics system and electronics, an initial back spar position of 0.7c is set.

Subjected to the σ_{yield} discussed in chapter 8 and the assumption that the carbon fibre should never be allowed to yield, an initial thickness for the spars web and flange and skin thickness can be calculated. For the preliminary skin design the shear flow is calculated to check the wing box for shear stresses. The first approximation of thin-walled beam theory confers the distribution of stress components across the wall thickness. Beam theory assumes the cross-section to be infinitely rigid in its own plane so that the stress components σ_2, σ_3 and τ_{23} are negligible.

If the shear stresses do not exceed the yield criterion the wingbox was checked for 2 additional considerations. A check is performed to see if the total shear flow through the structure adds up to the total torque. This process is iterated to find the shear flows trough the wing box and the front and aft skin sections to find the optimised skin thickness.

Spar webs may buckle due to the shear loads and the wing skins due to the normal stresses. To prevent this, stiffeners are placed on the spar webs and stringers on the wing skin. This breaks the larger areas up into smaller, stronger areas. The fact that the stringer strain should equal the top-skin strain and the fact that they share the total load between them gives a requirement for the stiffener area.

To prevent the stringers themselves from buckling under the applied loads, ribs are used to again break the stiffeners into shorter loaded units, without literally breaking them up. The forces in the spar webs, skin and stiffeners are calculated so that the number and size of spars and stringers and stiffeners is determined so that they total structure can withstand the ultimate loads without buckling.

The analysis is done with a Matlab code that automatically scales the wing if initial parameters like the wingspan, the wing area and the MTOW change. In this way every change to the aircraft is automatically incorporated in the wing structure. The Matlab routine iterates until the optimum ratio between skin thicknesses, number of spars, spar thicknesses, stringer numbers, spacing and size and stiffener and rib locations is found that minimises weight.

It is obvious that not all formulas and calculations can be shown here. To give an idea of the process an example calculation for the shear flow and rate of twist calculation is shown here. Figure 17 shows the setup of the problem [42].
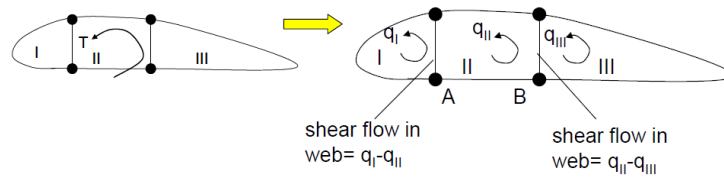
Figure 17: Front and aft spar thickness from root to tip

For this situation there are 2 governing equations [42]:

$$Torque = 2A_1q_1 + 2A_2q_2 + 2A_3q_3 \tag{8}$$

$$\left(\frac{\delta\theta}{\delta z}\right)_i = \frac{1}{2A_iG}\oint_s \frac{q_s}{t}ds \tag{9}$$

Where q is the shear flow, A the cell area, t the wall thickness and G the shear modulus. Equation 9 holds for all 3 cells, and the rate of twist $\frac{\delta\theta}{\delta z}$ is the same for all 3 cell [42]. This results in a system of 4 equations with 4 unknowns: the 3 shear flows and the rate of twist. This is solved in Matlab by setting up this system of equations in a matrix:

$$
\begin{pmatrix}
2A_1 & 2A_2 & 2A_3 & 0 \\
\frac{1}{2A_1 G}\left(\frac{l_1}{t_2}+\frac{h}{t_1}\right) & -\frac{1}{2A_1 G}\left(\frac{h}{t_1}\right) & 0 & -1 \\
-\frac{1}{2A_2 G}\left(\frac{h}{t_1}\right) & \frac{1}{2A_2 G}\left(\frac{2h}{t_1}+\frac{0.9chord}{t_2}\right) & -\frac{1}{2A_1 G}\left(\frac{h}{t_1}\right) & -1 \\
0 & -\frac{1}{2A_3 G}\left(\frac{h}{t_1}\right) & \frac{1}{2A_3 G}\left(\frac{h}{t_1}+\frac{l_3}{t_2}\right) & -1
\end{pmatrix}
\begin{pmatrix}
q_1 \\
q_2 \\
q_3 \\
\frac{\delta\theta}{\delta z}
\end{pmatrix}
=
\begin{pmatrix}
Torque \\
0 \\
0 \\
0
\end{pmatrix}
$$
$$(10)$$

In the matrix system in equation 10 q_i are the shear flows, t_2 is the skin thickness, t_1 is the spar thickness, h is the spar height and l_1 and l_3 are the section lengths of the first and third cell. This system of Ax = b is solved for all 100 sections in Matlab simply by setting x = A\b.

5.4.2 Wing structure results

The wingbox has 2 spars, 1 at 0.25c and the other at 0.70c. They are C-shaped beams where the length of the top and bottom flange are 35 percent of the height. The thickness of both spars varies between the root and the tip and can be found in figure 18. As can be seen the highest spar thickness is at the root with a thickness of 0.139 m, and the lowest thickness is found at the tip with only 2 mm of thickness. The skin of the wing is the same over the entire wing, and has to be 10 mm.

As carbon fibre has a relatively high Youngs modulus but a low shear modulus, it was found that the rate of twist limitation is harder to meet. The maximum loading case with all safety factors and loading factors included now causes a rate of twist of 9.6°, slightly below the design limit. The deflection goes up to 6 meters or slightly below 10 percent of the wingspan, far below the limit of 15 percent.

The best shape of the stringers was found to be a U-shape with all 3 sides equally long at 5 cm. The thickness is then 3 mm, resulting in a stringer area of 4.5 cm^2. The number of stringers on the top and bottom skin is kept the same for simplicity. At the root there are 42 stringers, which gradually reduces to 10 at the tip. The stiffener spacing at the root is 0.5 m and linearly reduces to 0.22 metres at the tip. As discussed in chapter 8 the stringers and stiffeners are made from a different material than the skin and spars. They are attached to the skin and spar webs using adhesive bonding.

The optimal rib spacing throughout the wing also varies. The lowest spacing of 0.75 metres is found at the root. This increases almost linearly to 1 metre at 40 percent of the wing, and to 2 metres at 75 percent of the wing. For the last 25 percent of the wing this distance is kept constant at 2 metres.
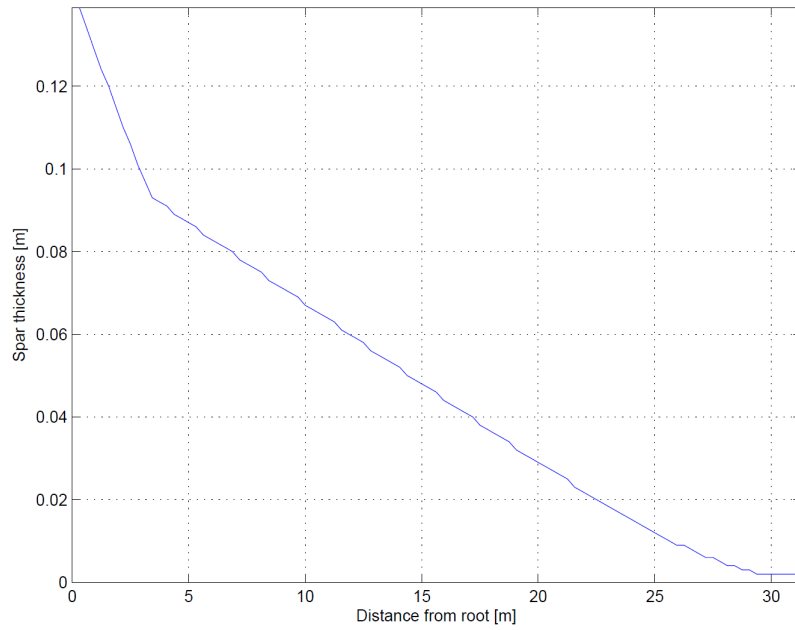
Figure 18: Front and aft spar thickness from root to tip.

5.4.3 Validation

The calculated numbers and dimensions allow for a calculation of the structural weight of the wing. The density is 1550 kg/m^3 for which the total weight is 13.9 tonne for 1 wing, bringing the total weight to 27.8 tonne. To validate these results a comparison is made with the Boeing 747-400. The wings of the 747-400 weigh 43.1 tonne for a MTOW of 397 tonne [44]. Both the 747-400 and the Jumbo City Flyer have a wing which weighs 11 percent of their MTOW for the wing structural weight. The estimate is that the structural weight of the Jumbo City Flyer can still be brought down, which means that using composites creates a lighter wing. An analysis in the Matlab program on an aluminium wing, with a SF of 1.5, confirms this as the weight is over 50 percent higher with this method.

A sensitivity analysis was performed on the wingspan. Using a range of wingspans it was found that a decrease of 5 percent in the wingspan yields a weight of 12.8 tonne for 1 winghalf, a reduction of 11 percent. This would however have a negative effect on the aspect ratio and hence on the L/D. Finding the optimum ratio between weight and the aspect ratio is an extensive iteration cycle that should help improve the performance of the Jumbo City Flyer.

5.5 Control system

For the Jumbo City Flyer, it was decided to make use of an irreversible control system. This system is lighter than a reversible control system and provides better handling characteristics. Also, this type of control system is less affected by flutter, cable/rod stretching and friction. The drawbacks of an irreversible control system are a higher cost and it is less maintenance friendly compared to a reversible control system [31]. Also a trend to use this type of control system within recent aircraft

such as the Boeing 787 and the Airbus A380 has been observed, proving that the advantages outweigh the disadvantages.

It was decided to make use of a so-called fly-by-optics system, driving self contained electro-hydraulic actuators. This control system does not require a large amount of hydraulic fluid and is thus lighter and easier maintainable than traditional control systems Additionally unlike fly-by wire this system is immune to electro magnetic interference [31]. From the perspective of maintenance, it was decide to use this system for both primary and secondary control surfaces.

For redundancy purposes the control system will consist of 3 independent circuits, each driving 1 of the 3 electro-hydraulic actuators per primary control surface. In section 7.4 it will be explained how these 3 systems are powered. The circuits are separated such that the impact of failures such as structural failure, engine separation or terrorist attacks are minimal.

6 Aerodynamic characteristics

The design and 2D characteristics of the wing are described in section 5. This chapter will focus on the 3D characteristics of the aircraft. The important aspects of the wing are:

- $C_{L,clean} = 1.76$
- L/D = 15.4
- High lift devices used are single fowler flaps

The lift in clean configuratin is determined in section 6.1. The high lift devices are sized in section 6.2. It also shows the lift curve for the Jumbo City Flyer in clean configuration and for landing. The incidence and twist angle are briefly discussed in sections 6.3 and 6.4. Section 6.5 will discuss the calculation of the lift over drag ratio during cruise.

6.1 Determination of total lift in clean configuration

The 2D lift curve of the airfoil selected for the Jumbo City Flyer wing is shown in section 5.1.3, figure 13. Due to 3D effects, the lift curve for the wing will look different. The requirement with respect to lift is that the maximum lift coefficient of the aircraft should be 1.7, following from the design point described in section 3.3. The lift force provided by the wing should be 1.05 times this value, according to Roskam [33], to account for negative lift from the tail needed to balance the aircraft. So, the maximum lift coefficient should be 1.79.

A method on how to generate the CL-α curve on the basis of a Cl-α curve is presented in chapter 12 of Raymer [45]. Raymer is preferred above Roskam because this method is also taught in classes at this faculty and therefore this method is more familiar to the authors. To construct the lift curve, 4 factors need to be calculated, they are listed below:

- The angle of attack at which no lift is created: $\alpha_{0,L}$
- The slope of the lift curve: $C_{L,\alpha}$
- The maximum lift coefficient: $C_{L,max}$
- The stall angle: α_s

The angle of attack at which no lift is created is a characteristic of the airfoil, being -4.7 degrees.

The slope of the 3D lift is graphed using equation 12.6 from Raymer [45], copied below as equation 11.

$$C_{L,\alpha} = \frac{2\pi A}{2 + \sqrt{4 + \left(\frac{A\beta}{\eta}\right)^2 \left(1 + \frac{\tan^2 \Lambda_{0.5C}}{\beta^2}\right)}} \frac{S_{exposed}}{S_{ref}} F \qquad (11)$$

In this equation, the correction for the Mach number β and the fuselage lift factor F are given by equations 12 and 13, respectively. The efficiency of the airfoil η is

around 0.95. The exposed area of the wing is established from the scale drawing of the Jumbo City Flyer aircraft made in CATIA.

$$\beta = \sqrt{1 - M_\infty^2} \tag{12}$$

$$F = 1.07(1 + d_{fus}/b_{wing})^2 \tag{13}$$

The maximum lift coefficient of this wing can be computed with equation 12.16 from Raymer [45], copied as equation 14:

$$C_{L,max} = \left[\frac{C_{L,max}}{C_{\ell,max}} \right] C_{\ell,max} + \Delta C_{L,max} \tag{14}$$

The maximum lift coefficient of the airfoil is known and the other 2 factors can be constructed from figures 12.8 and 12.9 in Raymer.

The stall angle is computed using equation 15, which is equation 12.17 from Raymer [45]. The only value unknown in equation 15 is $\Delta\alpha_{C_{L,max}}$, which is a statistical value found in figure 12.10 of Raymer.

$$\alpha_s = \frac{C_{L,max}}{C_{L,\alpha}} + \alpha_{0,L} + \Delta\alpha_{C_{L,max}} \tag{15}$$

With these 4 parameters known, the lift curve is constructed. The result is shown in figure 19 along with the lift curve for the flapped wing. It is important to note that the maximum lift coefficient is 1.76, where 1.79 is needed. Designing a wing that provides this lift was not possible without a too large increase in drag.

It is thought that it is realistic that the value of 1.76 is achieved. Wings of modern aircraft have dozens of different airfoils sections throughout the span of the wing and are known to have gone through a very detailed optimisation program. This optimisation is not started for this wing, due to the time constraint. If the above requirement cannot be met, the stall speed in clean configuration should be increased from 76 m/s to 77 m/s.

6.2 Sizing of the high-lift devices

The maximum lift coefficient during take-off and landing of 2.1 and 2.3 respectively are obtained from the design point. Analogous to the clean configuration, the wing should again provide for 1.05 times that value, meaning the maximum lift coefficients become 2.21 and 2.42 for take-off and landing, respectively.

The wing in clean configuration does not produce enough lift, so there is a need for high-lift devices. In this section it is estimated that the airfoil is improved such that it can generate a lift coefficient of 1.79 in clean configuration. Resulting in an increase in lift coefficient (ΔC_L) of 0.63.
To size the high-lift devices, the method presented in chapter 12.4 of Raymer [45] is followed. It is the same method as presented during the lectures on wing design for the course AE2101. ΔC_L is presented in equation 16:

$$\Delta C_{L,max} = 0.9 \Delta C_{\ell,max} \left(\frac{S_{flapped}}{S_{ref}} \right) \cos \Lambda_{hinge-line} \tag{16}$$

In equation 16 , $\Delta C_{\ell,max}$ is a characteristic dependent on the type of flap used. Values are indicated in table 12.2 in Raymer. The hinge line of the flap has a nearly straight line, making it safe to assume that $cos\Lambda_{hinge-line}$ equals 1. Results to fulfill the requirement on lift are stated below:

- Single Fowler flaps are used.
- The wetted area affected by the flaps is 47 percent of the wing area.
- The flap chord is 25 percent of the wing chord.
- The location of the flaps on the wing is between 3.1 metre and 16.3 metre from the centre of the wing or from 0.1 b/2 to 0.52 b/2

To construct the flapped wing curve, the values for $C_{L_{\alpha,flapped}}$, $\alpha_{0,L}$, and the stall angle need to be determined.

An equation for the change in zero lift angle of attack is given by equation 17, taken from Raymer [45], where $(\Delta \alpha_{0,L})_{airfoil}$ is typically -15 degrees in landing configuration:

$$\Delta \alpha_{0,L} = (\Delta \alpha_{0,L})_{airfoil} \frac{S_{wf}}{S} \cos \Lambda_{hingeline} \tag{17}$$

The stall angle can again be computed by equation 15 and $C_{L_{\alpha,flapped}}$ is found according to equation 18:

$$C_{L,\alpha,flapped} = \frac{S'}{S} C_{L,\alpha,clean} \tag{18}$$

In this equation, S$'$ is the wing area with extended flaps. For this calculation, it is assumed that the Fowler flaps, when fully deployed, increase the chord of the airfoil by 15 percent.

The wing has been sized for clean configuration and landing. A check is performed to see whether the take-off requirement can also be met. Raymer states that 60-80 percent of the ΔC_L, can be accounted for during take-off. Reason for this is that flaps are only partially deployed. An increase of 67 percent of the extra lift needed for landing fulfills this requirement for take-off . That is satisfactory. Wind tunnel tests will have to be performed to check the actual performance on scale models to verify the results obtained in this section. Note that there is enough place on the wing to increase the wetted area from the flaps. Another possibility to increase the lift is to add leading edge devices.

The sizing of the high-lift devices finalises the wing design. The lift polar for both the clean and the flapped configuration of the Jumbo City Flyer are given in figure 19. An overview of the wing planform was given in figure 10.
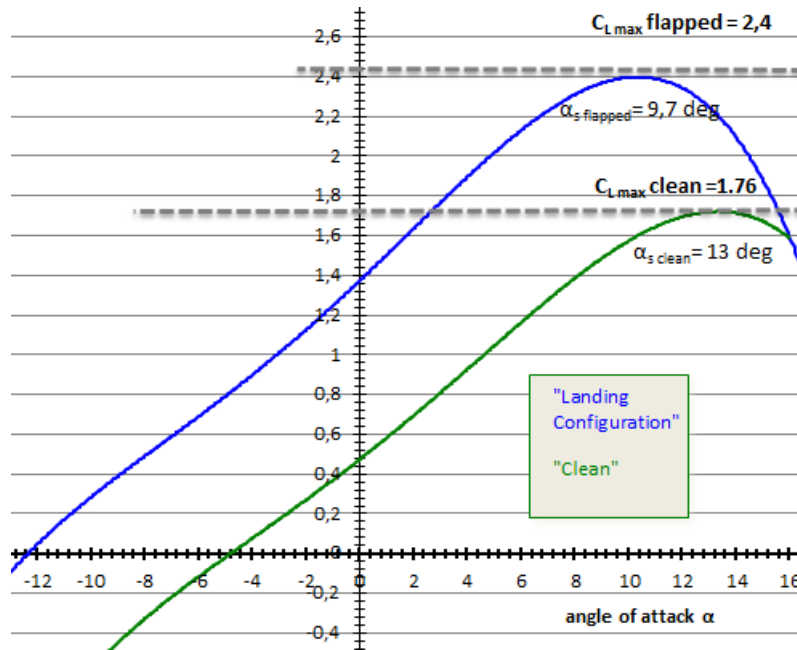
Figure 19: Lift curve for the Jumbo City Flyer

6.3 Incidence angle

During cruise, the aircraft will have a lift coefficient of around 0.7. This relates to an angle of attack of 3 degrees, as can be seen in figure 19. The wing will thus be mounted with an incidence angle of 3 degrees, to have the fuselage in a horizontal position.

6.4 Twist angle

The possibility of having a twist angle is not investigated. More advanced programs and preferrably wind tunnel tests have to be used to investigate the best choice.

6.5 Determination of drag

At this point, the whole aircraft is sized. A complete drawing is available in CATIAThis makes a first analysis on drag characteristics possible. For this, the method in Roskam [33] is followed. It is preffered over the method of Raymer [45] because it is more elaborate. More factors are required to construct the drag characteristics. To compute the total drag of the aircraft in clean configuration, 5 factors are calculated, listed below:

- The drag of the wing.
- The drag of the fuselage.
- The drag of the nacelles and the propellor of each engine.
- The drag of the empennage.
- The trim drag.

A drag polar cannot be constructed with this method, because it is only valid for the linear part of the lift curve. The drag coefficient during cruise is found to be

0.046, making the L/D value during cruise 15.4. This is too low for a final design. Roskam [33] states that modern commercial airplanes have L/D values ranging from 14 to 18. It is noted that the Roskam series was written in the 1980's and that the Boeing 787 and Airbus A380 have L/D values in cruise of up to 20 [46, 37, 47]. So, optimisation has to be performed on this subject.

While designing, little attention has been paid to minimising the drag, it is only constructed as last step. For future investigation, the design should be updated while paying attention to increasing L/D by minimising drag. This could either be done by performing windtunnel tests, but using advanced computational fluid dynamics methods are also an option. The application of winglets is another option to investigate.

6.6 Verification of results

The method proposed in Roskam to find the lift curve for 3D characteristics is an elaborate and time-consuming method. To verify the results in this section, it should be followed and the results should be within 10 percent. Due to a lack of time, this is not done. The fact that Raymer is a respected source within the aerospace community and the fact that the method used is taught in a class at this faculty is considered a good enough verification. Validation of the result should be done by testing the wing in a windtunnel.

The method of Roskam to determine the drag is verified with the method of Raymer. The same parameters are applied into the equation of Raymer as those that were used for the Roskam method. Both methods give almost the same $C_{D,0}$, with a difference of less than 4 percent. The methods differ significantly in the calculation of the Oswald span efficiency method, e. The equation of Roskam gives a value of 0.92, where the method of Raymer gives a value of 0.76. Torenbeek [36] does not offer a method on how to obtain e. This is something that needs more research in the future of this project because the effect on the drag due to lift is very noticable. An Oswald efficiency factor of 0.76 gives a L/D of 14.6, where an e factor of 0.92 gives an L/D of 16.0. In section 6.5, the value of 0.85 has been used.

To validate the results of section 6.5, windtunnel tests should be performed.

7 Propulsion and power

This section shows the design process for all parts of the aircraft that power it during the different phases of the mission. It also details the choice of fuel and its advantages and disadvantages, as well as the fuel system required. The Jumbo City Flyer will run on LNG as fuel, and uses 4 turboprops with a required power of 13,300 kW each.

7.1 Engine performance

For the Jumbo City Flyer to take off 53,300 kW of power needs to be provided by the engines. That means that each of the 4 engines need to provide around 13,300 kW of power. The only engine found capable to provide that much power is the Kuznetsov NK-110. However, this is a contra-rotating turboprop, a type of turboprop that has been disregarded with noise levels in mind. No other turboprop currently exists that can provide that amount of power, but looking at how the power available for turboprops has developed over time, it is expected that an engine can be developed that is capable of providing that power by 2025.

It is expected that an engine capable of providing the power required for the Jumbo City Flyer will be close to the most powerful turboprop of its time. Currently, the Europrop TP400 is the most powerful turboprop in Western Europe and America, so the TP400 is used as a reference for calculation purposes where necessary. The engine able to fly the Jumbo City Flyer needs an increase of 37 percent in power compared to the Europrop TP400.

The 53,300 kW power requirement is based on the take-off weight and the W/S-diagram. This is the take-off power requirement. However, the aircraft will need to provide a different amount of power to fly during cruise. Assuming steady flight, this value is calculated using the lift force and lift-to-drag ratio as specified in chapter 6.5. With this, it is found that the 4 engines need to provide 27.5 MW of power, so 6.87 MW each, to keep flying at a constant height and speed. The placement of the engines has been treated in section 3.2.3.

7.1.1 Engine control system

For the control of the Jumbo City Flyer's engines, it was decided to use a so-called full authority digital engine control (FADEC). Based on a power setting chosen by the pilot, this system automatically controls ignition, fuel flow, prop setting and allows for automatic start-up. As less engine parameters require the pilots attention, their workload is decreased. Also, the engine is protected for out of limit power requirements by the pilot. Concluding the FADEC increases overall efficiency and can increase safety, for instance by giving full power in case of stall. It needs to be noted thatthis system increases the aircraft's complexity. Also, since FADEC-failure results in immediate engine failure, redundancy in the form of multiple FADEC's need to be provided.

7.2 Power extraction requirements

During all parts of the mission of an aircraft, a certain amount of electrical, mechanical and pneumatical power is required, which are called the power extraction requirements. The estimation of these amounts was done using Roskam [33] and the results are listed in table 13.

Table 13: Power extraction requirements for cruise

Power requirements	Power [kW]
Electrical power extraction	28
Mechanical power extraction	163
Pneumatic power extraction	564
Total power extraction	756

For the electrical power extraction requirement it was assumed that the Jumbo City Flyer has the same requirement as a civil jet transport would according to Roskam [33].

The mechanical power extraction requirement consists of the mechanical power required for the fuel pumps and hydraulic pumps. The calculation was done with the method for piston-propeller driven aircraft, as is suggested by Roskam [33]. The value for the fuel pump efficiency is taken from Roskam [33], whereas the specific fuel consumption is taken from the Europrop TP400.

Adjusted data from the Boeing 767 is used for the hydraulic power extraction requirement, as this is the closest fit to the Jumbo City Flyer that data was found for. The data was adjusted to reflect the fact that the aircraft is a larger aircraft than the Boeing 767.

7.3 Auxiliary power units

The auxiliary power units of an aircraft are to provide energy for functions other than propulsion. They are used to start the engines and to power accessories and run systems for preflight checks. They can be used in emergency situations in the case of an engine failure.

It is expected that the aircraft will require about the same amount of power from the APU as a Boeing 747-400, so at this stage it is assumed that the Jumbo City Flyer will use APU's similar to the 2 PW&C PW901A's used on the Boeing 747-400, so these are taken as reference. They provide 90 KVA each, so this adds up to 180 KVA, or 144 kW.

7.4 Electrical system

The electrical system will provide power for lightning, flight instruments and avionics, flight controls, passenger accommodations and engine start. The primary power source for the Jumbo City Flyer will be 4 generators, each driven by 1 of the engines, providing AC. A generator circuit breaker will be placed in the connection

between the generators and the alternating current (AC) buses. Finally a converter will be placed in between the 4 AC buses and the 4 direct current (DC) buses.

A battery will provide the aircraft of DC power when the engines are inoperative, while AC power will be provide by an APU in the tail. Additionally, the aircraft will get 2 provisions to connect up with ground power. In case of emergency a ram air turbine will provide power for the primary control surfaces and instruments.

As indicated above, an example of an electrical function is to power the lighting of the aircraft. The following types of lighting will be installed on the Jumbo City Flyer in the following way:

- White strobe lights and navigation lights on the wing tips
- 1 beacon light on the top and bottom of the mid-fuselage.
- 2 taxi lights in the nose gear.
- 2 landing lights in the nose gear and 2 at the wing root.
- 1 logo light on each side of the stabilizer
- Separate cabin and cockpit lighting

For further development of the electrical system the following guidelines have been formulated:

- Electric cables should be shielded to protect from lightning and interference from each other.
- Care should be taken to make all parts accessible for maintenance.
- Buses and wirebundles should be separated in order to limit impact, for example of uncontained engine failure
- The battery should be shielded from primary structure/passengers

7.5   Taxiing system

In the taxiing phase of the mission profile the aircraft engines are highly inefficient. In a 17 minute taxiing operation, a Boeing 747 consumes 1 tonne of fuel and emits 3.2 tonne of CO_2 [48]. This can greatly be reduced by adding electrical taxiing systems to the aircraft.

Several electrical taxiing systems exist, such as a taxi bot on the airport or an APU-powered electrical motor built into the landing gear. The taxi bot is able to perform the 17 minute taxiing mission, but only use 25 to 50 litres of fuel and emits only between 60 and 150 kg of CO_2 [49] and the built-in electrical motor promises to reduce fuel consumption by 70 to 85 percent [50].

Implementing such a system means that an aircraft can have its engines turned off during all ground operations up to a few minutes before take-off. This not only reduces the fuel used, but also the foreign object damage incurred during taxiing, as well as lowering the noise. For the Jumbo City Flyer, this is especially valuable, as its mission consists of short range flights, meaning the time spent on the ground is relatively long and reducing costs of ground operations has a great impact. Combining all this, the taxi bot is valuable addition for reducing the environmental impact and costs of the aviation industry, and specifically, the Jumbo City Flyer.

7.6 Fuel analysis

The fuel selected for the Jumbo City Flyer is liquefied natural gas (LNG). This type of fuel is stored in slightly pressurised tanks at -162° Celsius as that is slightly below its boiling temperature. Regular fuel tanks are not designed for these temperatures, so specialised tanks will need to be used. This will increase the weight of the aircraft. However, the advantages offered by the use of LNG were found to offset the possible disadvantages. Both are listed below.

Advantages of LNG

- Lower fuel weight compared to conventional fuel.
- Reduction of CO_2-emissions between 74 and 90 percent.
- Reduction of NO_x-emissions around 85 percent.
- Reduction of the emission of reactive hydrocarbons between 70 and 93 percent.
- Usage can increase engine thermal efficiency.
- Fuel cost of LNG is lower than that of conventional jet fuels.

Disadvantages of LNG

- Requires pressurised tanks to store the fuel, increasing aircraft weight.
- Airport facilities for tanking LNG are required.
- Increased storage space for LNG compared to conventional jet fuels.
- Requires insulation to keep the fuel cool, increasing aircraft weight.

In designing the fuel system, specific guidelines need to be observed. These are to ensure the proper functioning of the fuel system and to prevent safety issues. These guidelines are listed below:

- Tanks and lines should not rupture in easily survivable crashes.
- Fuel lines should be located away from easily damaged structural parts.
- Fuel lines should be kept away from equipment that can generate sparks.
- No fuel lines are to be placed near the landing gear well.
- Tanks are kept away from engines, if necessary dry bays and firewalls are implemented.
- Vents are located such that fuel and fuel vapour remains clear of the aircraft in all cases.
- Fuel quantity sensors are located such that fuel quantity can be measured throughout entire mission.
- Fuel pumps are located such that fuel can be distributed to any engine for any attitude.
- The use of tip tanks is avoided.
- Refueling areas are designed such that explosion danger is minimised.

7.6.1 Cryogenic storage

To prevent the LNG from warming up too much, thermal insulation is required for which 2 materials are considered. The 2 considered insulators are silica aerogel [51] and phenolic foam. The former is the best insulator available apart from a vacuum, but this is very expensive [52]. To determine whether a single material or whether a combination is the best option, a calculation was made using all relevant characteristics.

The relevant characteristics are listed in table 14, and following an analysis it was decided to use a mix of 10 percent of aerogels and 90 percent of phenolic foam as insulation. These percentages are based on the surface the respective materials are used to cover. By using this 90/10 combination, the most critical parts, e.g. near the engines since these generate a lot of heat, are coated in aerogels and are extra insulated. The insulating layer is wrapped in carbon fibre to allow for a maximum operating pressure of 5 bar.

An estimation what the result of the 90/10 combination is has been made and the results can be found in table 14. This was done using current prices for the silica aerogel, though it is noted that prices for those are rumoured to drop in the near future [53].

Table 14: Result of the 90/10 combination for Aerogel and phenolic foam.

	Aerogel	Phenolic foam	Total
Thermal conductivity [W/m/K]	0.004	0.019	-
Volume [m^3]	0.755	33.97	34.7
Thickness of insulation [cm]	1	5	-
Density [kg/m^3]	2	38	-
Price [$/m^3]	1,000,000	334	-
Total weight [kg]	1.5	1291	1293
Total price [$1000]	755	11.7	767

The thickness of the insulating layer varies due to varying tank sizes, but only a few millimetres is needed at maximum. By sizing the fuel tanks this way, the heat increase due to the heat flux is limited to values deemed acceptable, being 900 J/s on the ground at 40° Celsius and 550 J/s during cruise per 2.1 m^3 fuel tank. The formula that was used is formula 19 from 'Thermodynamics - an Engineering Approach' [54]. Where $\triangle$T is the temperature difference, k the thermal conductivity, A the area covered with the insulator, and t the thickness of the insulation layer.

$$\frac{\delta Q}{\delta t} = \oint_s \overrightarrow{\triangledown} Tk dA = \frac{0.1 \triangle T k_{aerogel} A_{aerogel}}{t_{aerogel}} + \frac{0.9 \triangle T k_{foam} A_{foam}}{t_{foam}} \qquad (19)$$

The available room for the fuel tanks was calculated using the space available in the wingbox between the ribs, as calculated in chapter 5.4. The tanks located in the wingbox on average have a height of 0.7 m, a width of 1.0 m and a depth of 3.1 m. Assuming those values, 64 fuel tanks would be required, 46 of which fit in the wings. This means that 88 m^3 is stored in the wings and 49 m^3 of fuel is stored in the fuselage, on the cargo deck. This results in 6 spanning metres of fuselage filled with the centre fuel tank.

The fuel does not need an active cooling system because of auto-refrigeration. The gas that is withdrawn is replaced as the liquid vaporises by absorbing heat from the remaining liquid and the vessel itself. Auto-refrigeration occurs when the gas is withdrawn at a rate so that cooling equals or exceeds the heat available from ambient sources [25].

With this combination of insulation materials, the temperature increase for a 3

hour flight, including taxiing and landing, is limited to about 5° Celsius, without considering auto-refrigeration effects. It is expected that between 1.2 and 1.4 percent of the total fuel weight will boil off during a 3 hour flight across 2000 km, from gate to gate because of this [26].

The boil-off gas would total, for all tanks combined, 50 g/s during cruise and 90 g/s on the ground at an ambient temperature of 40° Celsius. Since the LNG evaporates to normal natural gas, it expands with a factor of 610. This comes down to 2 litres of gas per tank per second, and 134 litres in total across all tanks. Since the fuel tanks can handle only a few bar of pressure, the added gas has to be removed. Attached to all tanks are pressure release valves which lead the gas to a central point. During cruise the APU can run on 20 percent of the boil-off gas, leaving 80 percent for the engines.

This means that on the ground the boil-off gas produced is too much to be used by the APU alone. This is solved in 2 different ways for the taxiing pre-flight and after the flight. Pre-flight the LNG is simply fueled to the aircraft at 3° Celsius below its boiling temperature. There is no serious boil-off for the first hour after tanking then and the main engines are running by that time.

For the taxi phase after the flight, the fuel will be boiling at 2 litres per second per tank. The handling of this is twofold. First, since the fuel tanks are approximately half empty at landing, there is a cubic metre per fuel tank available for the evaporated natural gas. For an average taxi run of 10 minutes this adds 1.2 m^3 of gas to the tank. This would raise the pressure in the gas to 2.2 bar. Adding a waiting line of 20 minutes at the airport, this becomes a pressure of 4.6 bar, still within working limits of the fuel tanks.

Secondly, a small refrigeration unit will be taken on board the aircraft to refrigerate some of the boil-off gas, while some of it can also be used by the APU. These 2 systems should allow for enough time to reach a gate at the airport from where the pressure release valves and jettison lines are connected to the airport's LNG refrigeration system to be able to re-use the boil-off. In the unlikely case that this is not enough the boil-off gas can be vented.

7.6.2   Fuel lines and pumps

The 64 smaller fuel tanks that are required are divided into 5 larger tanks. Of these, 26 tanks are grouped in 2 inboard units, the 20 smallest tanks are grouped in 2 outboard units, and the rest in 1 centre tank with a volume of 49 m^3. This means that the fuel tanks in the wing have connection lines through the ribs, 2 in the lower corners and 1 in the top middle to allow the fuel to flow through under all possible flight angles.

The fuel lines run underneath the fuel tanks in the wing. Connected to every main fuel tank are 2 pumps, bringing the total to 10 pumps. During normal operations only 1 pump is needed per fuel tank, so the second pump is there for redundancy.
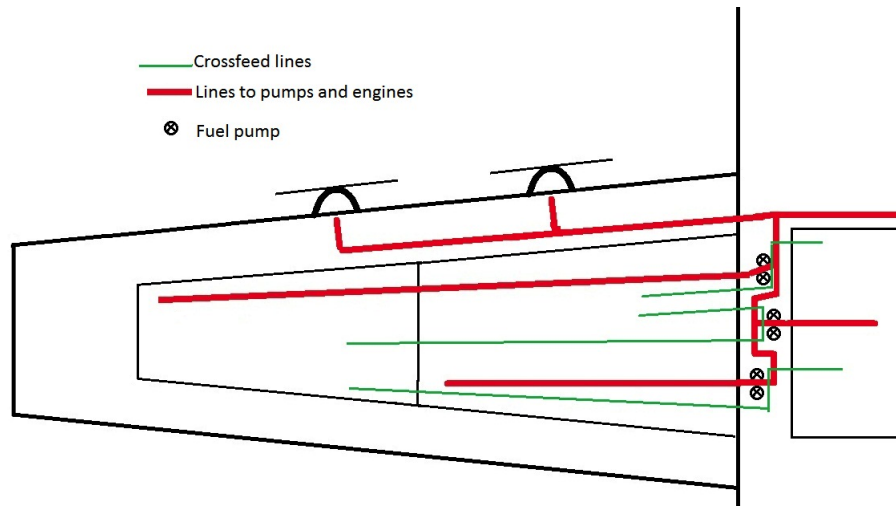
Figure 20: Schematic of the cryogenic fuel system

Since the fuel used is cryogenic, the risk of a freezing fuel pump is relatively high if water gets into the fuel lines.

Pumps specially designed to separate the engine part from the rotary vanes by using magnets will make sure that the engine part itself cannot freeze. From the pumps a series of valves control whether the fuel runs to the engines, to the other fuel tanks to solve imbalance issues, or to the outside air in case a fuel dump is needed. A schematic of the fuel system with the fuel lines, cross feed lines and the pumps can be seen in figure 20.

To allow boil-off gas to escape in case of an emergency the vents on top of the fuel tanks will be connected to the refrigerator, the engines, but also to lines that run to the outside air at the wingtips.

To protect all aircraft systems from freezing, all the fuel lines that transport cryogenic fuel will be lined with a thin layer of insulator. This has to be done as carbon fibre loses much of its strength when below -120° Celsius. With the current insulation system they will never be that cold.

7.7 Emissions

An aim of using LNG as fuel was to reduce the CO_2-emissions of the Jumbo City Flyer compared to the Boeing 747-400. Based on emission factors [27] and the fuel weight, the amount of CO_2 that is emitted for a flight by the Jumbo City Flyer was calculated and the same was done for the Boeing 747-400.

The method used to compare the performance of the Jumbo City Flyer with that of a Boeing 747-400 was to use the Breguet formulae to calculate the fuel used on a mission with a fully loaded aircraft carrying enough fuel to fly the mission and loiter for 45 minutes. The unknowns for the Boeing 747-400 were the amount of passengers, empty weight, payload weight, take-off weight and the lift over drag ratio. These were all found via different sources [55, 56, 57, 58] and implemented

into the Breguet formulae, with the range changed for each route of the 50 busiest routes the Jumbo City Flyer could perform. This was compared to data found from Fuelplanner [59] and an error margin of about 20 percent was found. This falls within the error range as expected from the Breguet formulae. The error margins are shown in figure 21.
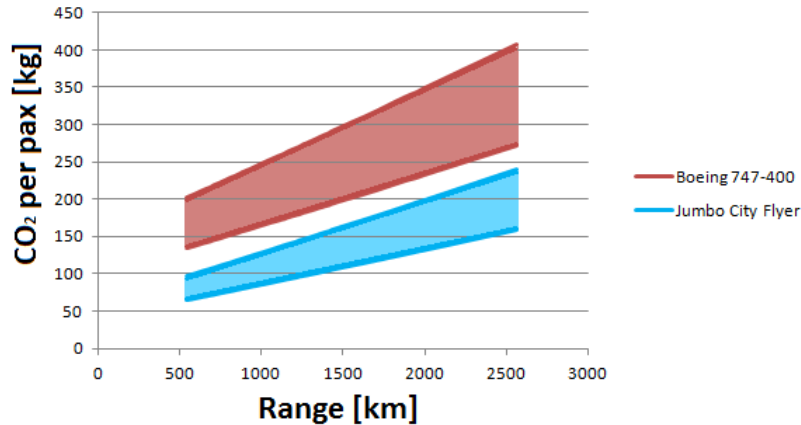
Figure 21: CO_2 emissions including uncertainties

Combined with the emission factors for both fuels, this resulted in the CO_2 emitted by the Boeing 747-400 and Jumbo City Flyer. This allowed the savings on emissions to be compared. These rang from 43 percent for a flight from Beijing to Hong Kong up to 52 percent for a flight from Los Angeles to San Francisco and can be seen in table 15, along with the route closest to the average distance of 1250 km as weighted by the amount of passengers.

Table 15: Comparison of CO_2-emissions of a Boeing 747-400 and Jumbo City Flyer on selected flights.

Flight	Distance [km]	CO_2 emitted [tonne]		Emitted CO_2/pax [kg]		
		B747-400	Jumbo City Flyer	B747-400	Jumbo City Flyer	Reduction [%]
Los Angeles - San Francisco	543	64.1	41.6	169	81	52
Narita - Incheon	1256	86.1	62.7	228	122	47
Beijing - Hong Kong	1991	110	84.9	290	165	43

7.7.1 Emission reduction contributors

A comparison between the Jumbbo City Flyer and the 747-400 shows 4 important contributors to the reduction of CO_2-emissions. The total theoretical optimal CO_2 reduction is calculated to be 80 percent during the cruise phase of the mission and the contribution to this 80 percent of each can be seen in figure 22. The method of calculation is to take the 747-400 as a starting point and change a certain parameter to see how this would change the emissions, based on the ceteris paribus principle, i.e., a single parameter is changed and everything else stays the same, e.g., the 747-400 now flies with LNG instead of Jet A-1, and the effect on the emissions is

analysed.
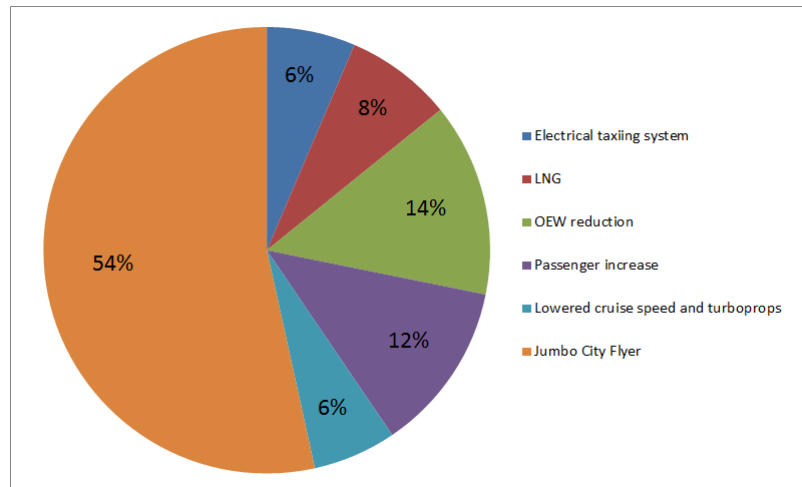
Figure 22: CO_2 reduction percentage per contributor.

A total of 4 factors which have the highest impact were analysed for the emission reduction: the fuel type, the operative empty weight reduction, the flight speed reduction, and the increased passenger payload.

Important to note is the fact that the individual reductions do not show directly in figure 22. For instance, reducing the flightspeed from Mach 0.85 to 0.62 would reduce the emissions per mission by 45 percent. The reason that the figure shows a reduction of 34 percent is the effect of diminishing returns when calculating percentage reductions, e.g., 2 reductions of 40 percent do not mean a total reduction of 80 percent, but of $1-0.6^2$, or 64 percent. The reduction caused by either is then 50 percent of the total.

The use of LNG instead of conventional fuel would reduce emissions by 25 percent [27], and as can be seen in the figure this would theoretically contribute to 18 percent of the total reduction. The next factor, the OEW reduction, causes a reduction based on the fact that a reduced required lift reduces the drag and therefore the engine output required. The same holds for the flight speed reduction, and both are based on the calculations in chapter 5. The last factor, the increased amount of transported passengers, causes an effect because the emissions are calculated per passenger taken per kilometre flown. Therefore taking more passengers on 1 of 2 otherwise identical aircraft results in a less CO_2 emitted per passenger km.

Emission calculations of the Jumbo City Flyer show that the total theoretical emission reduction of 80 percent is not met. This is due to a number of factors. First of all, the estimated reduction in this figure is for the cruise phase. On a typical mission of 1250 km this consists of 58 percent of the mission duration. The reduction during take-off, landing and climbing is less than the 80 percent due to, among others, higher propulsion levels. However, the use of an electrical taxiing system contributes in reducing the emissions by about 4 percent [60]. The fact that the 747-400 has a higher L/D than the Jumbo City Flyer currently also lowers

the reduction achieved by the Jumbo City Flyer, but with optimisation this should be solved. A third reason is that the fuel that is needed for a mission of the Jumbo City Flyer is still based on the Breguet range formulae wherein the fractions are all estimated on the safe side. This means that the actual fuel used by the Jumbo City Flyer will be lower, and hence the emissions too.

It should be noted that the 80 percent reduction is achieved using a modified Boeing 747-400. The total achievable reduction for the Jumbo City Flyer is different, but the result from the modified Boeing 747-400 is expected to be a close estimate of what reduction is possible for the Jumbo City Flyer in cruise. Also, after a sensitivity study was conducted into the effect of using Jet A-1 instead of LNG, it was confirmed that the percentages are similar, so the effects the contributors have in percent on the total reduction are roughly equal, e.g., using LNG on the Jumbo City Flyer as opposed to Jet A-1 lowers the emissions by 25 percent, and provides 18 percent of the reduction when considering all contributors.

7.8 Verification and validation

The engine that the Jumbo City Flyer requires has not been developed yet, but an estimated 37 percent increase in power is required. With regard to existing engines and the trend for increase in power for turboprops this is expected to be within reach before 2025. It is important that attention is paid to the sizing of the new engine. For now the Europrop TP400 has been used as reference, but in case these parameters change, e.g. the propeller diameter or engine weight, this needs to be taken into account in the design.

The method used to estimate the power extraction requirements was published in 1987 and derived from statistical relations for aircraft of the time. Also, the turboprop relations provided are for twin engine turboprops. The Jumbo City Flyer is a quadruple engine turboprop. It is therefore expected that when aircraft that have been designed since and the fact that the Jumbo City Flyer has 4 engines as opposed to 2 are taken into account, the statistical relations will change. For example, the electrical power extraction is likely to be higher, even if only considering in-flight entertainment systems. The power requirements are thus expected to be higher than calculated here. However, the results found were deemed acceptable with regard to the data available.

The emission analysis performed shows that the Jumbo City Flyer emits less CO_2 per passenger than a Boeing 747-400 on the same mission. This is as expected, as the Jumbo City Flyer is designed specifically for this flight.

8 Material selection and composition

The selection of the material is 1 of the most important and critical steps in the structural design process. If not done properly, the design may show poor performance, may require frequent maintenance and in the extreme case fail prematurely.

Due to time limitations the material selection process is only performed for 2 main structural components of the aircraft, the wing and fuselage structure. The structures consist of multiple elements like the wingbox, ribs, frames, stringers or stiffeners and skins. Since different loads are carried by these components, they are split up in 2 groups: plates/skins and stringers/stiffeners. The 2 materials are selected that are most suitable for both components.

First the most important material properties need to be investigated. Section 8.1 describes the process that was used to determine these properties. Then the selection process is treated in section 8.2. When the most advantageous materials are known, the feasibility of implementation is examined in section 8.3. Next, custom laminate configurations are created to optimise the properties per structural component. The results of the laminate material properties are presented in 8.4. Finally in section 8.5 an overview is given of the application of other materials in the design.

8.1 Driving material properties

The material selection process requires knowledge of the performance requirements of the structure and components. Table 16 shows the loading conditions and other required parameters for each of the structural parts.

Table 16: Loading conditions per structural part.

	Plates/Skins	**Stringers/Stiffeners**
Type of loading	axial, bending, torsion	axial
Mode of loading	static, fatigue, impact	static, fatigue
Service life	60,000 flight cycles	60,000 flight cycles
Operating environment	temperature: 203K - 313K; humidity conditions: 0-100%	temperature: 203K - 313K; humidity conditions: 0-100%

A service life in terms of flight cycles has been determined based on reference aircraft. FAR indicated that on average commercial aircraft are designed for 20,000 flight cycles [16]. However, a higher amount of cycles is considered for the Jumbo City Flyer, because the short range mission results in approximately 3 times as much load cycles per day. To maintain the same service life in years, the Jumbo City Flyer is designed for 60,000 flight cycles. Next to the service life, the manufacturing processes for production and total cost, including manufacturing and assembly, should be taken into account in the material selection process.

Considering these conditions, the most important material characteristics are listed in order of importance, ranging from most important to least, in table 17.

Table 17: Most important material properties.

Plates/Skins	Stringers/Stiffeners
Mass density	Mass density
Strength	Young's modulus
Young's modulus	Fatigue strength
Fatigue strength	Strength
Cost	Cost
Impact resistance	
Humidity resistance	

With the driving material properties determined, the selection process can take place. The method of selection and corresponding results will be discussed in the following section.

8.2 Selection process

Based on the important properties that are determined, a set of aerospace materials is compared. The comparison is performed in multiple selection stages. In the end, the material that passes all selection stages while having the lowest density is considered the best material choice for that specific structural component. The first stage of the stringers/stiffeners selection is shown in figure 23, which compares the modulus-density ratio, or material index, of all aerospace materials.
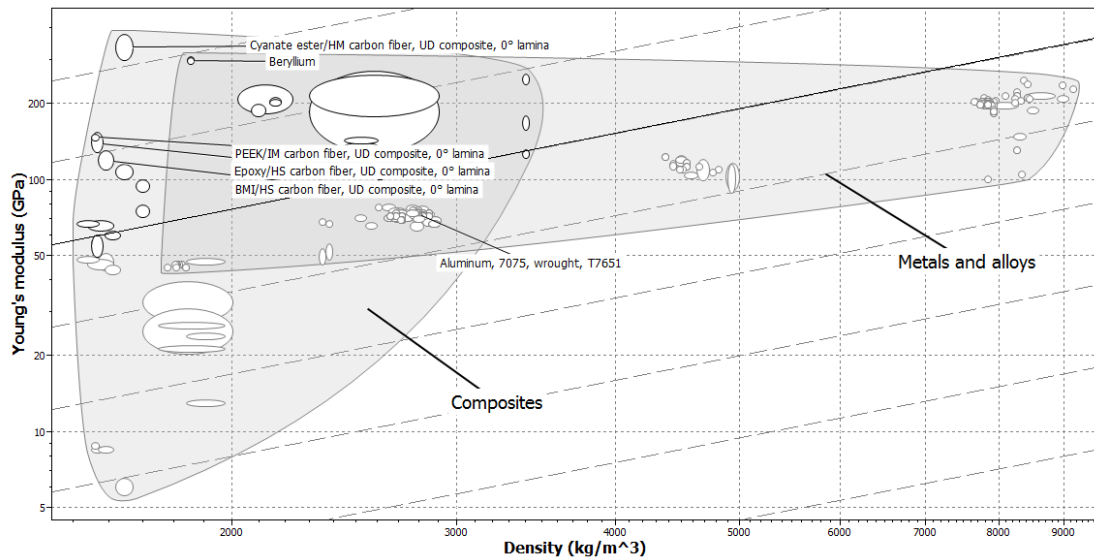
Figure 23: First selection stage for plates/skins.

A high material index is favourable for minimum mass design of the stringer/stiffeners. Materials with a high material index can be found in the upper-left corner of figure 23. The best results of the first selection stage are labelled in the figure. Additionally aluminium 7075-T651 alloy is indicated as a reference, since this is the alloy that is most used in the Boeing 747-400 for the earlier mentioned structural components.

As the figure shows, composite materials have relatively low density while maintaining high modulus compared to metals and alloys. This also applies for other important material properties. Table 18 shows a comparison of carbon/epoxy composites and conventional aluminium alloys for airframe applications [61].

Table 18: Comparison of carbon/epoxy characteristics compared to conventional aluminium alloys for airframe applications.

Weight reduction	Acquisition cost
Savings of 15-20%	Material cost increase
Cost of reduction $60-$100 per kg	Reduction due to high conversion rate
Reduction in number of joints	Reduction due to reduction in joints
	Fabrication cost generally increase
Performance	**Repair costs**
Smoother, more aerodynamic form	Reduction due to fatigue resistance
Improved aeroelastic properties	Reduction due to corrosion immune
More resistant to acoustic environment	Reduction due to fretting resistance
More resistant to service environment	Increase because of impact sensitivity
Improved fire containment	Increase due to material being prone to delamination
Improved crash resistance	

Better fatigue resistance is a very important advantage of composite materials, since many load cycles will occur during the service life of the Jumbo City Flyer. Other properties like resistance to acoustic environment are also important factors, since the use of turboprops will cause more noise and vibrations.

Completing the selection stages and considering the advantages of composite materials leads to the final material selection. epoxy HS/carbon fibre composite came out of the selection process as the best material for both the plates/skins as the stringers/stiffeners. For the stringers/stiffeners another laminate structure of the composite material will be used than for the plates/skins, since stringers and stiffeners will mainly carry axial loads, compared to combined loads for the plates and skins. This will further be explained in section 8.4. Now the material is selected, it should be first verified whether implementation of the material into structural parts is feasible.

8.3 Feasibility

Considering the customer requirement of the first test flight in 2025, the feasibility of implementing of epoxy HS/carbon fibre composite in structural parts should be considered. This is also important since the use of composite materials in large structural components is a relatively new concept in the aerospace industry. A trend showing the use of composite materials in aircraft is shown in figure 24.

As the figure shows, there has been an exponential increase in the use of composite materials since the year 2000. Introduction barriers like cost-intensive testing of composite materials in structural parts of the aircraft are now breached, which allows the usage of composite materials to grow even more in the coming years.
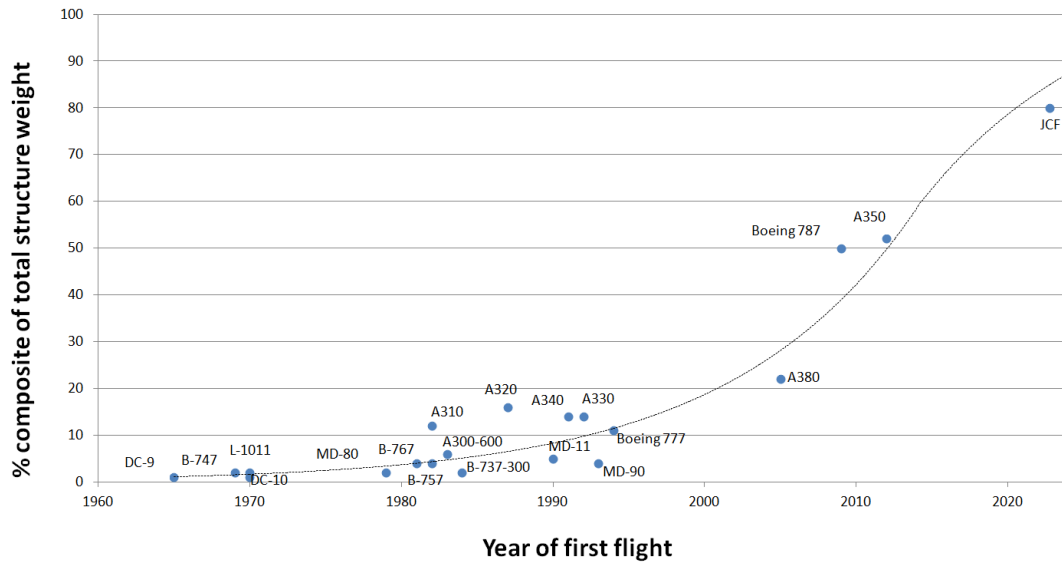
Figure 24: Use of composite materials in commercial aircraft.

Following the trend curve as indicated, it can be seen that in 2025 about 85 percent of the structural mass can be made of composite materials. Taking into account the many uncertain factors that may influence the technological development, it is estimated that approximately 80 percent of the Jumbo City Flyer's total structure mass can be made of composite materials.

8.4 Material composition and properties

Material properties for composite materials are only given for laminates with a 0° fibre orientation. Fibre orientation in each layer as well as the stacking sequence of various layers in a composite laminate can be controlled to generate specific physical and mechanical properties for the composite laminate. Using methods described in Baker [61] and Mallick [62], optimised laminate configurations have been calculated.

For the stringers/stiffeners a 0° laminate angle is the best option, since it is assumed that only pure axial loads are carried by these components. For the laminate design of the plates/skins it is determined that a laminate where half of the plies are +45° and -45° fibre angles, while the other half of the plies are unidirectional with 0° fibre angle. The resulting material properties for these laminates are shown in table 19.

Table 19: Custom laminate material properties.

Material property			Plates/skins	Stringers/stiffeners
Laminate configuration			$[(0°)_{2n}/(\pm45°)_n]_s$	$[(0°)_{6n}]_u$
Young's modulus	E_x	[GPa]	80.54	141.5
	E_y	[GPa]	23.96	10.65
Shear modulus	G_{xy}	[GPa]	20.80	5.02
Poisson's ratio	ν_{xy}		0.69	0.33
	ν_{yx}		0.21	0.25
Tensile strength	σ_x	[MPa]	1283	1955
	σ_y	[MPa]	259	46.6

These values will be used for the structural calculations further on in the report.

8.5   Other materials

Besides the main structural components, material selection for other aircraft components also needs to be considered. However, due to time limitations, these will not be determined through the same selection process as the main structural components, but are based on reference aircraft. Figure 25 shows the use of other materials throughout the design.
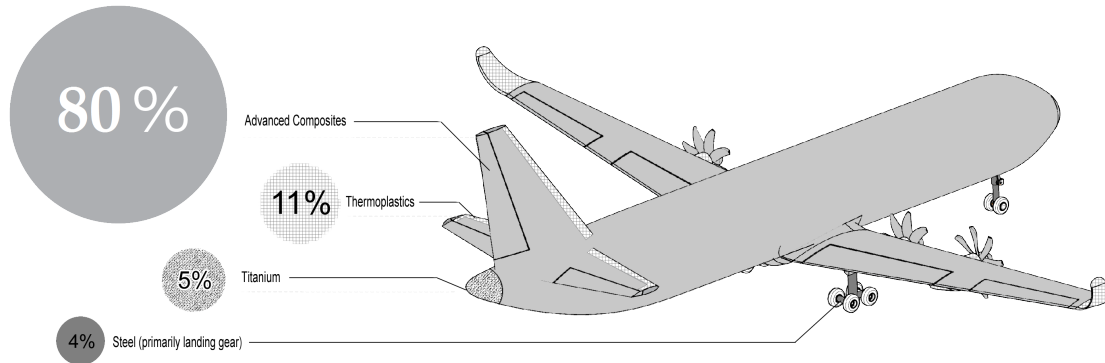
Figure 25: Use of materials in the Jumbo City Flyer.

As the figure shows, thermoplastics will be used at leading edges since thermoplastic materials have better impact resistance. Steel will be used in the landing gear to cope with high impact loads during landing. Also small amounts of conductive materials will be used in the main structural components. As the selected composite does not conduct electricity, a conductive liner will be implemented to protect the aircraft in case of a lightning strike.

9 Empennage design

Once the analyses on the wing and the weight and balance are done, the results can be used to design the empennage. The empennage is an essential subsystem for the stability and control of an aircraft. Therefore, it should be designed such that it contributes to meeting the requirements regarding stability and control [20] and amount to the following:

- Ensuring equilibrium of moments in steady flight.
- Restore this equilibrium relatively fast and with adequate damping after a disturbance.
- Generate forces to change the equilibrium in order to manoeuvre.

To design an empennage which meets these requirements for the most common flight conditions is what this chapter will deal with. It will be explained how the main results were obtained. These results consist of the optimal size of the horizontal and vertical tailplanes and the optimal lengthwise wing position from a stability and control point of view, which turned out to be 82.0 m^2, 71.4 m^2, and 49 percent along the fuselage, respectively. Furthermore, the control surface areas were found to be 20.9 m^2 for the elevator and 23.8 m^2 for the rudder. Further commuted parameters of the horizontal tail and vertical tailplane can be found in tables 20 and 21, respectively.

During the design process of the empennage emphasis was placed on the longitudinal stability and control. This is due to the fact that the longitudinal stability of an aircraft can be discussed and analysed independently from its lateral and directional stability, whereas the lateral stability and the directional stability are interdependent: a change in the sideslip angle affects the lateral behaviour and a change in the roll angle affects the directional behaviour.

Furthermore, longitudinal motion can be modelled relatively accurately by using simple derivations, while lateral and directional characteristics of an aircraft are more difficult to determine. This is because aerodynamic interference between the fuselage, wing and the empennage come into play [1].

Due to these reasons and to keep the analysis congruent with the rest of this report, only the longitudinal stability and control will be discussed in detail. This analysis can be found in sections 9.1 and 9.2. Nonetheless, to still ensure directional stability and control during operation an analysis on this, although not as elaborate, was still done by using the same principle, but by using a more concise method. This will be explained in section 9.4. The same has already been discussed for the lateral stability and control in section 5.3.

9.1 Static longitudinal stability

Different set-ups are possible for the aircraft during flight. These changes may be due to the following:

- Shifting of the c.g. in a certain range.
- Different high-lift device settings.

- Changing landing gear positions.

The empennage should be sized such that the aircraft remains statically stable in each configuration. With static stability it is meant that the aircraft has the tendency to return to its initial state after a disturbance. For longitudinal motion, then, it can be said that for an aircraft to be longitudinally statically stable it should be able to react to a disturbance in angle of attack by generating an opposite pitching moment to restore the initial state of equilibrium. It should be noted that whether the aircraft actually gets back to its initial state of equilibrium is a question of dynamic stability, which is not further assessed here as this is a sophisticated process which would require in-depth research.

The aircraft should be statically stable, both with the elevator and the horizontal stabilizer in a fixed condition, better known as the stick-fixed condition, as well as with the elevator and horizontal stabilizer in a stick-free condition, where it is free to trail with the wind [1]. In the analysis, however, only the stick-fixed condition was looked at, but very similar equations could be applied to the stick-free condition. The only difference is that in the stick-free condition the elevator deflection becomes a function of the angle of attack and should be accounted for properly.

As mentioned before, static stability is a measure of the tendency of an aircraft to return to its initial equilibrium. Taking the aforementioned definition of longitudinal static stability in account, the following condition should be met:

$$C_{m_\alpha} = \frac{\delta C_m}{\delta \alpha} < 0 \tag{20}$$

Hence, a positive change in angle of attack should generate a negative pitching moment coefficient. It can be shown that there exists a point on the aircraft in which equation 20 becomes equal to zero and beyond which it is greater than zero. This point is called the neutral point (n.p.). Since the aircraft would not create an opposite moment in and beyond this point anymore, the point about which the moments are taken should always stay in front of the neutral point. Usually the point about which moment are taken is the c.g. of the aircraft, which was also the case for this analysis. It should be noted that the definitions of all subsequently used symbols can be found in the the list of symbols .

The equation for the pitching moment is given in equation 21, where the last term indicates the contribution of the tail to C_m. If this equation is differentiated with respect to α, an expression for the neutral point can be found by setting $C_{m\alpha}$ equal to zero. Since in this case the c.g. would be exactly at the neutral point, x_{cg} can be replaced with x_{np}. $C_{m\alpha}$ can then be written as in equation 22.

$$C_m = C_{m_{ac}} + C_{L_{A-h}} \frac{x_{cg} - x_{ac}}{\bar{c}} - \frac{C_{L_h} S_h l_h}{S\bar{c}} \left(\frac{V_h}{V}\right)^2 \tag{21}$$

$$\frac{x_{np}}{\bar{c}} = \frac{x_{ac}}{\bar{c}} + \frac{C_{L\alpha_h}}{C_{L\alpha}}(1 - \frac{d\epsilon}{d\alpha})\frac{S_h l_h}{S\bar{c}}(\frac{V_h}{V})^2 \tag{22}$$

Where:

$$C_{L\alpha} = C_{L\alpha_{A-h}} + C_{L\alpha_h} \frac{S_h}{S}(1 - \frac{d\epsilon}{d\alpha})(\frac{V_h}{V})^2 \tag{23}$$

Emperic research [1] has shown that $\frac{x_{np}-x_{cg}}{\bar{c}}=0.05$ is a good value to choose as a stability margin, which ensures that the c.g. of the aircraft remains at least 5 percent of the mean aerodynamic chord (MAC) in front of the neutral point. This margin is imposed on equation 22, which can then be rewritten as:

$$\frac{x_{cg}}{\bar{c}} = \frac{x_{ac}}{\bar{c}} + \frac{C_{L\alpha_h}}{C_{L\alpha}}(1 - \frac{d\epsilon}{d\alpha})\frac{S_h l_h}{S\bar{c}}(\frac{V_h}{V})^2 - 0.05 \qquad (24)$$

Here, $(\frac{V_h}{V})^2$ denotes how the speed of the airflow at the tail is affected due to interference from the fuselage as compared to the undisturbed airflow at the wing. It was decided to mount the horizontal tailplane on the fuselage, as it is assumed that the large fuselage dimensions already provide sufficient space between the wake from the engines and the tail. Mounting the tailplane on the vertical tail would then only make the tail structure heavier and disturb the airflow on the vertical tail. From statistics it can then be found that $(\frac{V_h}{V})^2$ can be approximated by using a value of 0.85.

Subsequently, values for $\frac{x_{ac}}{\bar{c}}$, $C_{L\alpha_h}$, $C_{L\alpha}$, $\frac{d\epsilon}{d\alpha}$ and l_h can be obtained by using the geometric, weight and balance and aerodynamic parameters computed in sections 3.2.3, 5, 10.1, 10.2 and 6. In addition, results from the conceptual design stage [3] and statistical data fromTorenbeek [36] are made use of. For a more detailed description of the used method the reader is referred to references [1] and [36].
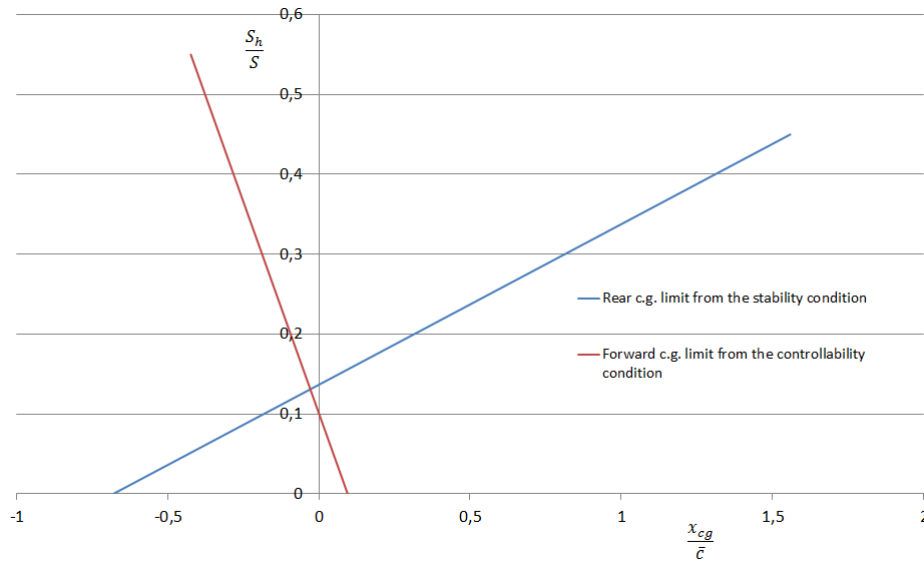
Figure 26: Stability and control restrictions on c.g. range.

Finally, if all required values are substituted in equation 24, it can be determined which horizontal tail area, S_h, is at least required for a certain c.g. position to ensure longitudinal static stability. If $\frac{S_h}{S}$ is then plotted as function of $\frac{x_{cg}}{\bar{c}}$, the rear c.g. limit is obtained, see figure 26. As can be seen, the requirement of static longitudinal stability constrains the most aft c.g. position allowed during flight. If the c.g. would shift any further to the aft, the stability limit of 0.05 would be violated and in the case that the c.g. would move even further, the neutral point

would be reached, meaning that the aircraft would no longer be statically stable. Therefore, the c.g. should at all times remain to the left of this line. It should also be noted that S_h increases as the c.g. moves further to the back, which is logical as the tail arm to counter the moment generated by the wing and fuselage decreases.

9.2 Longitudinal control at low speeds

After having determined the aft c.g. constraint, the forward limit needs to be computed in order to obtain the range in which the c.g. is allowed to travel during flight. The latter follows from the controllability of the aircraft.

If the aircraft is in an equilibrium state, the sum of the moments is equal to zero and the aircraft is said to be trimmed. This means that C_m equals 0 in equation 21. This equation can then be rewritten as:

$$\frac{x_{cg}}{\bar{c}} = \frac{x_{ac}}{\bar{c}} - \frac{C_{m_{ac}}}{C_{L_{A-h}}} + \frac{C_{L_h}}{C_{L_{A-h}}} \frac{S_h l_h}{S\bar{c}} \left(\frac{V_h}{V}\right)^2 \tag{25}$$

where $\left(\frac{V_h}{V}\right)^2$ and $C_{m_{ac}}$ are the same as in section 9.1 and C_{L_h}=-0.8 as a adjustable tail is assumed. The values for the remaining coefficients can be found by using a similar approach as in section 9.1. As the aim is to determine the most forward c.g. constraint, the sizing condition for which this is the case should be used. This is usually the landing configuration as the fuel mass is then at its lowest, which causes the c.g. to move forward. In addition, the flaps are fully deployed causing an even further shift and since the tail effectiveness decreases at very low speeds, it should still be possible to trim the aircraft. Therefore, the stall speed is used for the computation of the coefficients. For an elaboration on this the reader is referred to reference [1].

After substitution of the relevant values in equation, 25, $\frac{S_h}{S}$ can be plotted as function of $\frac{x_{cg}}{\bar{c}}$ in the same figure as before, see figure 26. This gives the forward c.g. limit from the controllability requirement. The resulting figure is called a scissor plot. As can be seen, the required horizontal tail area, S_h, increases as the c.g. moves forward. This is due to the fact that the flaps are deployed and the wing arm is also getting larger, requiring an even bigger tail force to counter it. Therefore, the c.g. should remain to the right of this line.
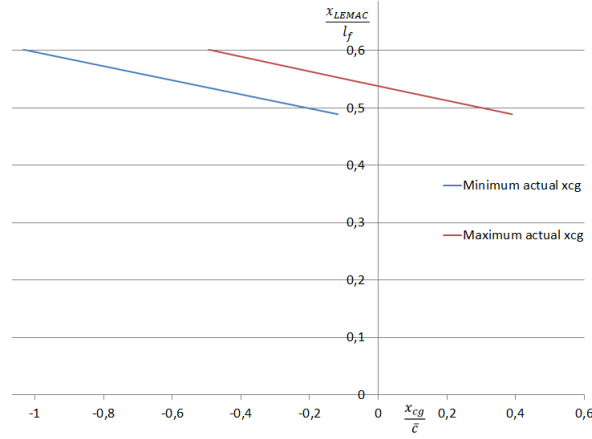
Figure 27: Shift of the c.g. range with wing position.

9.3 Preliminary design of the horizontal tailplane

Using the results from sections 9.1 and 9.2 the optimal size of the horizontal tailplane and the optimal location to position the wing can be obtained. It is known in what range the c.g. should remain for a certain S_h during flight to meet the requirements with respect to stability and control. In order to find the optimal S_h, it needs to be known how the c.g. range varies with the wing position. To determine this, the same procedure as described in section 10 can be applied to 2 additional wing positions.

The positions used are a 10 percent forward and a 10 percent backward shift of the wing, achieved by changing the leading edge position of the MAC. Subsequently, it is possible to plot the wing position, expressed in terms of the fuselage length, $\frac{x_{LEMAC}}{l_f}$, as a function of the $\frac{x_{cg}}{\bar{c}}$. The result can be seen in figure 27. Since the c.g. is expressed with respect to the MAC. a backward wing shift is equivalent to a forward shift of the fuselage and therefore the c.g. moves forward on the MAC The opposite is true for a forward wing shift.

Once the variation of the c.g. is known with respect to the wing position, the forward and rear limit, obtained from the control and stability conditions respectively, can be combined and aligned in the same figure. It should be noted that due to this, the maximum allowable c.g. range and the actual c.g. range are combined. The optimal solution for $\frac{S_h}{S}$ is then the minimum where the actual and the allowable c.g. range exactly coincide. To find this location, the vertical axis indicating the wing position was scaled as long as this minimum was found. This can be seen in figure 28.

Attention should be paid to the fact that the minimum $\frac{S_h}{S}$ can only be in the upper part of the scissor plot. Furthermore, the matching points of the 2 c.g. ranges must be on the same horizontal line, as they represent the c.g. limits for a specific wing location.
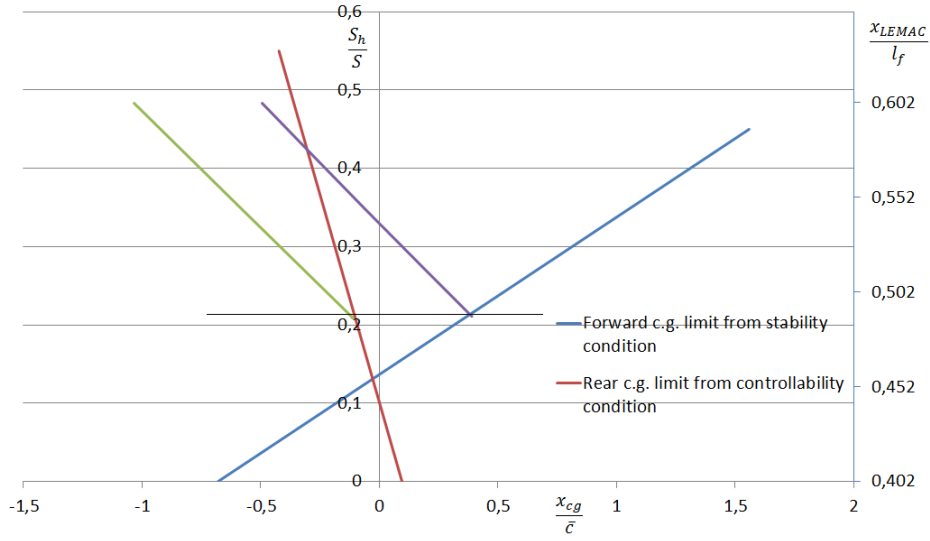
Figure 28: Matching of the actual c.g. range with the allowed c.g. range.

From $\frac{S_h}{S}$ and the wing area already determined, the tail dimensions follow. An overview of the results is given in table 20, where the coefficient S_e/S_h was obtained from statistical data.

Table 20: Final horizontal tail parameters.

Parameter	Value
$S_h/S[-]$	0.21
$S_h[m^2]$	82.0
$A_h[-]$	5
$b_h[m]$	20.25
$\lambda_h[-]$	0.5
$C_{root,h}[m]$	5.4
$C_{tip,h}[m]$	2.7
$\Lambda_{LE,h}[deg]$	12.4
$S_e/S_h[-]$	0.255
$S_e[m^2]$	20.9

9.4 Design of the vertical tailplane

In this final section of the empennage design, the design of the vertical tail is explained. The procedure used, is described in the AE3201 Systems Engineering and Aerospace Design lecture notes [1]. The most important vertical tail parameters are collected in table 21.

Table 21: Final vertical tail and rudder parameters.

Parameter	Value
S_v/S [-]	0.18
S_v [m^2]	71.4
A_v [-]	1.9
h_v [m]	11.6
λ_v [-]	0.3
$C_{root,v}$[m]	9.43
$C_{tip,v}$[m]	2.83
$\Lambda_{LE,v}$ [deg]	35
S_r [m^2]	23.8

The first step in sizing the vertical tail, is to determine the value for the abscissa in figure 29, which is 0.19 for the Jumbo City Flyer. Next, with the corresponding ordinate and statistical values [63], the tail and rudder area can be estimated.

Note that it was decided that the Jumbo City Flyer's rudder will be split. This is common for aircraft with a large tail [1]. The lower rudder is then used during cruise, decreasing the effects of lateral-directional coupling. Additionally, this increases safety as it reduces the control force required if 1 of the rudders is stuck in a given position.
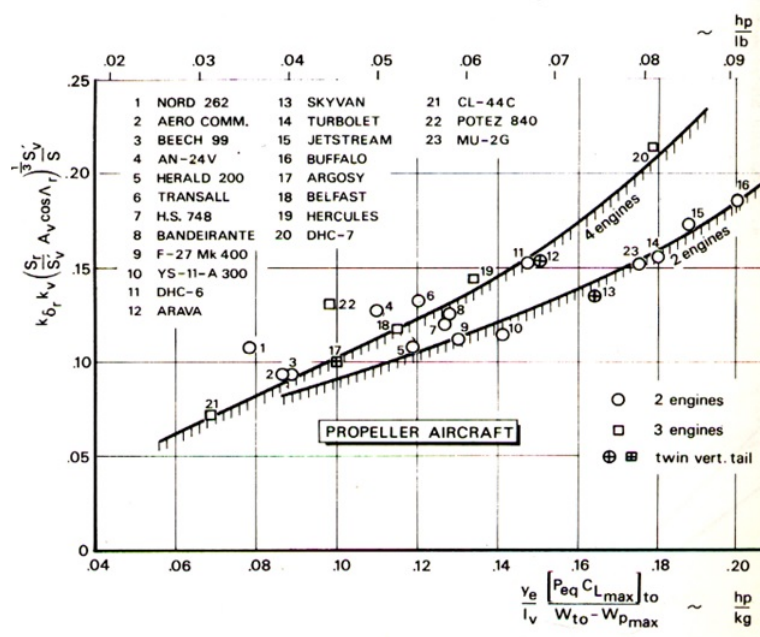
Figure 29: Fast method for vertical tail design [1].

10 Weight and balance

This chapter details how the weight of the aircraft and its components is estimated and explains how the location of the centre of gravity of each component is found. The weight and centre of gravity locations results obtained are used for the sizing of the empennage in chapter 9 and analysis of stability and control characteristics. The Jumbo City Flyer has a MTOW of 239 tonne and the c.g. is positioned at 31 metres from the nose of the aircraft.

10.1 Weight estimation

Initial class I weight estimation resulted in a take-off weight of 197 tonnes, with an empty weight of 79.4 tonne and fuel weight of 46.7 tonne [20]. After the first weight estimations, the aircraft is broken down into primary and secondary components and a class II weight estimation method as detailed in Roskam [32] is applied. This results in a new aircraft maximum take-off weight of 239 tonnes, the total of the 6 major aircraft component weights, which are listed in table 22.

Table 22: Aircraft component weight breakdown and c.g. position.

Aircraft component	Weight [tonne]	% of total weight	Position of c.g. [metre]
Structures	60.7	25.4	35.48
Powerplant	15.4	6.4	32.20
Fixed equipment	36.2	15.3	30.34
Payload	68.7	28.7	25.25
Crew	1.17	0.5	30.00
Fuel	56.7	23.7	34.00
Total	239	100	31.18

The class II weight estimation method applicable for commercial transport airplanes is used for the Jumbo City Flyer. This process consists of averaging results from 2 separate methods: the General Dynamics (GD) and the Torenbeek methods for each airplane component and summing up these values to get the total maximum take-off weight. The assumptions made during weight estimation and c.g. location process for the different aircraft components are documented in the relevant sections.

10.1.1 Structure

The aircraft structure group consists of 4 parts, being the wing, empennage, fuselage, and landing gear.

- Wing weight
- Empennage
- Fuselage
- Landing gear

The wing weight is calculated taking into account 4 engine mounts on the wings and attachment of high lift devices at the trailing edge of the wing. The wing system is equipped with Fowler flaps. The c.g. of the wing is located at the aerodynamic centre (a.c.) and assumed to run along the longitudinal direction of the respective

MAC.

The empennage consists of 2 parts, the horizontal and vertical tail. The horizontal tail is mounted on the fuselage and the horizontal tail will have variable incidence stabilisers.

The fuselage weight is increased if any inlets are located on or in the fuselage and when the main gear is attached to the fuselage, but both are not the case. However, the weight does increase due to the fuselage being pressurised.

The main and nose gear used for the Jumbo City Flyer are both retractable, and therefore the total landing gear weight is calculated using the GD method. The Torenbeek method splits up the main and nose gears and also takes into account whether the landing gear is retractable or fixed.

10.1.2 Powerplant

The powerplant group is made up of 4 parts.

- Engines
- Propeller
- Fuel system
- Propulsion system

The total engine weight is estimated by using the weight of the Europrop TP400 as a benchmark multiplied by the number of engines for the Jumbo City Flyer. The Europrop TP400's weight is chosen as reference for the engine weight for the Jumbo City Flyer because it is assumed that the Jumbo City Flyer will be powered by engines similar, but more powerful, to the Europrop TP400.

The fuel system calculation assumes that the aircraft makes use of regular Jet A-1 fuel and that the fuel system consists of several integral tanks. The Jumbo City Flyer uses LNG as a fuel and is therefore to have a different and more heavy fuel system, as the fuel also needs to be insulated to reduce heating of the LNG. The addition of 1 tonne to the result obtained is assumed to be an appropriate representation of the actual weight. The fuel system is discussed in detail in section 7.6.

The propulsion system consists of the engine controls, engine starting system, propeller controls, and oil system and oil cooler.

10.1.3 Fixed equipment

The fixed equipment weight consists of the following 11 separate parts:

- Flight control system.
- Hydraulic and pneumatic system.
- Electrical system.
- Instrumentation, avionics and electronics.
- Air-conditioning, pressurisation, anti- and de-icing systems.
- Oxygen system.
- Auxiliary power unit.

- Furnishings.
- Baggage and cargo handling equipment.
- Auxiliary gear.
- Paint.

For the calculation of the flight control system weight, it was assumed that the Jumbo City Flyer will have powered flight controls with hydraulic control actuators. However, using this in the calculation, it was found that for the Torenbeek method the hydraulic and pneumatic system is estimated to be heavier than the control system it is a part of. Therefore, for the Torenbeek method, unpowered flight is assumed with the estimated heavier weight for the hydraulic and pneumatic system added to it.

For the weight calculation of the air-conditioning, pressurisation, and anti- and de-icing systems, the length of the passenger cabin is sum of the upper deck cabin and lower deck cabin lengths.

The auxiliary power unit (APU) weight is the largest possible, as the Jumbo City Flyer is estimated to be in the top range of required APU's.

The furnishings weight is estimated using the values appropriate for a short-range aircraft and the design ultimate cabin pressure is assumed to be the air pressure at around 2.5 km height. This is what is generally used for aircraft flying at an altitude of 11 km and is assumed appropriate for the Jumbo City Flyer at an altitude 8.5 km.

The weight of the paint is estimated using the highest value available to provide a conservative estimate.

The next step in the process is to determine the centre of gravity of each of the components of the aircraft. This will be done in section 10.2.

10.2   Centre of gravity

In this section, the centre of gravity of the Jumbo City Flyer and that of its components is determined and the methodology to do so explained. It is important to find the c.g. because it affects an aircraft's flight stability and control characteristics as well as tail manoeuvre loads and ground loads acting on the nose gear.

The c.g. for Jumbo City Flyer is determined by taking the sum of the product of the approximate c.g. positions and weights of the respective aircraft components divided by the total weight of the aircraft components. Equations 26 and 27 calculate the c.g. in both longitudinal and vertical direction of the aircraft, respectively. The reference point is on the centre line, 1 m in front of the nose of the aircraft and 10 metres below it. This is done so all the parts of the aircraft are behind and above this reference point.

$$x_{cg} = \frac{\sum x_i * W_i}{\sum W_i} \qquad (26) \qquad\qquad z_{cg} = \frac{\sum z_i * W_i}{\sum W_i} \qquad (27)$$

The c.g. position of the aircraft component is determined by analysis of fractions of c.g. positions of aircraft systems from reference aircraft. The individual c.g. for the aircraft components are tabulated in table 22.

10.2.1 Load and balance diagram

With the Jumbo City Flyer general layout arrangement, cabin seating and cargo hold layout decided upon in section 11, and the c.g. position of the different aircraft components determined, the load and balance diagram is constructed and shown in figure 30. For the construction of the load and balance diagram, it is assumed the cargo is loaded first, followed by the upper deck, then the lower deck and finally the fuel is pumped into the Jumbo City Flyer.
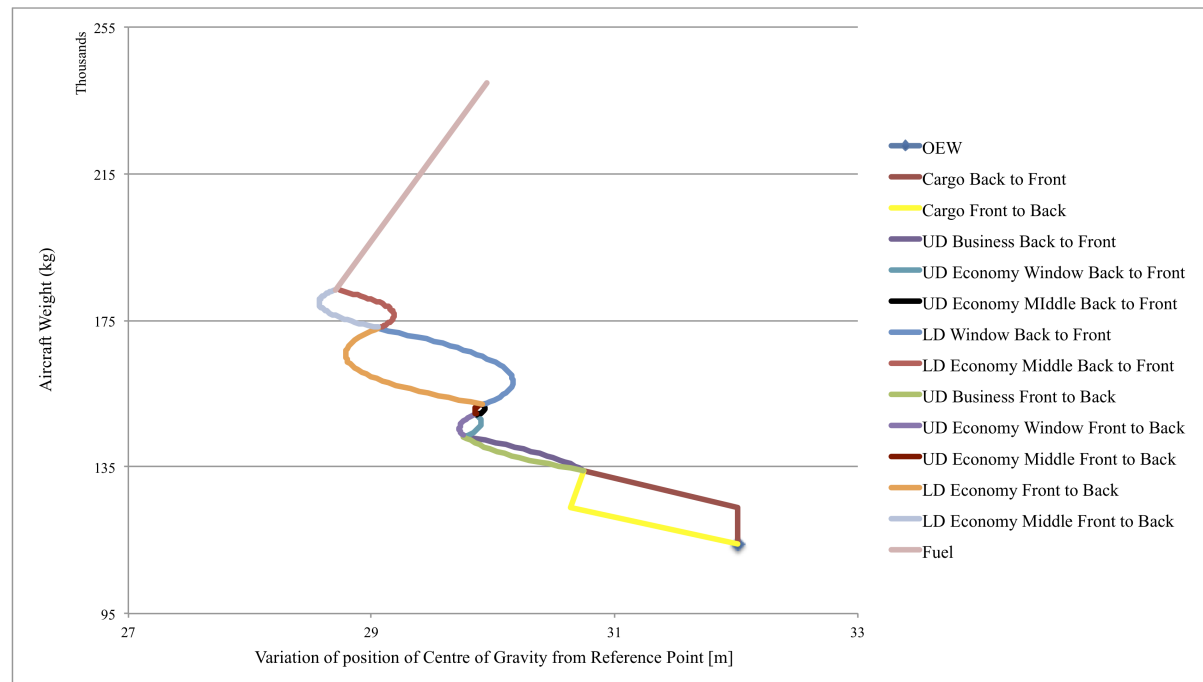
Figure 30: Variation of the centre of gravity position with changing aircraft weight.

The loading of passengers in the cabin and baggage or cargo increases the overall weight of the aircraft and causes a shift of the c.g. forward, i.e., towards the nose of the aircraft, relative to the c.g. of the aircraft at OEW. However with the addition of fuel the c.g. of the aircraft moves back towards the aft.

For the empty aircraft it is assumed the upper deck is loaded first, followed by the lower deck. The business class passengers take their seats first, then followed by the assumption that the window seats in the economy are filled first and finally the seats in the middle row. Likewise for the lower deck, followed by the middle seats for both back-to-front and front-to-back directional loading.

10.3 Verification and validation

The calculation of the aircraft component weight takes the average of 2 methods, as mentioned at the beginning of this chapter 10. As shown in table 23, the Jumbo

City Flyer is within reasonable limits in terms of structural and fixed equipment, and OEW in comparison with the passenger transports, according to data obtained from Torenbeek [36].

Table 23: Typical average empty weight fractions for the aircraft type in comparison with Jumbo City Flyer.

Aircraft Category	Percentage of MTOW			
	Structure	Propulsion	Fixed equipment	OEW
Short haul turboprop	32.0	12.5	13.5	58.0
Long haul jets	24.5	8.5	9.0	42.0
Long haul turboprops	27.0	12	12	51
Jumbo City Flyer	25.5	6.5	15.4	47.9

However, formulae for these methods are derived from statistical data of reference aircraft of similar size and type, of which it can be assumed that aircraft data is relatively old and does not take into account the technological advances in structural and material weight savings for the respective aircraft systems. It is assumed that the lower structure, propulsion and fixed equipment weights is due to technological advancement.

11 Fuselage design

In this chapter the fuselage will be studied in detail. In section 11.1 the cabin design is studied, where the seating arrangement, the environmental system and the water and waste system are discussed. The dimensions of the fuselage will be discussed in section 11.2, after which the structural aspects will be studied in section 11.3. In section 11.4 the cargo hold is designed and finally in section 11.5 the flight deck will be sized.

11.1 Cabin design

In this section the interior of the cabin is discussed. The aim of the cabin design is to transport passenger in the most comfortable way.

11.1.1 Passenger seating configuration

The Jumbo City Flyer has 2 classes being business and economy class. The business class is positioned at the front of the upper deck, the remainder of the upper deck and the lower deck is economy class.

The business class is composed of 16 rows in a 2x2x2 configuration, which results in 96 business seats. The economy compartment on the upper deck is composed of 15 rows, the first 10 rows are in a 2x3x2 configuration resulting in 70 economy seats on the upper deck. The last 5 rows are in a 2x2x2 configuration, resulting 30 economy seats. The lower deck has 37 rows installed. The first 32 rows are in a 3x3x3 configuration and the last 5 in a 2x2x2 configuration, resulting in 318 economy seats.

Having good illumination in the cabin adds to the comfort of the passengers, therefore the cabin has bigger windows than standard aircraft. This increases the passenger experience of flying. Because of time limitations no research is conducted with respect to the window's size. Structural calculations are thus still required to investigate the effect of cut outs in the fuselage.

In total 96 business and 418 economy seats are placed. The fuselage includes room for 15 toilets and 12 galleys. The emergency exits are type A doors as required by regulations [18]. For aircraft that can transport more than 299 people all exits must be type I or A. In this case type A is used and for every 110 passengers 1 exit per fuselage side must be added. In table 24, figure 31 and figure 32 the information explained is summarised.

Table 24: Passenger seat configuration.

	Upper deck	Lower deck
Business class rows	16	-
Business seat configuration	2x2x2	-
Business seats	96	-
Economy class rows	15	37
Economy seat configuration	2x3x2 and 2x2x2	3x3x3 and 2x2x2
Economy seats	100	318
Number of toilets	6	9
Number of galleys	4	8
Number of type A doors	2 pairs	4 pairs
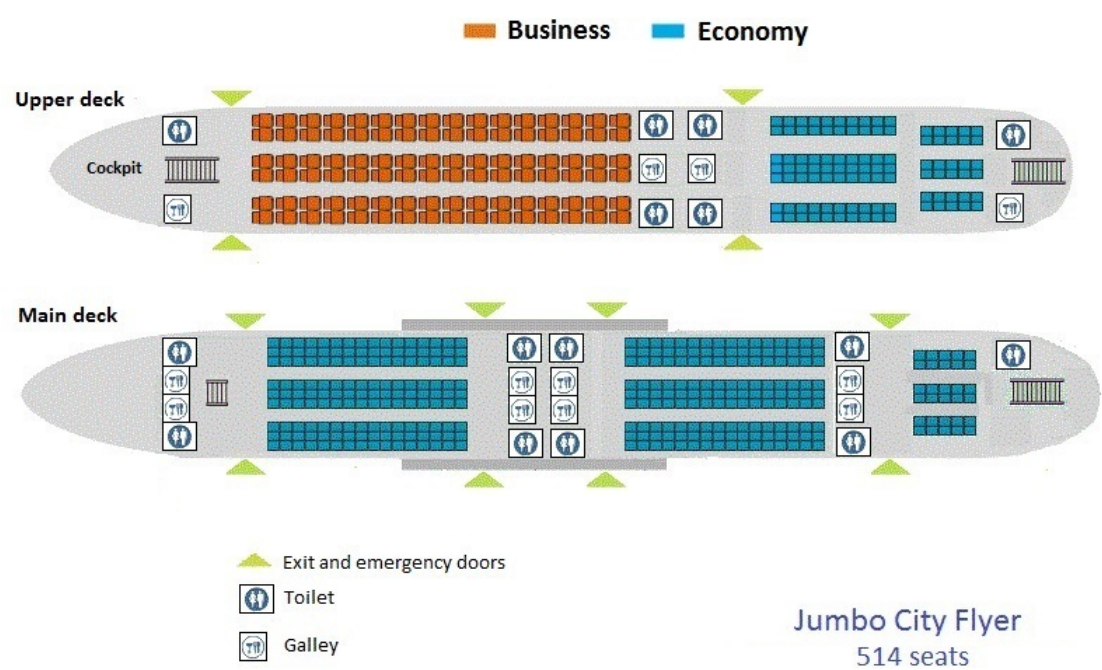
Figure 31: Passenger seat configuration.
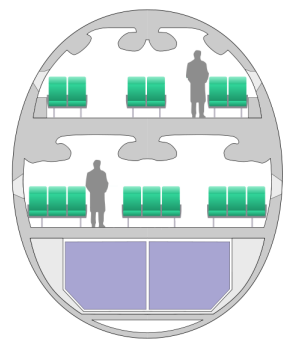
Figure 32: Cross section of the fuselage.

11.1.2 Environmental system

The environmental control system creates a comfortable environment for the passengers during flight. In this section the pneumatic environmental control systems for the fuselage will be discussed.

To have a controlled environment in the cabin several systems need to be implemented. First metering and control systems need to be installed to monitor constant pressure, temperature, oxygen and humidity levels. Emergency de-pressurization system are implemented to account for pressurisation defects. The engines or APU can be used to power the pneumatic systems. Air is compressed by the engines and pumped into the cabin. A back-up oxygen system is provided in case of failure of the main system.

Another relevant system for the comfort of the passenger is the air conditioning vent system. This complex system of tubes and vents will allow comfortable air conditions in the cabin. To achieve this environmental control in the cabin isolation is needed. The required cabin air required is 560 litre per minute per passenger [31].

11.1.3 Water and waste system

For the comfort of the passengers a water and waste system is provided. It is assumed that 1 litre per passenger is sufficient [31]. The system is to be pressurised with air from the pneumatic system. In this system a liquid is used, thus to prevent freezing the system needs to be heated. An electrical heat exchanger can be used for both hot water and preventing the system to freeze.

The toilets in the aircraft use waste tanks as a waste system. This self-contained system mixes the waste with chemicals in the tanks. At least 1 lavatory per 30 passengers has to be provided [31]. Panels to access the waste tanks need to be implemented for service.

11.1.4 De-icing, rain, and fog systems

The aircraft needs to be equipped with a subsystem to prevent problems when encountering icing conditions. Primarily de-icing and anti-icing systems are used. Several types of de-icing can be used, e.g., de-icing boots, electro-impulse systems. For icing special care is needed for pitot tubes, the leading edge of the wing and tail, flight controls and the wind-shield.

For weather conditions like rain and fog several systems are considered. To ensure visibility for the pilot, window wipers should be installed. Also, to prevent fogging a defog system is to be implemented. A decision still has to be taken which type of system will be used for the systems described in this section.

11.1.5 Escape systems

To ensure the safety of crew and passengers a well-organized escape system must be provided in the aircraft. Regulations state that all passengers on board should be able to exit the aircraft within 90 seconds. As stated in section 11.1.1, 12 exits are spread throughout the fuselage. These exits need to be properly marked in the cabin and at each exit there will be slides and rafts. For the emergency routes running over the wing, anti-skid material will be used. Finally, life jackets should be available under each seat.

11.2 Dimensions and layout

In section 11.1 the seat configuration and location of the toilets, galleys, stairs, doors and emergency exits were defined. From the CS-25 regulations [18] the dimensions for these items are determined and are presented in table 25.

Table 25: Dimensions of cabin interior parts.

Item	Height	Length [m]	Width [m]	Amount
Toilet	-	0.92	0.92	15
Galley	-	0.76	0.92	12
Emergency doors	1.83	1.07	-	6 pairs
Stairs	-	1.5	-	2
Seat Pitch Economy	-	0.84	-	-
Seat Pitch Business	-	1.12	-	-
Seat Width Economy	-	-	0.50	-
Seat Width Business	-	-	0.58	-
Aisle width economy and business	-	-	0.50	2

Since the economy cabin is wider than the business cabin, the economy section will determine the width of the overall fuselage. As shown in figure 31 the Jumbo City Flyer has a 3x3x3 configuration on the lower deck with a width of 0.50 metres per seat, 2 aisles of 0.50 metres and 0.35 metres of clearance on every side. This results in a fuselage width of 6.2 metres.

The height of the upper and lower deck is 2.10 metres, respectively. Both floors have a thickness of 0.1 metres. There are 2 empty spaces at the top and the bottom of the fuselage of 0.5 metres each and the cargo hold is 1.8 metres of height. This results in a height of 7.2 metres, hence the Jumbo City Flyer has an elliptical fuselage.

The length of the fuselage can now be determined since the lengths of all the cabin's separate items are known, see table 24 and 25. Be aware that if sufficient room is provided for the toilets, automatically there will be sufficient room for the galleys. This can be observed in figure 31, where it can be seen that the galleys and toilets are always placed together in the fuselage and that the toilets require more space than the galleys.

Lengths of the upper and lower cabin are shown in table 26 and 27 respectively.

Table 26: Dimensions of upper cabin.

	length [m]	Amount	Total length [m]
Cockpit	4	1	4
Toilet	0.92	4	3.68
Stairs	1.5	2	3
Emergency doors	1.07	2	2.14
Seat pitch business	1.12	16	17.92
Seat pitch economy	0.84	15	12.60
TOTAL			43.34

Table 27: Dimensions of the lower cabin.

	length [m]	Amount	Total length [m]
Cockpit	4	1	4
Toilet	0.92	5	4.6
Stairs	1.5	2	3
Emergency doors	1.07	4	4.28
Seat Pitch Economy	0.84	37	31.08
TOTAL			46.96

11.3 Fuselage structural design

The fuselage structure and skins will be made of an epoxy HS/carbon fibre as explained in chapter 8. It is assumed that the design process of a carbon fibre fuselage is similar to that of an aluminium fuselage. This means a semi-monocoque structure, which is a hybrid of a reinforced shell and a compressive structure, including frames and longerons. These frames and longerons are attached to the structure using adhesive bonding. The fuselage structure has to carry all subsystems, and transfer the loads to the wings. The exact sizing for all loads is a future step in the design process. For a preliminary design, the frame depths were set at 17 cm, the frame spacings at 51 cm and the longeron spacings at 23 cm [23], and the result can be seen in figure 33.
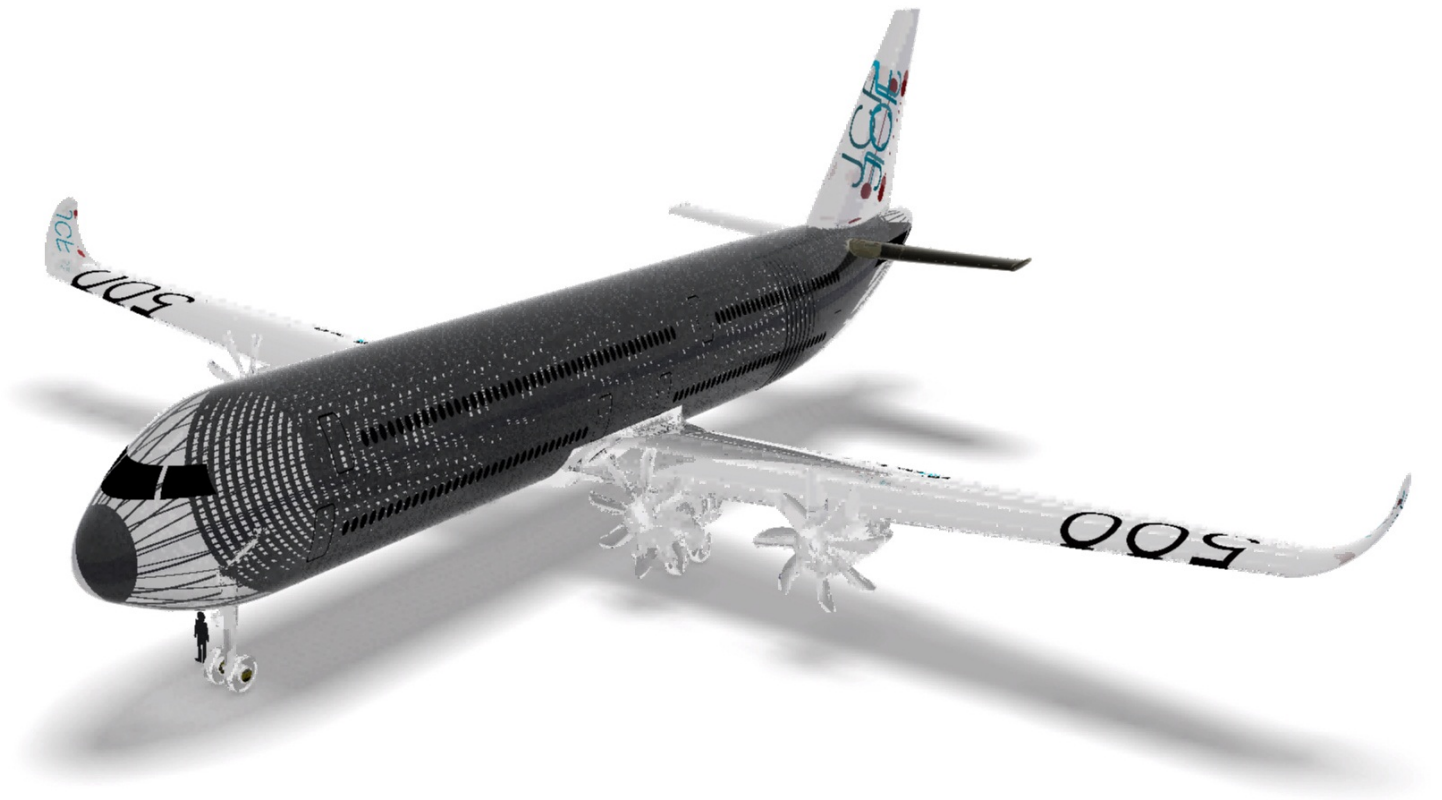
Figure 33: Structure of the fuselage.

The cabin altitude is the pressure inside the cabin as experienced by the passengers. As cabin structures become lighter and strongr, the trend is to decrease cabin altitude as this increases passenger comfort. The Boeing 767 for instance has a cabin altitude of 2100 m [64], whereas the Airbus A380 has a cabin altitude of 1500 m [65].

Since the Jumbo City Flyer flies lower than any of these aircraft, the pressure difference for the fuselage structure is lower. This means the cabin pressure can be dropped to 1200 m, which means higher passenger comfort levels. The pressure on itself only requires a thickness of 1.8 mm in the bulkheads, which are the front and rear end of the fuselage tube, and 0.22 mm in the skin of the fuselage according to pressure vessel theory, purely to withstand the pressure. Extra thickness will have to be added to carry all other loads, but as discussed before, this will have to be done in the next step of the design. Figure 33 also shows the bulkhead in the nose.

11.4 Cargo hold

In section 11.2 it was explained that the cargo hold has a height of 1.8 metres and width of maximum 5.5 metres. The largest standard container that exists is the LD1 container, which is a half container, and 2 can fit next to each other in the cargo hold. One container can load up to 1.6 tonne. The dimensions of this container are show in figure 34. The loading into the fuselage can be seen in figure 32.
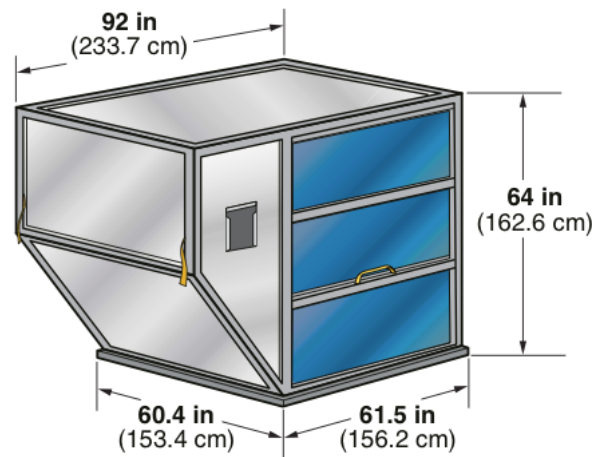
Figure 34: Dimensions of a LD1 container.

After calculating the space required for fuel, landing gear and wing box it was estimated that 32 LD1 containers can fit in the aircraft. This is enough to transport the design capacity 20 tonnes of cargo and luggage.

11.5 Flight deck design

For the design of a flight deck 4 considerations must be taken into account [31]:

- The pilots and the crew members must be able to reach the controls in a comfortable way.
- The pilots and the crew members must be able to see all flight essential instruments without undue effort.
- Communication by voice or touch must be possible without undue effort.
- Visibility from the cockpit must adhere to minimum standards (CS-25).

These considerations are the reason that the flight deck is designed around the pilot.

11.5.1 Avionics

In this section the basic instrumentation for the cockpit, flight management and avionics of the aircraft will be discussed.

The cockpit instrumentation layout should be compact and functional. The crew must be able to see all crucial flight instruments, control and warning devices. The crucial instruments for the pilot are attitude, speed and altitude indicators. Regulations state that every aircraft should have these instruments in the cockpit. Other control and warning devices can be divided into different panels, e.g., glass, primary flight display, navigation display, and engine indication and crew alerting system. This is beneficial for clarity for the pilot and maintenance of the aircraft.

12   Undercarriage layout

In this chapter the layout of the undercarriage is designed. Section 12.1 through section 12.4 discuss the different positions of the landing gear, the general layout of the landing gear and the tyres, the ground operations aspect and the brake and shock absorption systems and the rectraction mechanism respectively. The results presented in this chapter were obtained using the methods explained in Roskam [22, 31].

The main functions of the landing gear are summarised first:

- Absorb landing shocks and taxiing shocks.
- Provide ability for ground manoeuvering.
- Provide breaking capability.
- Allow for aircraft towing.
- Protect the ground surface.

These functions are fulfilled by a retractable landing gear in tricycle configuration. The main gear has 2 struts with 4 tyres and the nose gear consists of 1 strut with 2 tyres. The struts have a length of 3.05 m to provide the required ground clearance. The highest tyre operating speed is encountered during landing and it is 78 m/s.

12.1   Type and position of the landing gear

As explained in section 3.2.6, the decision was made to use a retractable landing gear in tricycle configuration. The next step is to decide on the amount of struts the main gear will have. By looking at the landing gears of reference aircraft it was chosen to use 2 struts, with 4 tyres each. For the nose gear 1 strut is used with 2 tyres.

The longitudinal position of the main landing gear was estimated during the calculation of the centre of gravity in section 10.2. The main landing gear was positioned at 34.3 metre from the nose, at half the wing chord. As such there is a distance of 4.1 metre between c.g. and the main gear, fulfilling the tip-over requirement. The nose gear is positioned at 4.0 metre from the nose.

The lateral position of the nose gear is at the centreline of the aircraft. The main landing gear is positioned at 3.85 metre from the centre of the fuselage, both left and right. As such, the main gear struts are positioned under the wing and will be stored in the fuselage when retracted.

Another consideration of the landing gear is the ground clearance. This has an impact on the length of the struts. Since the propellors of the TP400 have a diameter of 5.3 metre and the engines are positioned underneath the wing, relatively long struts are required. It was determined that struts of 3.05 metre provide the required ground clearance of 5 degrees. Table 28 summarises the information given.

Table 28: Landing gear positions.

	Main gear	Nose gear
Longitudinal distance from the nose [m]	34	4
Distance from the centre of the fuselage [m]	3.5	0
Number of struts [-]	1	2
Length of the struts [m]	3.05	3.05

Once the position of the landing gear and the characteristics of the struts are known the loads per strut can be calculated. This is done using the moment equilibrium at the ground, according to the equations given in Roskam [31, 22]. The results are:

- Maximum static load for nose strut: 341 kN.
- Maximum static load per main strut: 1083 kN.

This results in an equivalent single wheel load (ESWL) of 170 kN for the nose gear and 271 kN for the main gear.

12.2   Type, size and inflation pressure of the tyres

In the previous section, the ESWL for both nose and main gear were determined. For the nose gear however, a second method is used to determine the ESWL and the highest load must be used for further design [31].

For the second method, the maximum dynamic load per nose gear tyre was determined, resulting in a load of 310 kN. The resulting maximum static load per nose gear tyre is 206 kN. The second method thus results in the largest ESWL for the nose gear. This result will be used in further calculations.
To determine the size of the tyre it is necessary to know the maximum tyre operating speeds for take-off and landing. They are calculated to be:

- Maximum tyre operating speed take-off: 75 m/s.
- Maximum tyre operating speed landing: 78 m/s.

With the maximum static loads and the maximum tyre operating speeds known, the size and the pressure of the tyres can be determined using table 2.12 in Roskam [31]. This results in the tyre sizes as shown in table 29. The definition of the different parameters are provided in figure 35.
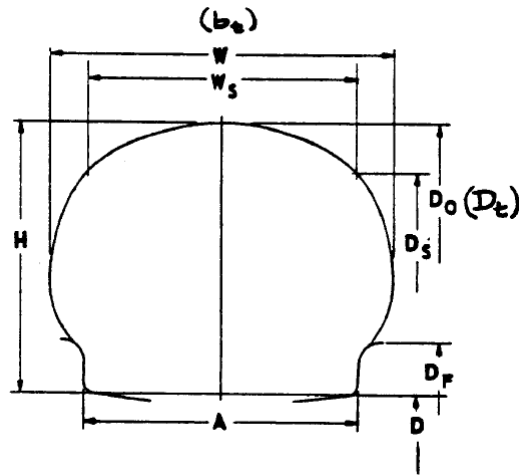
Figure 35: Definition of the tyre measures.

Table 29: Tyre characteristics.

	Main gear	Nose gear
Outside diametre (D_o) [m]	1.32	1.24
Section width (W) [m]	0.52	0.43
Bead seat diametre (D) [m]	0.51	0.45
D_o (max-min) [m]	1.32-1.30	1.24-1.21
W (max-min) [m]	0.46-0.44	0.44-0.41
Maximum shoulder diametre ($D_{s,max}$) [m]	1.17	1.1
Maximum shoulder width ($W_{s,max}$) [m]	0.46	0.37
Maximum speed [m/s]	100	94
Section height (H) [m]	0.41	0.40
A [m]	0.41	0.35
Unloaded inflation pressure [PSI]	200	195

As a last point, it must be taken into account that the tyres grow approximately 4 percent in width and 10 percent in diameter during their operational lifetime. To account for this, a tyre clearance is used. It has been calculated using the method explained in Roskam [31]. This resulted into the following clearances:

- Reserve width main landing gear: 0.047 m
- Reserve radius main landing gear: 0.16 m
- Reserve width nose landing gear: 0.042 m
- Reserve radius nose landing gear: 0.15 m

12.3 Ground operations

While on the ground, the aircraft must be able to taxi from the gate to the runway. As explained in 7, a taxibot will be installed in the nose gear, hence the engines are not required for taxiing. Although this taxibot eliminates the need for a push back tug, it should still be possible for tugs or towing equipment to connect with the nose gear.

The ground manoeuvring capability of an aircraft is measured in terms of its minimum turn radius. Different turning radii data of the Airbus 330 were used as main reference [66] to determine the manoeuvering capability of the Jumbo City Flyer. The reason for using the A330 as main reference is that this aircraft has a similar fuselage length and wheel base as the Jumbo City Flyer.

A final criterium that was investigated were the critical angles for foreign object damage. It was observed that these angles were too small compared to reference aircraft. The simplest solution to tackle this problem, is to make use of splash guards on the nose gear.

12.4 Brake and shock absorption systems

So far in this chapter, the landing gear has been designed to protect the ground surface, for aircraft towing, and for manoeuverability on the ground. The landing gear must also be able to brake and absorb all shocks. The braking system should be able to:

- Decelerate and stop the plane.
- Help to steer the plane.
- Hold the airplane when it is parked.
- Control the speed when taxiing.

Disc brakes will be used for the Jumbo City Flyer. They are commonly used on aircraft. The most effective brakes are those made of carbon, which are up to 40 percent lighter than conventional brakes. However, they can be twice as expensive as conventional brakes. Therefore it was opted to use anti-skid brakes, they are about 90 percent as effective as carbon brakes, but without the additional costs.

Concluding, the landing gear needs to absorb the shocks that occur during landing and taxiing. This is done using oleo-pneumatic struts. The size of these struts was calculated using the method explained in Roskam [31], resulting in a length of 0.88 metre and 0.63 metre of diameter for the main landing gear and 0.11 metre of length and 0.40 metre of diameter for the nose landing gear.

12.5 Retraction mechanisms

At this stage the landing gear is sized but it has to be possible to retract it. This is done using a retraction actuator. This actuator is a hydraulic system. The location of the actuator has 2 criteria that must be taken into account:

- The retracted actuator length cannot be less than half the extended actuator length.
- The force-stroke diagram of the retraction actuator should not show large peaks [31].

The location is determined using the method explained in [31]. Figure 36,37 and 38 show the main and nose landing gear renders including the retraction actuator.

Figure 36: Main gear deployed.

Figure 37: Main gear retracted by 45 degrees.
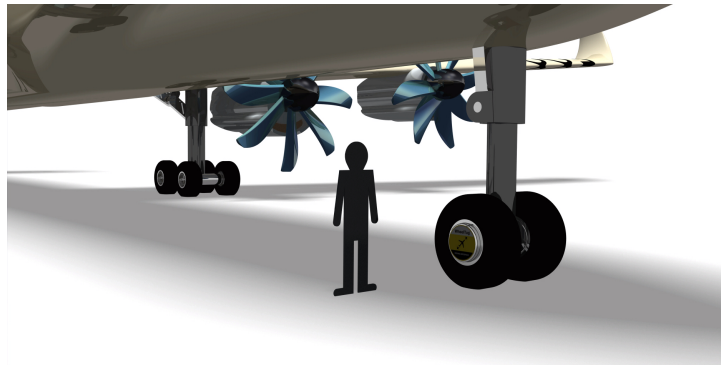
Figure 38: Nose gear deployed.

13 Systems engineering

During the design phase, critical reliability issues can be addressed to identify the strong and weak points. Therefore a reliability, availability, maintainability and safety analysis has to be performed and the and operability characteristics need to be analysed, this is described in section 13.1. To asses the potential risks the Jumbo City Flyer encounters during its lifetime, a risk analysis is performed in section 13.2.

13.1 Reliability, availability, maintainability, and safety analsyis and operability characteristics

The performance of the Jumbo City Flyer needs to be analysed before the design progresses into the next phase. This is done with a reliability, availability, maintainability, and safety (RAMS) analysis, along with determining the operability characteristics. For this, the main focus is on:

- Fulfilling of the objectives by the aircraft.
- Identifying bottlenecks.
- Identifying critical items.
- Allocation of resources.
- Development of a maintenance plan.
- Development of a worst case scenario.

The reliability defines how well the aircraft can perform the mission it is designed to do. The Jumbo City Flyer has been designed specifically to perform a mission that consists of transporting 500 passengers over a distance of up to 2500 km at a cruise altitude of 8.5 km with a cruise speed of Mach 0.62. It is expected that the Jumbo City Flyer has a high reliability and that it outperforms other aircraft on this mission with respect to reliability.

Availability, which is defined as whether the aircraft is available to perform the mission it is designed for, can be influenced by maintenance problems, but also by other factors. These include adverse weather conditions, lack of catering or crew or delays due to passengers being late. Only the maintenance aspect can be taken into account at this point. It is expected that the Jumbo City Flyer performs at least as well in the availability aspect as aircraft currently used for this misison.

Maintainability of an aircraft quantifies the ease with which it can be maintained to correct or isolate defects, meet future requirements, and make future maintenance easier. It therefore influences the availability, as increasing the maintainability will mean less time spent in a storage hangar. The Jumbo City Flyer will have less scheduled maintenance as it has a predominantly composite structure. It will also make use of bolted repairs, which are as permanent and damage tolerant when applied on composite material as they are on metal structures [67]. However, if the aircraft is scheduled for maintenance, the tanks need to be emptied. This can increase the maintenance time and cost. The aircraft is already designed to meet future requirements. Future maintenance aspects are expected to mostly depend on advances in the composite materials field, so they can not be accounted for at

this moment.

Safety is a major factor in aviation, as a failure of critical systems can have catastrophic results. This is especially true for the Jumbo City Flyer, as it is to be among the largest passenger aircraft. Therefore safety measures have been taken to ensure the aircraft is as safe as possible. Due to the short range mission of the Jumbo City Flyer, it will be exposed to a lot of pressurisation cycles. However, it is less susceptible to fatigue than most current aircraft as it has a structure composed of mostly composite materials. Composite materials are harder to inspect for small damage, so extra safety margins were taken into account. Another safety measure is that the engines are placed as close to the fuselage as possible, to reduce the impact on stability an engine failure has. In the case of a landing gear failure, the fuel tanks will be emptied before attempting a landing. Thus, a fuel dumping system is implemented into the design of the aircraft.

For operability of the aircraft, a closer look is taken at the functioning of the aircraft and its subsystems. A big influence on operability is the fact that LNG is used as fuel. For maintenance, the fuel has to be removed from the tanks to prevent pressure rising because of boil-off gas. This means that an aircraft may be grounded longer than an aircraft operating on conventional fuel. A related operability issue is the fact that special handling equipment needs to be used at airports, as LNG needs to be stored and tanked at around -160° Celsius. For the taxiing phase, the fact that an electrical taxiing system is used means that the aircraft still needs to be able to taxi using its engines in case the other system fails. This has been taken into account in the design.

13.2   Risk analysis

The Jumbo City Flyer can encounter certain undesirable situations during a flight, so-called risks. An example of this would be a bird strike. To get a clear overview of what the impact of different risks is on the Jumbo City Flyer, a risk maps is made. All risks considered and their probability and impact are stated in table 30. The resulting risk map is shown in figure 39. The x-axis represents the impact of the risk and on the y-axis the probability of an impact is shown. Far right and up are undesirable risks.
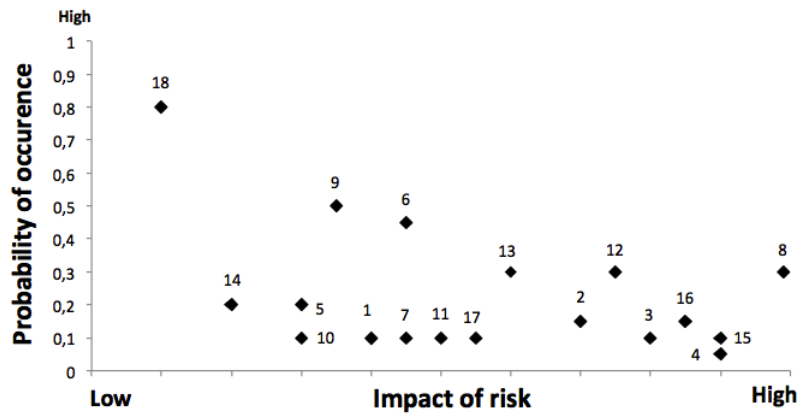
Figure 39: Risk map for the Jumbo City Flyer.

Table 30: Risk probability.

	Risk	Probability	Impact
1	Fuel contamination	0.1	0.4
2	Engine failure	0.15	0.7
3	Depressurisation	0.1	0.8
4	Fatigue	0.05	0.8
5	Bird strike	0.2	0.1
6	Weather damage	0.45	0.45
7	Electronical failure	0.1	0.45
8	Structural integrity	0.3	0.99
9	Fuel leak	0.5	0.4
10	Fire	0.1	0.3
11	Brake failure	0.1	0.5
12	Loss of control	0.3	0.75
13	Landing gear failure	0.3	0.45
14	Communication failure	0.2	0.2
15	Terrorist threat	0.1	0.9
16	Mid air collisions	0.15	0.8
17	Fuel exhaustion	0.1	0.43
18	Lightning strike	0.5	0.3

As an example, 4 risks are elaborated:

- **Risk 2: Engine failure**
  The engines will be used almost continuously, with several take-off and landing runs every day. The probability that 1 engine fails is estimated at 0.15, while the impact could be high when a part of the propellor breaks off and hits a part of the plane. In the case of a multiple engine failure, the Jumbo City Flyer can land safely with 2 engines.
- **Risk 4: Fatigue**
  The fatigue resistance of composites is an advantage of composite materials over metals. Many load cycles will occur during the service life of the Jumbo City Flyer, so using composites is a large benefit. Expansion and contraction are the most frequent causes of fatigue. The Jumbo City Flyer will experience

these cycles several times a day. Due to the good fatigue resistance, the probability of occurrence is low. If the material fails however, the impact will be high.

- **Risk 9: Fuel leak**
  LNG has a high ignition temperature, about 650°C, compared to about 315°C for gasoline. It also has a narrow range of flammability, i.e. in concentrations in air below about 5 percent and above about 15 percent, natural gas will not burn. The high ignition temperature and limited flammability range make accidental ignition or combustion of LNG unlikely.

  The fact that LNG is lighter than air further enhances its safety. This in contrast to other fuels such as diesel, petrol or LPG, which are heavier than air and pool on the ground creating a fire hazard. The result is a moderate impact of the risk.

  A fuel leak will in no case provide a risk of asphyxiation as the air circulation system in the cabin is separated from air system in the cargo hold. Connection valves are in place that will only open in case of a sudden depressurisation, but since outside air will be entering the aircraft and oxygen masks are present for everyone this will not be problem.

- **Risk 18: Lightning strike**
  When lightning strikes the plane, the lightning does not penetrate the skin. Instead, the charge moves around outside of the aircraft. The Jumbo City Flyer itself acts as a big conductor. Therefore, a layer of metal is woven within the carbon fibre composite materials in the structure to cope with lightning strikes. The lightning moves through the metal, with the least amount of resistance, to the static dischargers. Static dischargers are placed on the wing, the wing tips and the tail.

14 Evaluation and presentation

In this chapter the cost-wise performance of the aircraft is analyzed and presented in section 14.1. Section 14.2 discusses the possibility of the family of the Jumbo City Flyer aircraft while section 14.3 examines the operational aspects of the aircraft. In section 14.4 the compliance matrix is shown comparing the customer requirements to the Jumbo City Flyer performance and finally section 14.5 discusses the development timeline for the Jumbo City Flyer.

14.1 Market fit

In this section, an estimation on the development cost is given, a first estimate for the price of the aicraft is given, and the operating cost on a typical flight are analysed.

14.1.1 Development cost

The final book of the Roskam series [35] gives a method to estimate the development cost for an aircraft. It gives statistical relations for the cost to design and engineer an aircraft, to support its development, to perform tests and simulations and to finance the whole operation. The method includes several factors on how much testing and simulation is done. Incorporated in the calculation for the Jumbo City Flyer is the fact that simulation is done on a much more detailed level then in the 1980's, when the Roskam series was written.

It is however hard to put any precision on the numbers used. Boeing for example had 800,000 hours of simulation time on Cray supercomputers for their 787 program [68]. A cost factor for this will always be a guess. The main assumptions when applying the formulae given in Roskam are stated below.

- The hourly cost rate of an engineer is $150. This includes things such as overhead and administration.
- The number of prototypes built is 7.
- The annual inflation rate is 3 percent.
- The cost of the avionics system is 10 percent of the cost of the complete aircraft.
- The number of aircraft built for static testing is 2.
- The manufacturing labor rate is $100 per man hour. This includes overhead and administration.
- The tooling labor rate is $120 per man hour.
- All prices given are calculated in 2025 dollars which include inflation.

The result from all calculations is that the development price of the Jumbo City Flyer will be around $10 billion. As mentioned before this number is corrected for inflation up to 2025. This includes the complete development cost, from the first sketches drawn during the project until the end of all testing and the delivery of the first airplanes. It also includes setting up the production line.

These cost might seem rather low. The development cost of the Boeing 787 was $32 billion [69] and the Airbus A380 program cost was around $16 billion [70]. Taking

into account that a lot of off-the-shelf technology will be used for this aircraft, it is expected to be a reasonable estimate.

14.1.2 Price of the aircraft

All the development costs have to be earned back and a profit has to be made, meaning the aircraft has to be sold. A preliminary estimation for the cost to design and build the Jumbo City Flyer, yields a price of $170 million per aircraft. This is the price without any profit margins.

Roskam gives an estimation for the total manufacturing cost [35]. By dividing this by the number of aircraft made, a cost price per aircraft is obtained. When a surplus for profit is added, a selling price of the aircraft can be estimated. In the same manner as for the previous section, the results of this section have a high error margin and are preliminary results only. Important assumptions, next to those mentioned in subsection 14.1.1, are listed below:

- The number of aircraft built each month at full capacity is 35. It is the same number as for the Boeing 737 [71].
- The total number of aircraft built is conservatively estimated to be 2000, before 2050. A current market of at least 300 aircraft exists for this plane [3]. Knowing that an annual growth of 8 percent is expected on the Asian market for the coming decades [2], the total market for this aircraft in 2050 is a bit less then 5200 aircraft. The market share of the Jumbo City Flyer would then be 39 percent. Again, this is a future prospect, which is by definition prone to errors.

With these assumptions and the statistical relations in Roskam [35], a cost price of $170 million is found. This includes the complete cost for designing and building the aircraft, but no profit for the manufacturer. A first estimate of the selling price would be $200 million. Compared to a Boeing 747-8, which costs around $350 million [72], this is relatively cheap.

14.1.3 Operating cost

To provide an accurate estimation of operating cost is hard at this moment, but it is estimated that by flying with the Jumbo City Flyer instead of the Boeing 747-400, airliners can save around 29 percent of their fuel cost. This makes for a 10 percent reduction of their total operating cost.

At this point, it is near to impossible to give numbers for the operating cost with any accuracy. Operating cost can be split in direct and indirect operating cost. Direct operating costs involve the cost of fuel, crew, landing fees, maintenance and more. Indirect operating costs involve passenger handling, facilities, advertisement, administration, and more. It was not possible to estimate these indirect costs for the year 2025. An attempt has been made with a method proposed in Roskam [35], but the results were too dependent on assumptions that could not be verified

and therefore the result was discarded.

When assuming that the cost for crew, landing fees, maintenance and all indirect operating cost are the same for the Jumbo City Flyer and the Boeing 747-400 in 2025, a preliminary comparison of the operating cost of these two aircraft can be made. To do this, the prices of Jet A-1 and LNG in 2025 have to be estimated. That is not entirely accurate, but by looking at trend lines in January 2013 from the United States Energy Information Administration [73] an estimation was made. The price of Jet A-1 has been nearly constant in the period between 1980 and 2000, going up since 2000 [74]. To calculate savings on fuel cost of the Jumbo City Flyer with the 747-400, the following assumptions are made:

- The prices of LNG and Jet A-1 are interrelated in the future. They will go up by the same amount.
- The cost to transfer natural gas to liquified natural gas adds a factor of 5 to the fuel cost [75].
- The typical mission for comparison is 1250 km.

Preliminary results on the fuel burnt on a typical mission are given in section 7.7. With this, it is found that the fuel cost per passenger can be reduced by around 29 percent with respect to the Boeing 747-400. Knowing that the fuel costs take up around 33 percent of the total operating expenses of an airliner, as calculated in section 2.3, airliners can save 10 percent of their total cost by using the Jumbo City Flyer.

14.2   Family of aircraft

Airliners often ask for a series of aircraft to be developped. They want smaller and larger aircraft of the same type. An aircraft that can carry 500 passengers, one that can carry around 400 and perhaps one that can carry 300, for example. By this, it is not meant to deliver the same aircraft with different seating arrangements and thereby vary the number of passengers, but a complete re-design of the aircraft is meant. Comparable to the Boeing 777-200 and 777-300, there will probably be a market need for the Jumbo City Flyer-500 and a Jumbo City Flyer-400. Note that a short range or a long range version of this aircraft is not considered at the moment. It is specifically designed for a short range mission.

To make a family of aircraft, it is easier to scale the aircraft down then to scale it up, take less passengers instead of more. When taking less passengers, the wing can remain very similar. The fuselage can be decreased in length and the engines can do with less thrust. When decreasing the length of the fuselage, the centre of gravity should be checked. If it moves, the wing should be repositioned. Also, the sizing of the tail should be redone. When decreasing the fuselage, the aircraft becomes lighter, creating less drag. Therefore, engines with less thrust can be implemented.

How a 400 passenger Jumbo City Flyer would look like is not calculated during this project. Throughout the design process, it is kept in mind that there might be a call for this aircraft. Updating the aircraft is expected to be a relatively fast process. It will require less work then designing an entirely new aircraft.

14.3 Operations and logistics

The operations and logistics description for the Jumbo City Flyer aircraft is given for 2 segments of the aircraft operation. There are the airborne phase and the ground operations. The airborne operations of the Jumbo City Flyer are briefly explained in the section 14.3.1 while the ground operations are elaborated in 14.3.2.

14.3.1 Airborne operations

The airborne operations of the aircraft are defined by the mission profile 7 in the section 4 Before the Jumbo City Flyer becomes airborne, pre-flight checks are carried out to ensure the airworthiness of the vehicle. Once airborne, assuming a clean bill of health for the structural and propulsive systems, it is important the aircraft communication, navigation, weather system function properly for successful accomplishment of the mission.

14.3.2 Ground operations

The ground operations refer to all activities required to keep the aircraft in good flying condition. These activities are partitioned into ramp/terminal handling and maintenance operations of the aircraft as illustrated by figure 40.
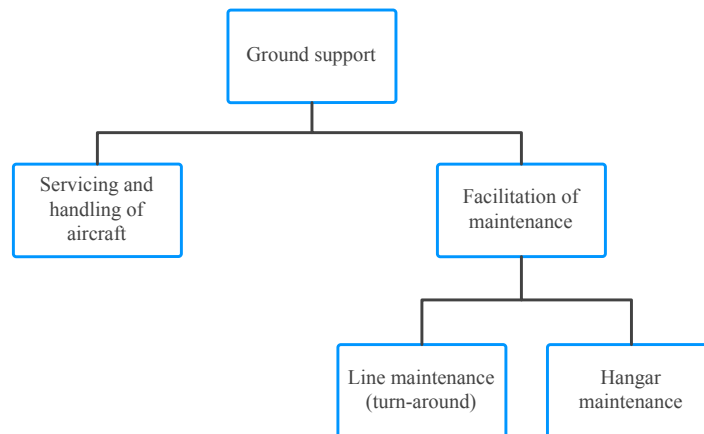
Figure 40: Ground support categories.

14.3.3 Ramp and terminal operations

For short to medium haul aircraft it is important to have shorter turnaround times to maximise the time the aircraft spends in the air. An estimate on the turnaround time is illustrated by figure 41. This is generated by appropiately allocating activity times after analysis of the turnaround times for the Boeing 737 series [76] and the Boeing 747 series [77].

Based solely on the fuel volume capacity, it is assumed that the Jumbo City Flyer with a capacity of 127 m^3 will have less fueling time in comparison with the aircrafts of similar size. The Boeing 747-400 aircraft has a volume capacity of 217 m^3.

However, the use of the LNG requires additional airport facilities for the storage and pumping.
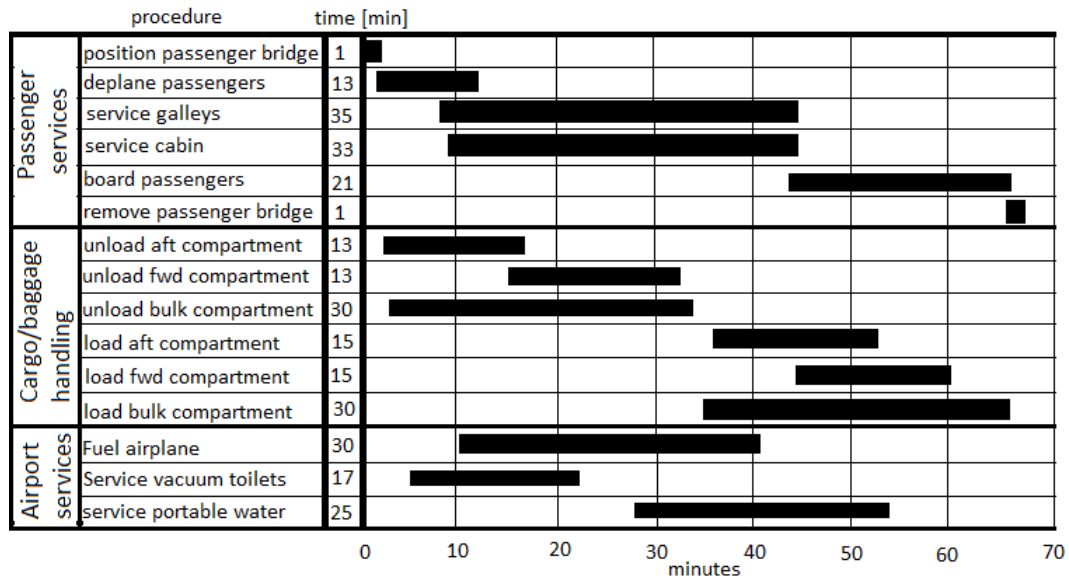
Figure 41: Estimate of ground handling times at terminal for the design.
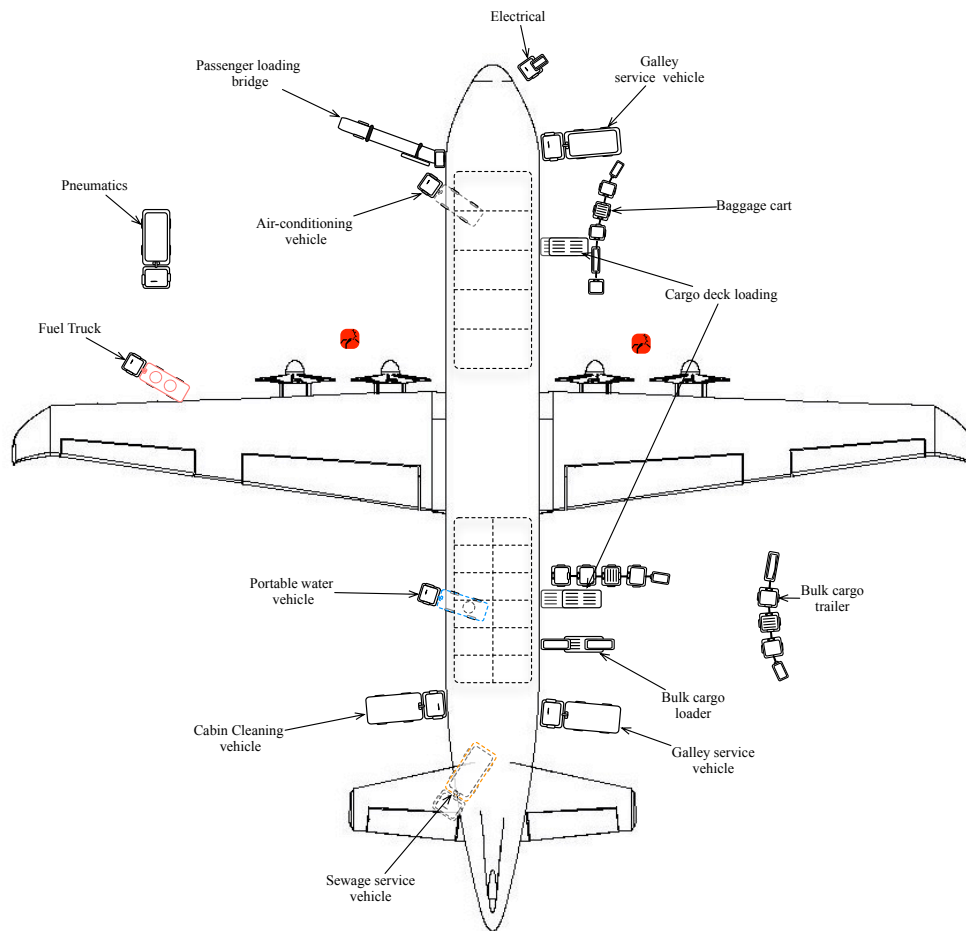
Figure 42: Schematic of Jumbo City Flyer being serviced during a turnaround with help of ground support systems.

14.3.4 Maintenance and Material Support

The maintenance activities for an aircraft are divided into the on-aircraft maintenance and off-aircraft maintenance. On aircraft maintenance is further divided into line and hangar maintenance activities [78]. In order to minimize time spent in maintenance, Jumbo City Flyer sub-systems are designed such that faults or discrepancies identified during flight can be reported to the maintenance control. This activity enables the maintenance to make adequate preparation and therefore saving time when the aircraft arrives for an unscheduled maintenance stop. A schematic diagram of this activity is shown in 43.
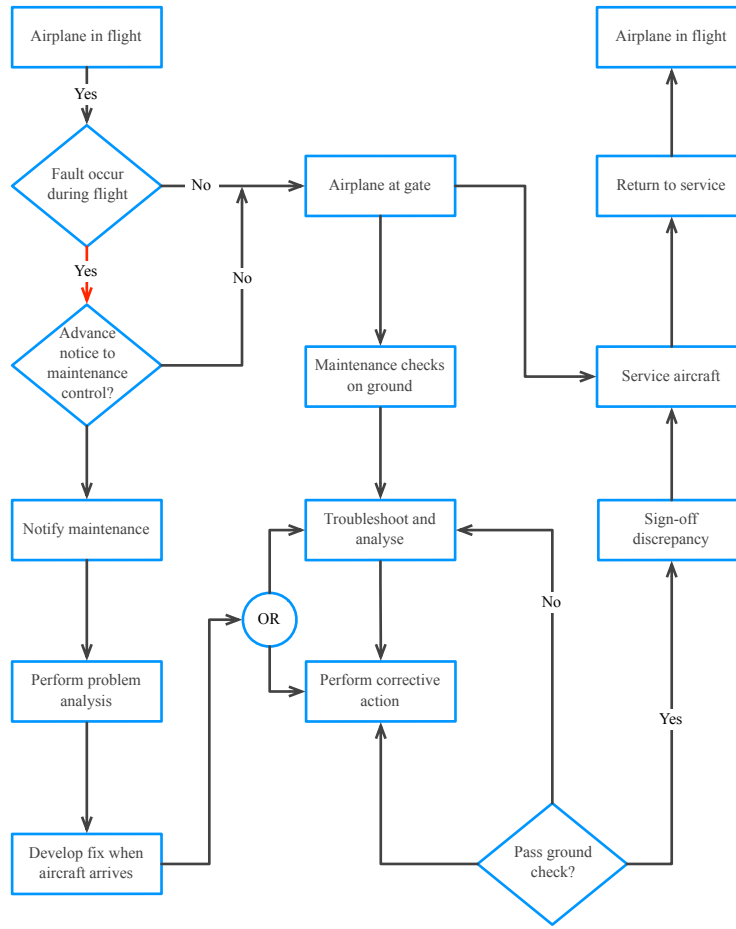
Figure 43: Schematic of maintenance operations procedure during aircraft turnaround.

The advantages of the overall dimensions of the Jumbo City Flyer aircraft mean it can utilise current aircraft maintenance building facilities. However, the height of the fuselage from the ground means that additional stands and jigs have to be customised for reaching and servicing of the aircraft. Service doors are placed at strategic points on the aircraft to enable easier access into the aircraft.

In support of the maintenance activities, the material section handles the parts and supplies required. The use of the composites will require special tools for early detection of faults.

14.4 Compliance matrix

The compliance table is shown in table 31. It shows which requirements are fulfilled, partially fulfilled, or not fulfilled, denoted with a $\sqrt{}$, $\pm \sqrt{}$, and -, respectively. The reasoning why a certain requirement is not met and further quantification for the Jumbo City Flyer are given below that.

Table 31: Compliance matrix

#	Project objective	Fulfilled
1	Carry around 500 passengers	$\sqrt{}$
2	Range of 2500 km	$\sqrt{}$
3	Ability to use alternative fuels	$\sqrt{}$
4	Available for 2025	$\sqrt{}$
5	Minimum cruise speed M = 0.6	$\sqrt{}$
6	The CO_2-emissions per passenger km should be reduced by 50 percent when compared to Boeing 747-400 on the same mission	$\pm \sqrt{}$
7	Safe and comfortable travel within regulations (CS25)	$\sqrt{}$
8	Low noise levels, in accordance with the future anticipated regulations from the Committee on Aviation Environmental Protection part 8	$\pm \sqrt{}$
9	Standard infrastructure requirements at the airport	$\pm \sqrt{}$
10	Airplane needs to be able to land and take-off on the busiest airports and comply with noise restrictions	$\sqrt{}$
11	Design has to comply with CS-25 regulations	$\sqrt{}$

Now the actual numbers of the Jumbo City Flyer are given. The numbers here go together with the numbers indicated in table 30.

1. The Jumbo City Flyer is able to carry 514 passengers in a 2 class configuration.
2. The Jumbo City Flyer is designed to have a range of 2500 km. The payload range diagram is given in section 4.4.4.
3. The fuel used is LNG.
4. In the design process only technologies are used with a technology readiness level of 6 or higher, indicating it is reasonable to expect a first flight in 2025. This is supported by the Gantt chart in section 14.5.
5. The cruise speed for the Jumbo City Flyer is Mach 0.62.
6. The Jumbo City Flyer has a reduction of 43 percent on a mission from Beijng to Hongkong with a range of 1991 km with respect to a Boeing 747-400 on the same mission, but reaches a 52 percent reduction on a 543 km flight from Los Angeles to San Francisco.
7. The Jumbo City Flyer is designed to operate safely and transport passengers comfortably while complying with all CS-25 regulations.
8. It turned out that determining the exact noise levels of the Jumbo City Flyer was too difficult in this stage of the design process. However, it does have the wheel tug system, which results in taxiing with engines off. This will reduce noise during ground operations. Also, since propellers have improved takeoff and climb performance, the Jumbo City Flyer can climb to an altitude relatively fast. Combined, it is expected that the Jumbo City Flyer will meet the requirement, but further in the design process this will have to be verified and parts of the design might have to change because of it.
9. The Jumbo City Flyer can use standard infrastructure with regard to passenger and cargo loading, but it will need a storage facility for LNG on each airport and with that also come special tanking facilities.
10. The take-off and landing distances achieved by the Jumbo City Flyer are sufficient to be able to land and take-off on the busiest airports.
11. The design of the Jumbo City Flyer complies with the CS-25 regulations.

14.5   Project design and development logic

After the DSE is concluded, 9 steps need to be taken to go through production to first flight. All steps are shown in figure 44 in a Gantt chart and briefly explained below, starting from an extra iteration to the first flight in January 2025.

1. **Extra iterations**
   The first step is extra iterations of the design. The recommendations need to be implemented and although the design and business idea is good, it can be improved upon. For the design, if the margins between initial assumptions and first results on the MTOW are within 5 percent, the first preliminary design sequence is finished.

2. **Pitch the idea for aircraft manufactures and sell the design**
   When the design is optimised an updated cost estimation and return on investment analysis are made. This then means the Jumbo City Flyer design can be sold to a respectable aircraft manufacturer, as that provides extra resources to improve the design in the detailed design phase and extra resources necessary for step 4.

3. **Preliminary design**
   With aircraft manufacturers joining, the preliminary design can be continued. Due to the innovations in the design of the Jumbo City Flyer, the use of LNG and composites, the preliminary design phase is longer compared to that of a conventional aircraft.

4. **Find funding**

5. **First order of the Jumbo City Flyer**
   Step 4 and step 5 are taken at the same time. Selling the aircraft to airline companies and finding funding go hand in hand. Since it is an economicallt efficient and low-emission aircraft, demand is expected to be high. For this and the following step, it is very important to have a big aircraft manufacturer supporting the buying the Jumbo City Flyer design as the connections, relations, and the influence of a large company are of major importance to get orders and secure suppliers to meet the deadline of 2025.

6. **Setting up production line**
   With the preliminary design finished, first orders in, and funding secured, contracts can be negotiated with suppliers and a start with the production line will be made. This needs to be done in time to have a full production line when starting with manufacturing of the first Jumbo City Flyer.

7. **Start detailed design**
   With the first aircraft ordered, the design enters the final phase, the detailed design.

8. **Manufactering**
   When the detailed design is finished, the production of the first Jumbo City Flyer commences.

9. **First flight January 2025**
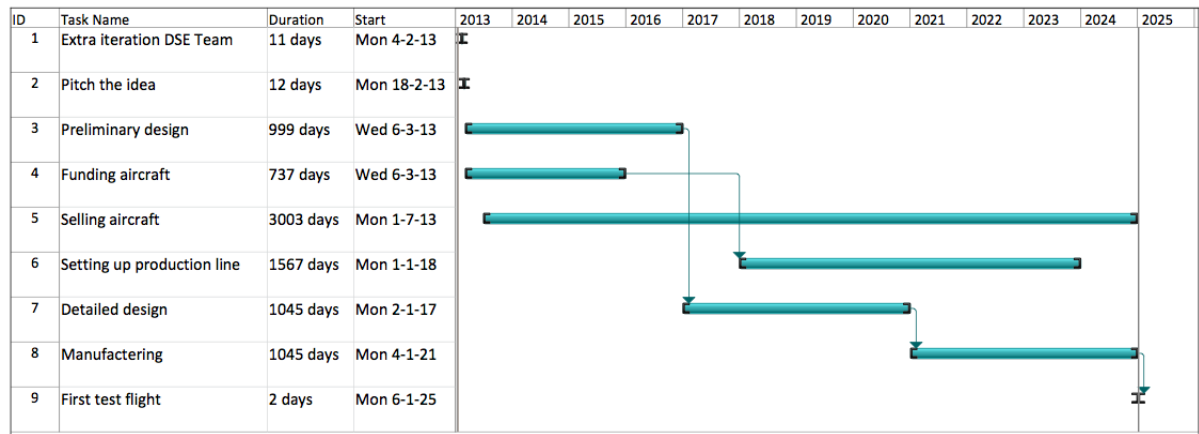
Figure 44: Post DSE gantt chart

15   Conclusion

The preliminary design and process for the Jumbo City Flyer, a high capacity, short range, and low emissions aircraft, has been presented. The design is dictated by the requirements set in the project brief. Market research shows that ranges up to 2500 km are responsible for most of the growth in the market. Therefore the designed maximum range is 2500 km. Due to increasing attention to the CO_2 emissions of the aviation industry, the emissions of the aircraft need to be lowered. This was set to be 50 percent lower per passenger km compared to a Boeing 747-400.

The design is compared to a Boeing 747-400 as this is an aircraft often used for these missions. The aircraft is intended to meet market demands in the short haul market, with a higher passenger carrying capacity and lower operating cost than current aircraft operating in the same market. This is achieved by optimising the design for this mission, as there is currently no aircraft optimised for this mission. It is expected that there is a market for up to 5500 aircraft by 2050.

The Jumbo City Flyer flies slower and lower than current aircraft performing these missions, namely with a cruise speed of Mach 0.62 at an altitude of 8.5 km. It was determined that the drag decreases significantly when flying at this speed and altitude, reducing the thrust and thus fuel required. It also enables the use of straight wings, which provide more lift and have a lower structural weight compared to swept wings. The increase in flight time because of the lower flight speed is marginal, only 20 minutes on a 2 hour flight. Lowering the flight speed also allows for turboprops, which are more efficient than turbofans at the selected cruise speed. Ground operations will be performed using an electrical taxiing system, which means there are no emissions during this phase of the mission.

The material selection process resulted in up to 80 percent of the Jumbo City Flyer being made out of epoxy HS/carbon fibre. Different types of fuel were studied for the required reduction of CO_2-emissions, e.g., LPG, Jet A-1 fuel, liquid hydrogen and LNG. It was concluded that LNG is the best option. An average reduction of 47 percent per passenger km compared to a Boeing 747-400 is achieved for the CO_2-emissions, taking as reference the 50 busiest routes, see appendix A. Also, a reduction in fuel costs is achieved since LNG is much cheaper than Jet A-1 fuel and this is expected to also be the case in 2025. It is concluded that airliners flying with the Jumbo City Flyer can lower fuel costs per passenger-km by 33 percent compared to a Boeing 747-400. The Jumbo City Flyer reduces the total costs for an airliner by almost 16 percent.

16 Recommendations

This section will outline the recommendations as identified during the design process of the Jumbo City Flyer and serve as a starting point for further refinement of the preliminary design of the aircraft. The recommendations are catalogued according to the different chapters of the design phase.

16.1 Fuselage design

The structural integration of windows into the fuselage needs to be studied in further detail. Passengers appreciate having a large windows, but addition of openings into the fuselage structure compromises it significantly.

Sizing and positioning of the structural components of the fuselage need to further analysed that is the type, position, and amount of stringers, frames, and longerons. Next to that, the integration of the wing and fuselage needs further study.

The amount of cargo containers that fit in the Jumbo City Flyer is determined by calculating the space there is left in the fuselage after the wingbox, landing gear and main fuel tank are sized and positioned. It must be studied if all this space is indeed available for cargo containers and it might be possible to store smaller containers in the tail.

16.2 Propulsion design

A heat exchanger is used to evaporate the LNG before it is burned in the engine. It is recommended to investigate whether and how the heat exchanger can be used to cool either the engines inlet air and thus increase thermal efficiency or can used to cool down the air used to cool the turbine blades.

The position and benefit of counter-rotating propellers on the Jumbo City Flyer need further investigation. For the A400M it is known this increases the lift at low speeds by 4 percent, decreases the tail fin by 17 percent and the surface of the horizontal stabiliser by 8 percent [79].

The noise performance has to be analysed according to CS-25. Too little information is available at this moment do make a detailed study of it. Using a taxi bot will eliminate all noise during the taxi phase of the mission.

16.3 Wing design

The wing skin currently has the same thickness over the entire wing. By varying the skin thickness throughout the wing, the wingbox design can be further optimised for weight savings while maintaining structural integrity.

Another step is to change the number of stringers that are attached to the bottom of the wingbox. The top and bottom skin have an equal amount of stringers, making the bottom side overdesigned. Improvements can be made here.

The engine is embedded into the wing, and as such it will have to carry part of the loads that run through the wing. This correlation has to be investigated as either the wing structure has to carry all the loads with a hole, or the engine pod will have to carry part of the loads.

16.4   Fuel storage, handling, and transport

For the Jumbo City Flyer's success, it is essential that the facilities for storing and tanking of LNG at airports worldwide are developed.

The emergency fuel dump system has to be designed to ensure that it can dump the fuel fast enough in case of an emergency. This includes sizing the fuel pumps and fuel lines to ensure a delivery of fuel to the engines at all points of the flight envelope.

It is recommended that the production of aerogels in large quantities is further investigated. It weighs 2 kg/m^3 and is the best insulator available. The problem is the high price it comes at, around 1 million dollars for 1 cubic metre. Making all insulation out of aerogels would save over a tonne of weight but would cost around 7.5 million dollar per aircraft. If aerogels can be obtained at lower prices in the next few years, the option of making the entire insulation system from aerogel is worth looking in to.

The integration of the centre fuel box with the wingbox and the landing gear in the cargo bay of the aircraft will have to be analysed in more detail. The better this is integrated, the more space is left for cargo.

16.5   Weight and balance

With the position and weight of the Jumbo City Flyer aircraft components calculated based on statistical data of aircraft designed and built before 1990, hence it is recommended that these calculations be made with equations or relations based on modern aircraft.

16.6   Empennage design

The horizontal stabilizer was designed to allow for a range in c.g. of 50 percent of the mean aerodynamic chord during flight. Margins of this magnitude are rare and therefore the controllability limit needs more research.

As mentioned, the effect of counter-rotating propellers was not accounted for in the analysis and should be looked into as it could decrease the tail size.

The lateral and directional stability and control were not analysed in as much detail as the longitudinal motion. The design of the vertical tailplane could be further improved if these asymmetric motions are researched further.

16.7 Undercarriage design

It is recommended that further research is conducted into the concept of an electrical taxiing system. The advantages of the concept have already been established, but the characteristics of such a system are as of yet unknown. When these are known, they need to be added and taken into account in the rest of the design of the Jumbo City Flyer.

16.8 Aerodynamic characteristics

An assumption made during the design of the wing is that the lift by the wing should be 1.05 times the weight of the aircraft, in all different conditions. The maximum lift coefficient needed with this assumption is 1.79. however maximum lift coefficient is achieved by the wing at this point is 1.76 with addition of high lift devices.

The design can be improved upon with regard to the maximum lift in clean configuration. This is the critical point for the aerodynamic design. The maximum lift in landing configuration is the driving constraint for the wing loading. If this wing loading can be increased, the wing can be scaled down. This means that the flaps should be redesigned, but there is room for improvement here. The ratio of flapped wing area over wing area can be increased and leading edge high-lift devices could be added. When the wing is scaled down, keeping the aspect ratio the same, the total moment on the root decreases.

Scaling down the wing has a noticeable effect on the structural wing weight. It also would have a considerable effect on the drag created by the wing and thus the lift over drag ratio. A quick sensitivity study shows that, when increasing the wing loading by 10 percent, the weight of the wing can be decreased by 10 percent. Note that this is a weight of 1.5 tonne, without the 'snowball effect'. The L/D would also benefit from this. Decreasing the wing area by 10 percent decreases the $C_{D,0}$ of the wing but increases the induced drag by the wing, because a higher lift coefficient is needed. The net effect is that the L/D is increased from 15.4 to 15.7, keeping the weight the same.

Another 4 percent decrease in wing weight can be achieved by choosing a thicker airfoil near the root. This was initially not considered due to the higher drag created. But if the wing structure can be decreased, an optimisation for this should be done. Another option when increasing the root thickness is to have the same wing weight but a larger aspect ratio.

A combination of the two recommendations above, scaling down the wing by 10 percent and increasing the aspect ratio from 10 to 10.5 and keeping the weight the same yields a L/D of 15.9. An optimisation of the above process is recommended when continuing the work done in this report.

The aerodynamic benefits of the winglets vs extension of the wing need further analysis.

16.9 Environmental impact

During the detailed design the environmental impact of the development, construction and end-of-life of the Jumbo City Flyer will have to be investigated. A strategy for reducing this impact has to be developed. This is an important aspect in the environmental impact of the Jumbo City Flyer during its life cycle and a good strategy is vital.

References

[1] Rocca, G. L., "AE3201 - Systems Engineering and Aerospace Design," Tech. rep., Delft University of Technology, 2011.

[2] Rao, A., *Project Guide Design Synthesis Excercise: Design of a Jumbo City Flyer*, Technical University Delft, 2012.

[3] vd. Beek, A., Decloedt, D., Eng'alut, I., v. Ginneken, P., Janssen, Y., Mehmood, H., Naardig, E., Nous, R., Tiemstra, J., and Verkaik, S., "Jumbo City Flyer Midterm report," December 2012, Bachelor Thesis.

[4] Airplanes, B. C., "Boeing Current Market Outlook 2012-2031," Booklet, Seattle, WA 98124-2207, 2012.

[5] S.A.S, A., "Navigate the future: Airbus Global Market Forecast 2012-2031," book, 31707 Bagnac Cedex, France, 09 12.

[6] "World's Top 50 busiest routes: As at Jul-2010," `http://centreforaviation.com/profiles/hot-issues/route-changes`, July 2010.

[7] Communications, I. C., "Passenger numbers to reach 2.75 billion by 2011," `http://www.iata.org/pressroom/pr/pages/2007-24-10-01.aspx`, 10 2007.

[8] (IMF), I. M. F., "Asia and Pacific: Regional Economic Outlook," April 2012.

[9] "JAL Anual Report 2009," Tech. rep., Japan Airlines, 2009.

[10] *Anual Report 2011*, American Airlines, 2011.

[11] *ANA Fact Book 2012*, All Nippon Airways, 2012.

[12] Liebeck, R., "Advanced Subsonic Airplane design and Economic Studies," Tech. Rep. CR-195443, NASA, 1995.

[13] "China Southern to finally commence long-haul A380 services, but operation still faces challenges," `http://centreforaviation.com/analysis/china-southern-to-finally-commence/-long-haul-a380-services-but-operation-still-faces-challenges-83737`, September 2012.

[14] "China Southern Airline Destinations," `http://www.csair.com/en/tourguide/before_ready/destination_info/domestic.shtml`, November 2012.

[15] Bill Hopwood, Mary Mellor, G. O., "Sustainable Development: Mapping Different Approaches," *Wiley InterScience*, 2002.

[16] The U.S Government Printing Office (GPO), *Part 25—Airworthiness Standards: Transport Category Airplanes*, November 2012.

[17] The U.S Government Printing Office (GPO), *PART 36—Noise Standards: Aircraft Type and Airworthiness Certification*, October 2012.

[18] European Aviation Safety Agency (EASA), *Certification Specifications and Acceptable Means of Compliance for Large Aeroplanes CS25*, 12th ed., 06 2012.

[19] (EASA), E. A. S. A., *Notice Of Proposed Amendment (Npa) No 2011-08*, 1st ed., May 2011.

[20] vd. Beek, A., Decloedt, D., Eng'alut, I., v. Ginneken, P., Janssen, Y., Mehmood, H., Naardig, E., Nous, R., Tiemstra, J., and Verkaik, S., "Baseline Report," November 2012, Bachelor Thesis.

[21] Roskam, J., *Airplane Design Part I: Preliminary Sizing Of Airplanes*, University of Kansas, Lawrence, 1986.

[22] Roskam, J., *Airplane Design Part II: Preliminary Configuration Design And Integration Of The Propulsion System*, University of Kansas, Lawrence, 1986.

[23] Roskam, J., *Airplane Design Part III: Layout Design Of Cockpit, Fuselage, Wing And Empennage: Cutaways And Inboard Profiles*, University of Kansas, Lawrence, 1986.

[24] Sadraey, M., "Wing Design," Tech. rep., Daniel Webster College.

[25] Jr., E. G. B., "Frequently Asked Questions About LNG," `http://www.energy.ca.gov/lng/faq.html#600`.

[26] Sedlaczek, R., *Oil-Off In Large- And Small-Scale Lng Chains*, Ph.D. thesis, Trondheim, May 2008.

[27] U.S. Department of Energy, *Voluntary Reporting of Greenhouse Gases*, 2007.

[28] of Air Quality, N. C. D., "CNG Vehicles," `http://daq.state.nc.us/motor/cng/`, April 2004.

[29] Goyal, P., "Present scenario of air quality in Delhi: a case study of CNG implementation," *Atmospheric Environment*, Vol. 37, No. 38, December 2003, pp. 5423–5431.

[30] Mills, M. M., "7. New Initiatives in High-Altitude Aircraft," `http://www.hq.nasa.gov/pao/History/SP-4404/ch7-13.htm`.

[31] Roskam, J., *Airplane Design Part IV: Layout Design Of Landing Gear And Systems*, University of Kansas, Lawrence, 1986.

[32] Roskam, J., *Airplane Design Part V: Component Weight Estimation*, University of Kansas, Lawrence, 1986.

[33] Roskam, J., *Airplane Design Part VI: Preliminary Calculation Of Aerodynamic, Thrust And Power Characteristics*, University of Kansas, Lawrence, 1986.

[34] Roskam, J., *Airplane Design Part VII: Determination Of Stability, Control And Performance Characteristics: FAR And Military Requirements*, University of Kansas, Lawrence, 1986.

[35] Roskam, J., *Airplane Design Part VIII: Airplane Cost Estimation: Design, Development, Manufacturing And Operating*, University of Kansas, Lawrence, 1986.

[36] Torenbeek, E., *Synthesis of Subsonic Airplane Design*, Delft University Press, 1982.

[37] Bargsten, C. J. and Gibson, M. T., "Select Technologies That Have Shaped Modern Aviation," Tech. rep., NASA, August 2011.

[38] Hepperle, M., "Java Foil," `http://www.mh-aerotools.de/airfoils/javafoil.htm`, December 2012.

[39] "XFLR5," `www.xflr5.com/`, November 2012.

[40] Gudmundsson, S., *Aircraft Preliminary Design Handbook*, 2011.

[41] Mulder, J., van Staveren, W., van der Vaart, J., and de Weerdt, E., *Flight Dynamics Lecture Notes*, Faculty of Aerospace Engineering, 2007.

[42] Megson, T. H. G., *Aircraft Structures for Engineering Students*, Butterworth-Heinemann, 2007.

[43] "AE2100 second year project Work Package 4," Tech. rep., Delft University of Technology, 2010.

[44] "747 Family," `http://www.boeing.com/commercial/747family/pf/pf_facts.html`, November 2012.

[45] Raymer, D. P., *Aircraft Design: A Conceptual Approach Third Edition*, American Institute of Aeronautics and Astronautics, Inc., 1999.

[46] Smit, H. and Fielding, J., "New Concepts for Environmentally Friendly Aircraft," Tech. rep., Cranfield University, 2009.

[47] Ramba, J., Dean, K., and McCall, T., "A380," `http://www.dept.aoe.vt.edu/mason/Mason_f/A380Dean.pdf`, December 2012.

[48] Suslik, D., "The Taxibot System Will Be Demonstrated Live This Week To Leading Airlines And Ground Handling Companies At Chateauroux Airport, France," *Isreal Aerospace Industries*, 2012.

[49] "Taxibot System," `http://www.iai.co.il/35095-39730-en/Groups_Military_Aircraft_Lahav_Products_TaxiBot.aspx`, December 2012.

[50] "Fuel Savings," `http://www.wheeltug.gi/fuel_savings.shtml`, January 2012.

[51] "Insulation Products," `http://aerogel.com/products/overview-product.html`, January 2013.

[52] "Stardust NASA's Comet Sample Return Mission FQA," Tech. rep., NASA, 2005.

[53] Kanellos, M., "Aerogel Prices to Drop by 90 Percent?" *Green Tech Media*, June 2011.

[54] Cengel, Y. and Boles, M., *Thermodynamics - an Engineering Approach*, Mc Graw Hill, 2010.

[55] "747-400 Payload Range Cabability," Tech. rep., Boeing, 2011.

[56] "Boeing 747-400," Tech. rep., Cathay Pacific, 2013.

[57] IHS, "Janes all the world aircraft," `https://janes.ihs.com/CustomPages/Janes/Home.aspx`, January 2013.

[58] "Boeing 747," Tech. rep., Global Security, 2011.

[59] "Fuel Planner," `http://www.fuelplanner.com`, January 2013.

[60] "Manufacturers aim for electric taxi EIS by 2016," `http://www.flightglobal.com/news/articles/in-focus-manufacturers-aim-for-electric-taxi-eis-by-2016-368554/`, January 2013.

[61] Baker, A., Dutton, S., and Kelly, D., *Composite Materials for Aircraft Structures*, American Institute of Aeronautics and Astronautics, Inc., 2004.

[62] Mallick, P., *Fiber-Reinforced Composites*, Taylor & Francis Group, 2007.

[63] Rocca, G. L., "Vertical Tail Data," .

[64] Elwood H. Hunt, Dr. Don H. Reid, D. R. S. D. F. E. T., "Commercial Airliner Environment Control System," May 1995.

[65] Aircraft, G., "Airbus A380 Specifications," .

[66] "Airplane Characteristics For Airport Planning," Tech. rep., Airbus, 2005.

[67] "Boeing 787 From The Ground Up," Tech. rep., The Boeing Company, 2008.

[68] "Boeing 787 Wind Tunnel Testing Under Way," `http://www.boeing.com/companyoffices/gallery/images/commercial/787/k63038.html`, December 2012.

[69] "Boeing celebrates 787 delivery as program's costs top $32 billion," `http://seattletimes.com/html/businesstechnology/2016310102_boeing25.html`, January 2013.

[70] "Airbus' Behemoth Hits Turbulence," `http://www.businessweek.com/stories/2006-06-13/airbus-behemoth-hits-turbulence`, December 2012.

[71] Becker, D., "The Boeing 737/757 Lean Story," `http://paceimpact.com/wp-content/uploads/2012/08/Boeing-Lean.pdf`, December 2012.

[72] "Jet Prices," `http://www.boeing.com/commercial/prices/index.html`, December 2012.

[73] "Natural Gas," `http://www.eia.gov/dnav/ng/ng_pri_sum_dcu_nus_m.htm`, December 2012.

[74] "Petroleum & Other Liquids," `http://www.eia.gov/dnav/pet/hist/LeafHandler.ashx?n=PET\&s=EMA_EPJK_PTG_NUS_DPG\&f=A`, December 2012.

[75] "Heren LNG Markets Daily," `http://img.en25.com/Web/ICIS/LMD_2.pdf`, December 2013.

[76] "Terminal Servicing 737," `http://www.boeing.com/commercial/airports/acaps/737sec5.pdf`, October 2005.

[77] "Terminal Servicing 747," `http://www.boeing.com/commercial/airports/acaps/7474sec5.pdf`, October 2005.

[78] Harry A. Kinnison, P., *Aviation Maintenance Management*, Mc Graw Hill, 2004.

[79] "The versatile airlifter for the 21st," `http://www.airbusmilitary.com/Aircraft/A400M/A400MAbout.aspx`, November 2012.

A   Appendix: Busiest routes worldwide

Table 32: The 50 busiest routes worldwide, sorted on number of passengers per month.

	From	Code	To	Code	# pass	dist. [km]
1	Tokyo Int'l AP	RJTT	Sapporo-New Chitose AP	RJCC	1253220	992.94
2	Seoul-Gimpo AP	RKSS	Jeju Int'l AP	RKPC	848151	605.26
3	Tokyo Int'l AP	RJTT	Fukuoka AP	RJFF	811521	890.46
4	Sydney AP	YSSY	Melbourne AP	YMML	780932	714.96
5	Beijing Capital Int'l AP	ZBAA	Shanghai Hongqiao Int'l AP	ZSSS	689287	1136.57
6	Hong Kong Int'l AP	VHHH	Taiwan Taoyuan Int'l AP	RCTP	680915	902.51
7	Tokyo Int'l AP	RJTT	Naha AP	ROAH	659166	1617.47
8	Congonhas-Sao Paulo AP	SBSP	Rio de Janeiro-Santos Dumont AP	SBRJ	624105	729.98
9	Tokyo Int'l AP	RJTT	Osaka Int'l AP	RJOO	620460	482.76
10	Mumbai-Chhatrapati Shivaji AP	VABB	Delhi-Indira Gandhi AP	VIDP	575133	1269.44
11	Madrid-Barajas AP	LEMD	Barcelona AP	LEBL	461228	495.92
12	Sydney AP	YSSY	Brisbane AP	YBBN	456540	760.55
13	OR Tambo Int'l AP	FAJS	Cape Town Int'l AP	FACT	453551	1300.39
14	Singapore Changi AP	WSSS	Soekarno-Hatta Int'l AP	WIII	442009	904.55
15	Soekarno-Hatta Int'l AP	WIII	Juanda Int'l AP	WARR	432091	695.51
16	Hong Kong Int'l AP	VHHH	Shanghai Pudong Int'l AP	ZSSS	402528	1371.55
17	Tan Son Nhat Int'l AP	VVTS	Noi Bai Int'l AP	VVNB	366256	1272.22
18	Los Angeles Int'l AP	KLAX	San Francisco Int'l AP	KSFO	350014	565.04
19	Guangzhou Baiyun Int'l AP	ZGGG	Shanghai Hongqiao Int'l AP	ZSSS	346472	1334.12
20	Beijing Capital Int'l AP	ZBAA	Shenzhen Bao'an Int'l AP	ZGSZ	345265	2004.61
21	Soekarno-Hatta Int'l AP	WIII	Ngurah Rai Int'l AP	WADD	338055	998.87
22	OR Tambo Int'l AP	FAJS	King Shaka Int'l AP	FALE	337720	490.54
23	Hong Kong Int'l AP	VHHH	Suvarnabhumi AP	VTBS	335622	1856.54
24	Beijing Capital Int'l AP	ZBAA	Guangzhou Baiyun Int'l AP	ZGGG	334859	2037.78
25	Beijing Capital Int'l AP	ZBAA	Chengdu Shuangliu Int'l AP	ZUUU	333918	1609.13
26	Soekarno-Hatta Int'l AP	WIII	Medan Int'l AP	WIMM	328486	1412.14
27	Singapore Changi AP	WSSS	Kuala Lumpur Int'l AP	WMKK	326533	349.70
28	Hong Kong Int'l AP	VHHH	Singapore Changi AP	WSSS	314422	2686.21
29	King Khalid Int'l AP	OERK	King Abdulaziz Int'l AP	OEJN	310970	856.73
30	Los Angeles Int'l AP	KLAX	John F. Kennedy Int'l AP	KJFK	310856	4025.71
31	Suvarnabhumi AP	VTBS	Phuket Int'l AP	VTSP	307619	701.62
32	Shanghai Hongqiao Int'l AP	ZSSS	Shenzhen Bao'an Int'l AP	ZGSZ	298428	1302.80
33	O'Hare Int'l AP	KORD	LaGuardia AP	KLGA	298378	1180.12
34	Melbourne AP	YMML	Brisbane AP	YBBN	292443	1411.58
35	Tokyo Int'l AP	RJTT	Kagoshima AP	RJFK	291368	1159.36
36	Soekarno-Hatta Int'l AP	WIII	Hasanuddin Int'l AP	WAAA	290388	1462.36
37	London Heathrow AP	EGLL	John F. Kennedy Int'l AP	KJFK	282205	11695.73
38	Mexico City Int'l AP	MMMX	Cancun Int'l AP	MMUN	278440	1317.81
39	Beijing Capital Int'l AP	ZBAA	Hong Kong Int'l AP	VHHH	272588	2125.62
40	Gimpo Int'l AP	RKSS	Gimhae Int'l AP	RKPK	271518	332.83
41	Narita Int'l AP	RJAA	Incheon Int'l AP	RKSI	265230	1303.73
42	Hong Kong Int'l AP	VHHH	Ninoy Aquino Int'l AP	RPLL	260819	1184.94
43	Hartsfield-Jackson Atlanta Int'l AP	KATL	Orlando Int'l AP	KMCO	260180	659.74
44	Ninoy Aquino Int'l AP	RPLL	Mactan-Cebu Int'l AP	RPVM	259582	567.82
45	Cairo Int'l AP	HECA	King Abdulaziz Int'l AP	OEJN	259417	1295.76
46	Mexico City Int'l AP	MMMX	General Mariano Escobedo Int'l AP	MMMY	259368	715.71
47	El Dorado Int'l AP	SKBO	Alfonso Bonilla Aragon Int'l AP	SKCL	258460	433.83
48	El Dorado Int'l AP	SKBO	Jose Maria Cordova Int'l AP	SKRG	257407	300.00
49	Suvarnabhumi AP	VTBS	Singapore Changi AP	WSSS	256418	1436.60
50	Melbourne AP	YMML	Adelaide AP	YPAD	255376	647.88
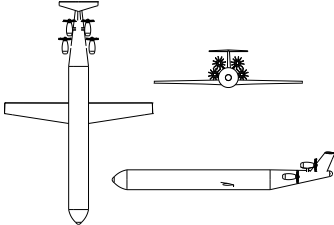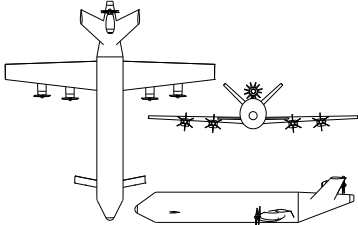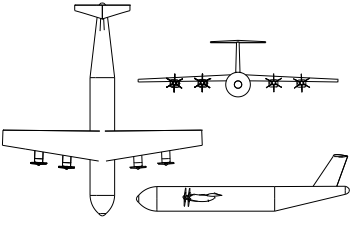
B Appendix: Domestic flights investigated by China Southern Airlines

Country	City	Airport	Longest Runway	Length (m)	Elevation (m)
Australia	Adelaide	Adelaide Intl		3100	6
Australia	Sydney	Kingsford Smith	16R/34L	3962	6
Australia	Melbourne	Tullarmarine Intl	16/34	3657	10
Australia	Brisbane	Brisbane Intl	(01/19)	3560	4
Brazil	Sao Paulo	Congonhas	17R/35L	1940	802
Brazil	Rio De Janeiro	Santos Dumont	02R/20L	1323	3
China	Shanghai	Pudong	17L/355R	4000	4
China	Beijing	Capital	(19/01) & 18L/36R	3800	35
China	Guangzhou	Guangzhou Baiyun Intl	02R/20L	3800	15
China	Chengdu	Shuangliu Intl	02R/20L & 02L/20R	3600	495
China	Shanghai	Hongqiao	18L/36R & 18R/36L	3400	3
China	Zhenzhen	Bao'an Intl	15/33	3400	4
Colombia	Bogota	**El Dorado Intl**		3800	2548
Colombia	Palmira	**Alfonso Bonilla Aragon Intl**		3000	964
Colombia	Medellin	**Jose Maria Cordova Intl**		3557	2141
Egypt	Cairo	Cairo Intl		4000	116
England	London	London Heathrow		3901	25
Hong Kong	Hong Kong	Hong Kong Intl	07R/25L & 07L/25R	3600	9
India	Delhi	Indira Gandhi Intl	(11/29)	4430	237
India	Mumbai	Chhatrapti Shivaji Intl	(09/27)	3445	11
Indonesia	Jakarta	Soekarrno-Hatta	07L/25R & 07R/25L	3660	10
Indonesia	Denpasar	Bali	(09/27)	2984	4
Indonesia	Medan	Medan Intl	(05/23)	2900	35
Indonesia	Makassar	Sultan Hasanuddin Intl		3100	14
Japan	Tokyo	Narita	16R/34L	4000	41
Japan	Tokyo	Haneda	16R/34L & 16L/34R	3000	6
Japan	Okinawa	Naha AB	18/36	3000	4
Japan	Osaka	Osaka Intl	14R/32L	2999	8
Japan	Sapporo	New Chitose	01R/19L & 01L/19R	2999	25
Japan	Fukuoka	Itazuke AFB	16/34	2800	10
Japan	Kagoshima	Kagoshima		3000	276
Korea	Seoul	Incheon	15R/33L & 15L/33R	3750	7
Korea	Seoul	Gimpo	14L/32R	3600	18
Korea	Busan	Gimhea		3200	2
Korea	Jeju	Jeju Intl	(07/25)	3000	36
Malaysia	Kuala Lumpur	Kuala Lumpur Intl		4124	21
Mexico	Apodaca	General Mariano Escobedo Intl		3000	390
Mexico	Mexico City	Mexico City Intl		3952	2230
Mexico	Cancun	Cancun Intl		3500	6
Phillipines	Manila	Ninoy Aquino Intl		3737	23
Phillipines	Mactan	Mactan-Cebu Int		3300	9
Saudi Arabia	Riyadh	King Khalid Intl		4205	625
Saudi Arabia	Jeddah	King Abdulaziz		4000	15
Singapore	Singapore	Changi Intl	02L/20R & 02C/02R	4000	7
South Africa	Johannesburg	Tambo Intl	03L/21R	4418	1694
South Africa	Durban	King Shaka Intl	(06/24)	3700	93
South Africa	Cape Town	Cape Town Intl	(01/19)	3201	46
Spain	Madrid	Barajas	18R/36L	4350	610
Spain	Barcelona	El Prat	07L/25R	3552	4
Taiwan	Taipei	Toayuan Intl	05R/23L	3350	32
Thailand	Bangkok	Suvarnabhumi Intl	01R/19L	4000	2
Thailand	Phuket	Phuket Intl		3000	25
USA	Atlanta	Hartsfield Jackson Atlanta Intl		3776	313
USA	Chicago	Chicago OÂ´Hare Intl		3962	205
USA	Los Angeles	Los Angeles Intl	07L/25R	3685	38
USA	New York	JFK Intl		4441	4

USA	New York	LaGuardia		2135	6
USA	Orlando	Orlando Intl		3659	29
USA	San Francisco	San Francisco Intl	10L/28R	3618	4
Vietnam	Ho Chi Minh City	Tan Son Nhat Intl	07R/25L	3800	10
Vietnam	Hanoi	Noi Bai	11R/29L	3800	12
china	changchun			3200	215
china	changsha			2490	66
china	dalian			3300	33
china	guiyang			3200	1139
china	guilin			2800	174
china	harbin			3200	139
china	haikou			3600	23
china	nanchang			2800	44
china	nanning			3200	128
china	sanya			3400	27
china	shantou			2500	sea levelish
china	shenyang			3200	60

C   Appendix: 3 concepts originating from the midterm

Table 34: Overview of the main features of the JCF500-1, JCF500-2, and JCF500-3.

Feature	JCF500-1	JCF500-2	JCF500-3
Range [km]	2500	2500	2500
Cruise speed	Mach 0.6	Mach 0.6	Mach 0.6
Crew [-]	12	12	12
Capacity (ec/bu)	430/78	426/78	426/78
Fuselage	Circular	Elliptical	Circular
	1 passenger deck	2 passenger decks	2 passenger decks
	Check-in luggage allowed	Check-in luggage allowed	No check-in luggage
	Cargo allowed	Cargo allowed	No cargo
Diameter [m]	7	h:7.5 w:6.5	6.1
length [m]	77	55	57
height [m]	24	16.4	16.3
Wings	Low fuselage mounted	Low, aft mounted	High fuselage mounted
	limited sweep	limited sweep	limited sweep
		Canard at the front	
Wingspan [m]	53	55	54
Wing area [m^2]	277	303	297
Aspect ratio [-]	10	10	10
Fuel	CNG	Jet A-1 Kerosene	LPG
MTOW	177	181	177
OEW	98	93	93
Fuel	32	42	37
Fuel system [tonne]	31	2.5	11
Engines	Open rotor (4)	Turboprops (4)	Turboprops (4)
	Mounted on fuselage	Mounted under wing	Mounted under wing
		Counter-rotating open rotor (1)	
		Mounted in V-tail	
Tail	T-tail	V-tail with open rotor	T-tail
Landing gear	Mounted under wings	Mounted under wings	Mounted under fuselage
Planform			

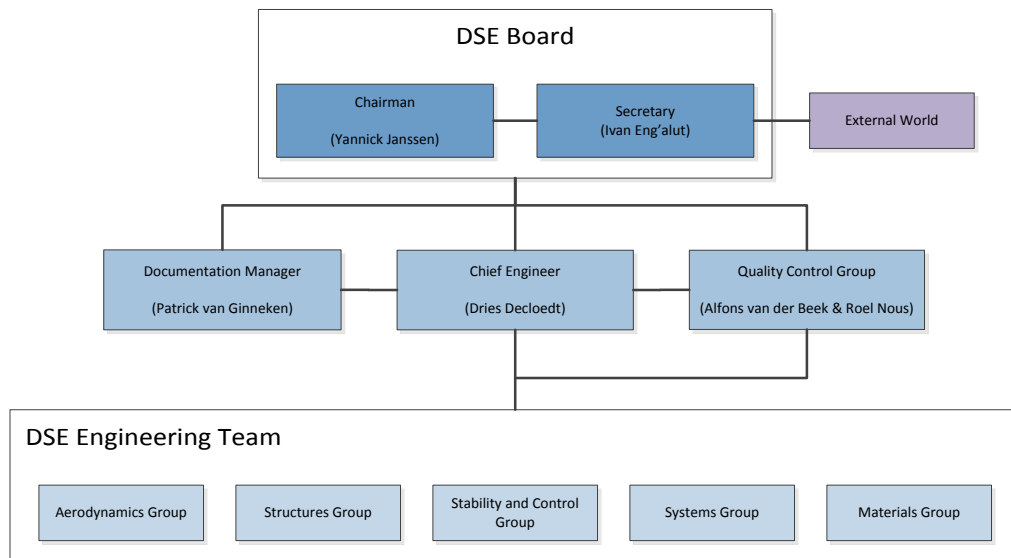# D Appendix: Group organisation

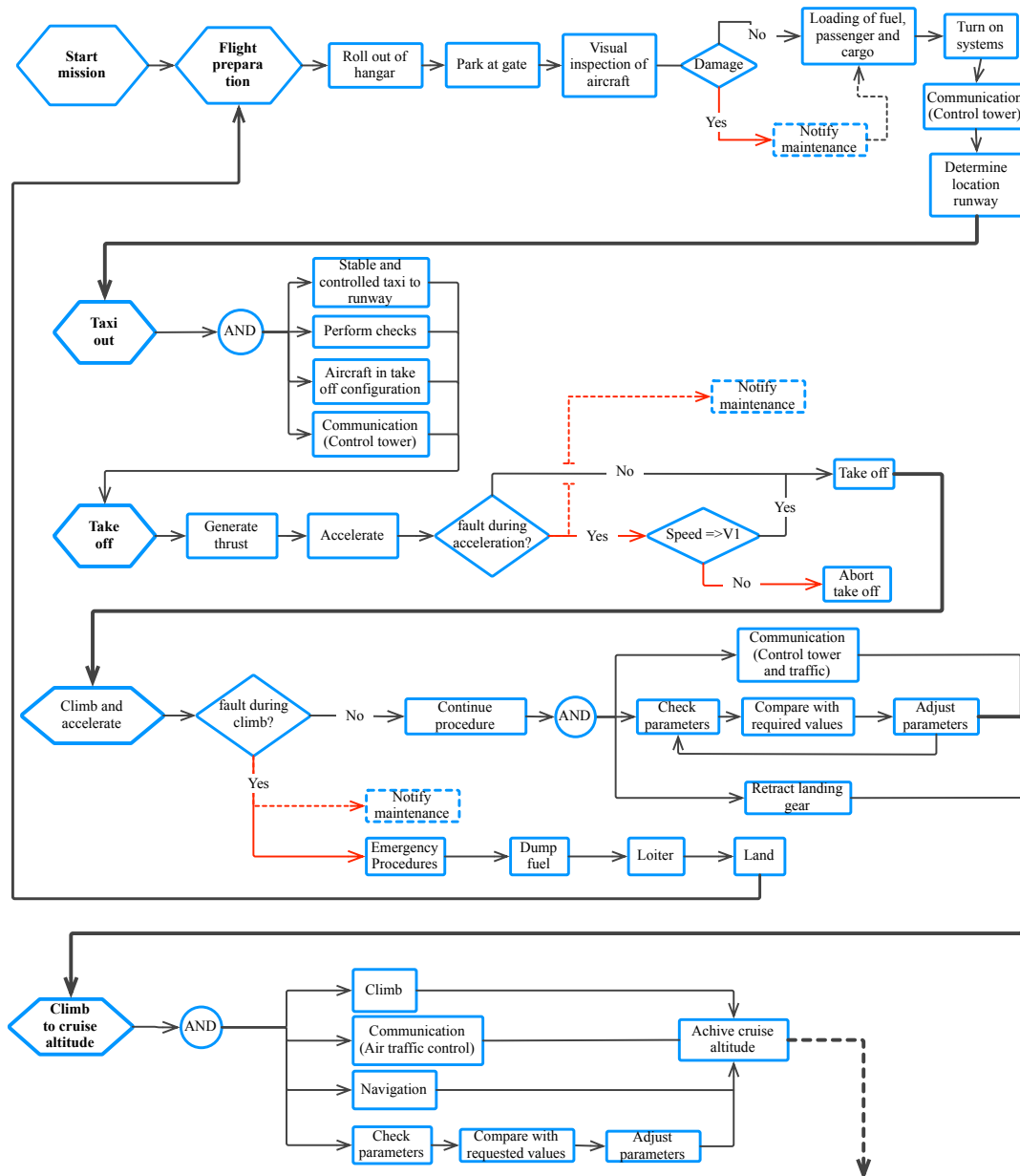Figure 45: Group organization.

E Appendix: Functional Flow Diagrams
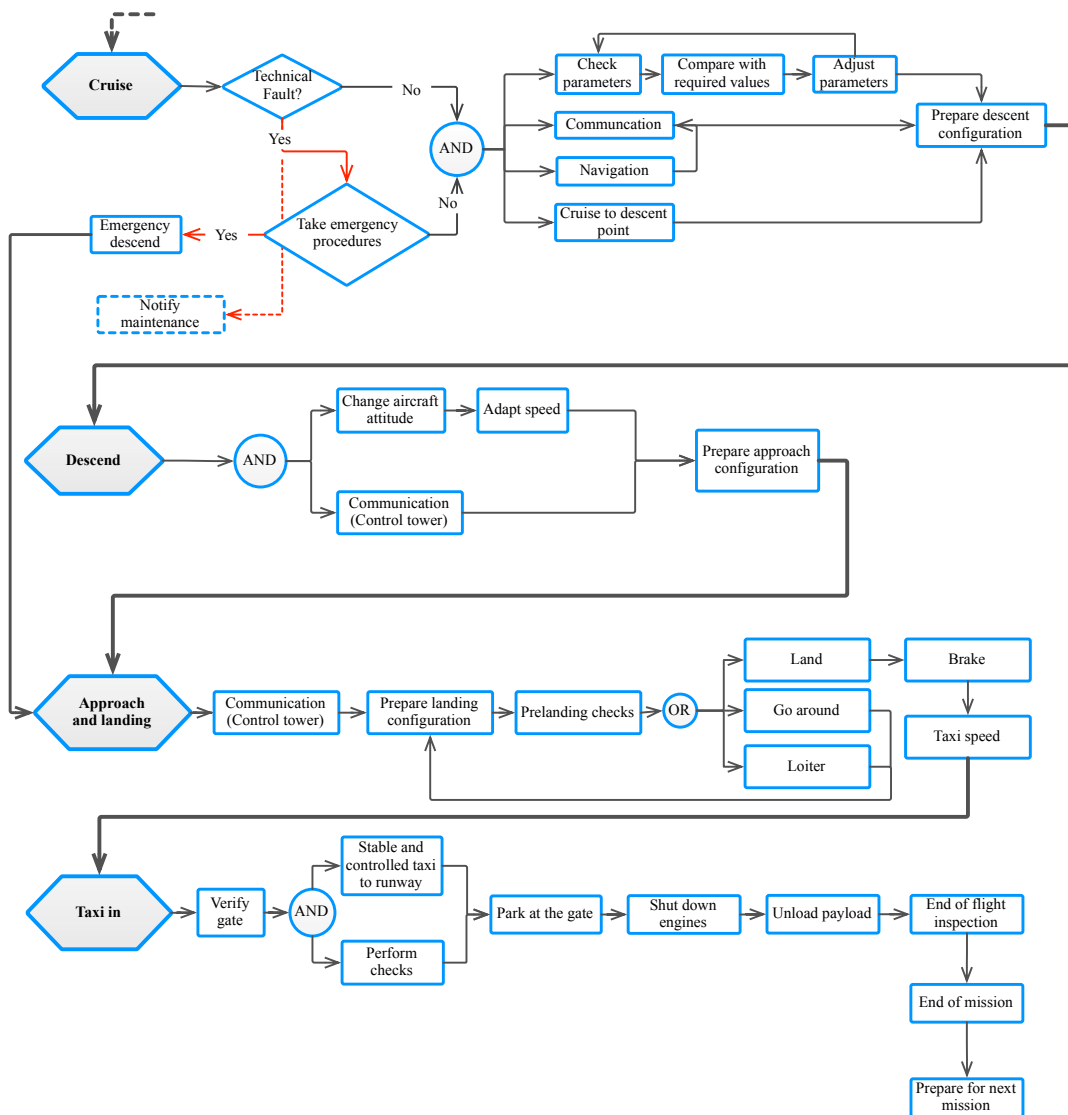

Figure 46: Functional Flow Diagram; Part 1

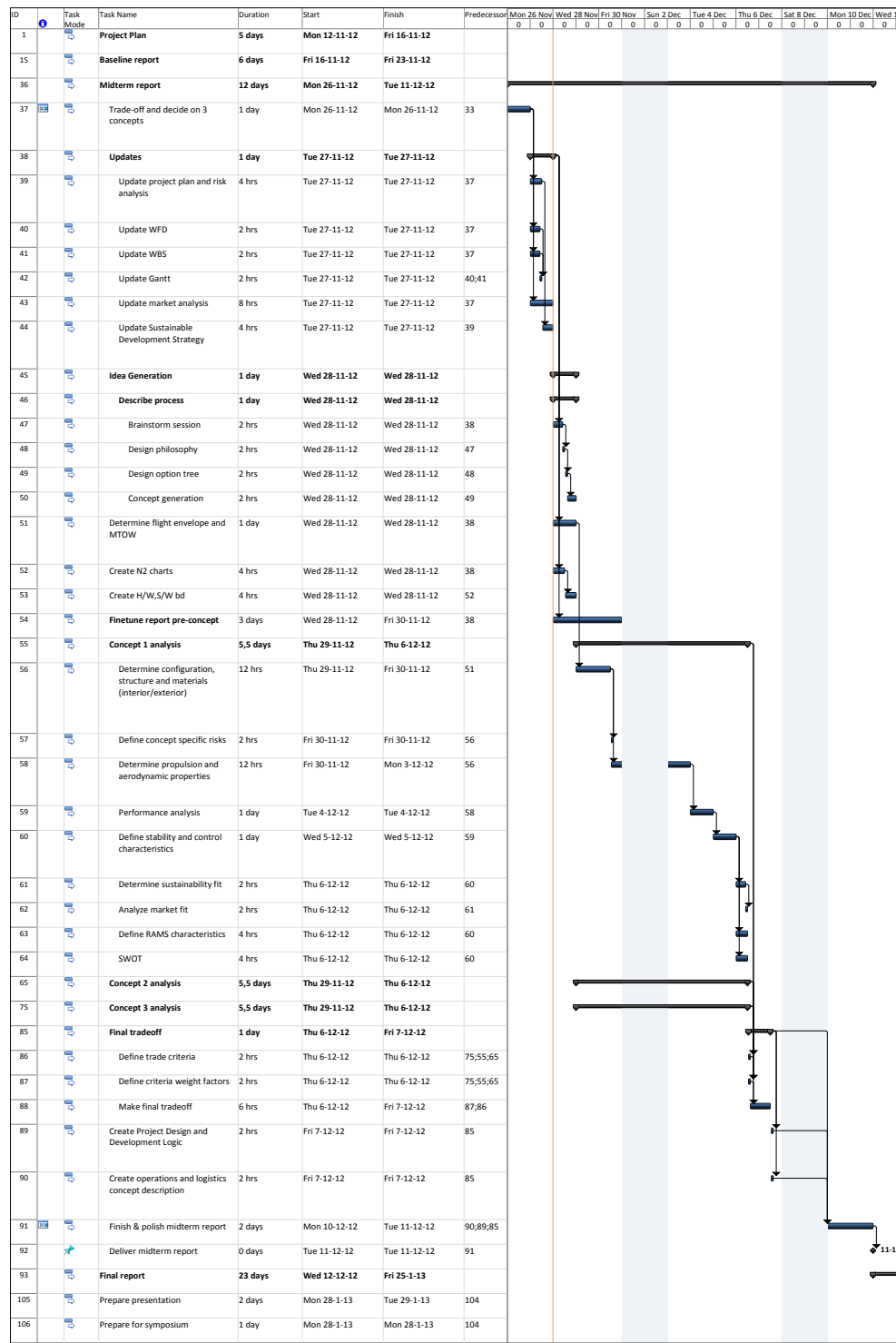Figure 47: Functional Flow Diagram; Part 2

F Appendix: Gantt chart

ID	Task Mode	Task Name	Duration	Start	Finish	Predecessor
1		**Project Plan**	**5 days**	**Mon 12-11-12**	**Fri 16-11-12**	
15		**Baseline report**	**6 days**	**Fri 16-11-12**	**Fri 23-11-12**	
36		**Midterm report**	**12 days**	**Mon 26-11-12**	**Tue 11-12-12**	
37		Trade-off and decide on 3 concepts	1 day	Mon 26-11-12	Mon 26-11-12	33
38		**Updates**	**1 day**	**Tue 27-11-12**	**Tue 27-11-12**	
39		Update project plan and risk analysis	4 hrs	Tue 27-11-12	Tue 27-11-12	37
40		Update WFD	2 hrs	Tue 27-11-12	Tue 27-11-12	37
41		Update WBS	2 hrs	Tue 27-11-12	Tue 27-11-12	37
42		Update Gantt	2 hrs	Tue 27-11-12	Tue 27-11-12	40;41
43		Update market analysis	8 hrs	Tue 27-11-12	Tue 27-11-12	37
44		Update Sustainable Development Strategy	4 hrs	Tue 27-11-12	Tue 27-11-12	39
45		**Idea Generation**	**1 day**	**Wed 28-11-12**	**Wed 28-11-12**	
46		**Describe process**	**1 day**	**Wed 28-11-12**	**Wed 28-11-12**	
47		Brainstorm session	2 hrs	Wed 28-11-12	Wed 28-11-12	38
48		Design philosophy	2 hrs	Wed 28-11-12	Wed 28-11-12	47
49		Design option tree	2 hrs	Wed 28-11-12	Wed 28-11-12	48
50		Concept generation	2 hrs	Wed 28-11-12	Wed 28-11-12	49
51		Determine flight envelope and MTOW	1 day	Wed 28-11-12	Wed 28-11-12	38
52		Create N2 charts	4 hrs	Wed 28-11-12	Wed 28-11-12	38
53		Create H/W,S/W bd	4 hrs	Wed 28-11-12	Wed 28-11-12	52
54		**Finetune report pre-concept**	**3 days**	**Wed 28-11-12**	**Fri 30-11-12**	38
55		**Concept 1 analysis**	**5,5 days**	**Thu 29-11-12**	**Thu 6-12-12**	
56		Determine configuration, structure and materials (interior/exterior)	12 hrs	Thu 29-11-12	Fri 30-11-12	51
57		Define concept specific risks	2 hrs	Fri 30-11-12	Fri 30-11-12	56
58		Determine propulsion and aerodynamic properties	12 hrs	Fri 30-11-12	Mon 3-12-12	56
59		Performance analysis	1 day	Tue 4-12-12	Tue 4-12-12	58
60		Define stability and control characteristics	1 day	Wed 5-12-12	Wed 5-12-12	59
61		Determine sustainability fit	2 hrs	Thu 6-12-12	Thu 6-12-12	60
62		Analyze market fit	2 hrs	Thu 6-12-12	Thu 6-12-12	61
63		Define RAMS characteristics	4 hrs	Thu 6-12-12	Thu 6-12-12	60
64		SWOT	4 hrs	Thu 6-12-12	Thu 6-12-12	60
65		**Concept 2 analysis**	**5,5 days**	**Thu 29-11-12**	**Thu 6-12-12**	
75		**Concept 3 analysis**	**5,5 days**	**Thu 29-11-12**	**Thu 6-12-12**	
85		**Final tradeoff**	**1 day**	**Thu 6-12-12**	**Fri 7-12-12**	
86		Define trade criteria	2 hrs	Thu 6-12-12	Thu 6-12-12	75;55;65
87		Define criteria weight factors	2 hrs	Thu 6-12-12	Thu 6-12-12	75;55;65
88		Make final tradeoff	6 hrs	Thu 6-12-12	Fri 7-12-12	87;86
89		Create Project Design and Development Logic	2 hrs	Fri 7-12-12	Fri 7-12-12	85
90		Create operations and logistics concept description	2 hrs	Fri 7-12-12	Fri 7-12-12	85
91		Finish & polish midterm report	2 days	Mon 10-12-12	Tue 11-12-12	90;89;85
92		Deliver midterm report	0 days	Tue 11-12-12	Tue 11-12-12	91
93		**Final report**	**23 days**	**Wed 12-12-12**	**Fri 25-1-13**	
105		Prepare presentation	2 days	Mon 28-1-13	Tue 29-1-13	104
106		Prepare for symposium	1 day	Mon 28-1-13	Mon 28-1-13	104

Figure 48: Gantt chart

G   Appendix: Renders

H   Appendix: DSE group